

AD-A118 518

DELAWARE UNIV NEWARK DEPT OF CIVIL ENGINEERING
NUMERICAL MODELING OF THE NEARSHORE REGION.(U)
JUN 82 J T KIRBY, R A DALRYMPLE

F/G 8/3

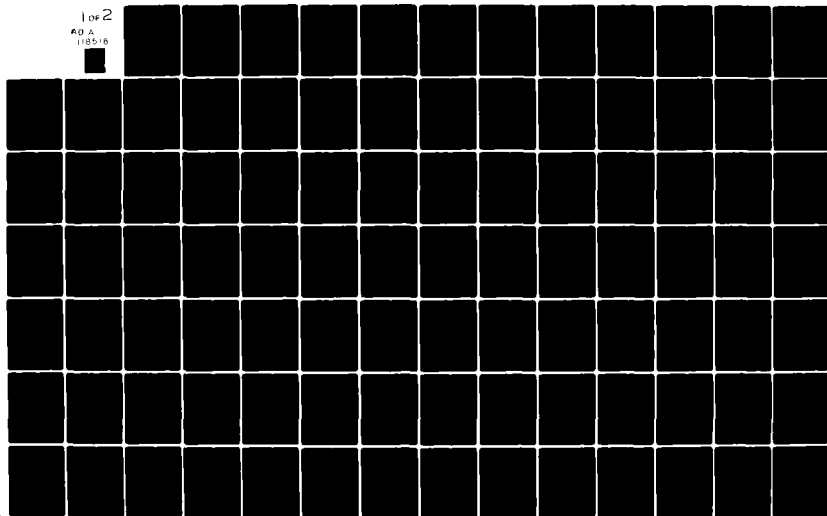
N00014-81-K-0297

NL

UNCLASSIFIED CE-82-24

1 of 2

AD A
118518



AD-A118518

**NUMERICAL MODELING
OF THE NEARSHORE REGION**

by
James T. Kirby, Jr.
and
Robert A. Dalrymple

Technical Report No. 11
Contract No. N00014-81-K-0297
with the OFFICE OF NAVAL RESEARCH, GEOGRAPHY PROGRAMS

Research Report CE-82-24

June 1982

OCEAN ENGINEERING PROGRAM

DEPARTMENT OF CIVIL ENGINEERING
UNIVERSITY OF DELAWARE
NEWARK, DELAWARE
19711

NUMERICAL MODELLING OF THE NEARSHORE REGION

by

JAMES T. KIRBY, Jr.

and

ROBERT A. DALRYMPLE

Technical Report No. 11

Contract No. N00014-81-K-0297

with the Office of Naval Research, Geography Programs

RESEARCH REPORT CE-82-24

June 1982

Ocean Engineering Program

Department of Civil Engineering

University of Delaware

Newark, Delaware

19711

SECURITY CLASSIFICATION OF THIS PAGE (When Data Entered)

REPORT DOCUMENTATION PAGE		READ INSTRUCTIONS BEFORE COMPLETING FORM
1. REPORT NUMBER ONR TR. No. 11	2. GOVT ACCESSION NO.	3. RECIPIENT'S CATALOG NUMBER
4. TITLE (and Subtitle) Numerical Modelling of the Nearshore Region		5. TYPE OF REPORT & PERIOD COVERED
7. AUTHOR(s) James T. Kirby, Jr. and Robert A. Dalrymple		6. PERFORMING ORG. REPORT NUMBER
9. PERFORMING ORGANIZATION NAME AND ADDRESS		8. CONTRACT OR GRANT NUMBER(s) N00014-81-K-0297
11. CONTROLLING OFFICE NAME AND ADDRESS Department of Civil Engineering University of Delaware, Newark, DE 19711		10. PROGRAM ELEMENT, PROJECT, TASK AREA & WORK UNIT NUMBERS
14. MONITORING AGENCY NAME & ADDRESS (if different from Controlling Office)		12. REPORT DATE June 1982
		13. NUMBER OF PAGES 163
		15. SECURITY CLASS. (of this report)
		15a. DECLASSIFICATION/DOWNGRADING SCHEDULE
16. DISTRIBUTION STATEMENT (of this Report) This report has been approved for public release and sale; its distribution is unlimited		
17. DISTRIBUTION STATEMENT (of the abstract entered in Block 20, if different from Report)		
18. SUPPLEMENTARY NOTES		
19. KEY WORDS (Continue on reverse side if necessary and identify by block number) Numerical models, nearshore circulation, longshore currents, rip currents		
20. ABSTRACT (Continue on reverse side if necessary and identify by block number) The thoeretical background and numerical formulation for two finite-difference models for predicting nearshore circulation are reviewed. The models are based on the time- and depth-averaged equations of continuity and momentum, with momentum flux terms derived from linear wave theory. Wave shoaling and refraction are determined by the method of Noda <u>et al.</u> (1974). The first model,		

DD FORM 1 JAN 73 1473 EDITION OF NOV 65 IS OBSOLETE

Unclassified

SECURITY CLASSIFICATION OF THIS PAGE (When Data Entered)

referred to as linear, neglects the effects of convective acceleration and lateral mixing, and calculates bottom friction using the small mean current assumption. The second, nonlinear model includes the neglected effects, and uses the full bottom stress relation as given by Liu and Dalrymple (1978). Both models solve iteratively for mean currents and mean free surface displacement at discrete grid points.

A calibration of both models is described based on comparison with field data obtained from the NSTS Torrey Pines experiment (Gable, 1979). Finally, various results obtained during previous studies utilizing the models are presented and discussed.

Unclassified

SECURITY CLASSIFICATION OF THIS PAGE(When Data Entered)

PD 118 518

Blank Page

p. ii, vi

p. 28, 44, 76, 110, 117, 120, 122

Jan 11 1982

6 Oct 82

ABSTRACT

The theoretical background and numerical formulation for two finite-difference models for predicting nearshore circulation are reviewed. The models are based on the time- and depth-averaged equations of continuity and momentum, with momentum flux terms derived from linear wave theory. Wave shoaling and refraction are determined by the method of Noda *et al.* (1974). The first model, referred to as linear, neglects the effects of convective acceleration and lateral mixing, and calculates bottom friction using the small mean current assumption. The second, nonlinear model includes the neglected effects, and uses the full bottom stress relation as given by Liu and Dalrymple (1978). Both models solve iteratively for mean currents and mean free surface displacement at discrete grid points.

A calibration of both models is described based on comparison with field data obtained from the NSTS Torrey Pines experiment (Gable, 1979). Finally, various results obtained during previous studies utilizing the models are presented and discussed.

TABLE OF CONTENTS

	<u>Page</u>
Abstract	1
List of Figures	vii
Chapter I. Introduction	1
Chapter II. Theoretical Development of the Models	3
1. Introduction	3
2. Theoretical Framework of the Models	3
2.1 Specification of the Boundary Value Problem . . .	5
2.2 Depth and Time Averaged Forms of the Equations . .	9
2.3 Radiation Stresses	12
2.4 Wind Stress	13
2.5 Bottom Stress	14
2.6 Wave Refraction and Shoaling Including Wave-Current Interaction	15
2.7 Wave Breaking Criteria	19
2.8 Lateral Mixing	20
2.9 Wave Height Decay	22
3. Overview of the Linear and Nonlinear Models	25
Chapter III. Formulation of the Numerical Models	29
1. Introduction	29
2. The Grid Scheme and Location of the Unknown Quantities	30
3. Boundary Conditions	34

	<u>Page</u>
4. Finite Difference Operators and Notation	36
5. Finite Difference Forms of the Governing Equations - Linear Model	37
6. Finite Difference Forms of the Governing Equations - Nonlinear Model	40
7. The Numerical Scheme for Refraction and the Wave Height Field	45
Chapter IV. Calibration of the Nearshore Circulation Models . . .	49
1. Field Data Used for Calibration	49
1.1 Choice of Field Data Used for Calibration	51
2. Calibration of the Models	61
2.1 Linear Model Calibration	63
2.2 Nonlinear Model Calibration	65
2.3 Response of Both Models Using Data Set 2	68
3. Discussion of the Calibrated Coefficients	72
Chapter V. Examples of Numerical Results Using the Nearshore Circulation Models	77
1. Introduction	77
2. Specific Applications of the Linear and Nonlinear Models	77
2.1 Plane Beach Applications	78
2.2 Barred Profile Applications	86
2.3 Applications to the Laboratory Wave Basin	90
2.4 Periodic Bottom Topography	91
2.5 Intersecting Waves Applications	102
Chapter VI. Conclusions	111

	<u>Page</u>
References	115
Appendix I. Using the Nearshore Circulation Program	119
Listing of Linear Model	125
Listing of Nonlinear Model	143

LIST OF FIGURES

<u>Figure No.</u>	<u>Title</u>	<u>Page</u>
2-1	Plan Definition Sketch For Coordinate System	6
2-2	Longuet-Higgins' Analytical Solution for Oblique Wave Attack on a Plane Beach	21
3-1	Grid Scheme	31
3-2	Velocity Components for Grid Block (i,j)	33
3-3	General Leapfrog Solution Scheme	43
4-1	Location of NSTS Torrey Pines Experiment	50
4-2	Instrumentation for NSTS Torrey Pines Experiment	52
4-3	Torrey Pines Nearshore Bathymetry, November 9, 1978	53
4-4	Torrey Pines Nearshore Bathymetry, November 18, 1978	54
4-5	Time Averaged Current Measurements, November 10, 1978	57
4-6	Average Field Velocity Profile, Data Set 1	58
4-7	Angular Distribution of Spectral Density, November 15, 1978	60
4-8	Average Field Velocity Profile, Data Set 2	62
4-9	Currents Induced in Model Using Nov. 9 Bathymetry. Nonlinear Model: Data Set 1	64
4-10	Longshore Average Depth Profile, Torrey Pines, Nov. 9	66
4-11	Variation of Longshore Current with Friction Factor in the Linear Model	67
4-12	Variation of Longshore Current with Lateral Mixing in the Nonlinear Model. $f = 0.015$	69
4-13	Variation of Longshore Current with Lateral Mixing in the Nonlinear Model. $f = 0.010$	70
4-14	Longshore Current in the Linear and Nonlinear Models. Data Set 2	71

<u>Figure No.</u>	<u>Title</u>	<u>Page</u>
4-15	Currents Induced in Model Using Nov. 18 Bathymetry. Nonlinear Model: Data Set 2	73
5-1	Set-up on a Plane Beach	79
5-2	Set-up at Shoreline Due to a Wave Group with a Period of 18 Seconds	81
5-3	Resonance of Wave Channel Due to Forcing at Seiche Period	82
5-4	Inshore Mean Free Surface Displacement Versus Time for the Nonlinear Model Application to a Plane Beach	83
5-5	Longshore Current Profile for Plane Beach. Linear Model	84
5-6	Longshore Current Profile for Plane Beach. Nonlinear Model	85
5-7	Barred and Plane Beach Profiles	87
5-8	Longshore Current Profile for Barred Beach. Linear Model	88
5-9	Longshore Current Profile for Barred Beach. Nonlinear Model	89
5-10	Experimental Streamlines in the Wave Basin (From Dalrymple <u>et al.</u> , 1977)	92
5-11	Currents in Model Basin Corresponding to Dalrymple <u>et al.</u> (1977)	93
5-12	Predicted and Measured Longshore Velocities for the Basin Test Case	94
5-13	Depth Contours for the Periodic Bottom of Noda (1973)	96
5-14	Current Vectors for Noda Topography. Linear Model	97
5-15	Current Vectors for Noda Topography. Nonlinear Model	98
5-16	Currents Induced by Bulge on a Plane Beach. Linear Model	100
5-17	Currents Induced by Bulge on a Plane Beach. Nonlinear Model	101

<u>Figure No.</u>	<u>Title</u>	<u>Page</u>
5-18	Definition Sketch for the Intersecting Wave Application	102
5-19	Current Vector Plot for a Rip Current Perpendicular to the Shoreline	108
5-20	Current Vector Plot for the Meandering Circulation Pattern	109

Chapter I

INTRODUCTION

The need for methods to accurately predict the magnitude and spatial distribution of nearshore currents is central to the present research efforts aimed at quantifying the transport of marine sediment in the beach and near-shore environment. Investigators have made significant strides in describing the mean wave-induced motions in the surf zone in the twenty years since the correct formulation of the averaged equations of motion. Using the concept of wave momentum flux, or radiation stress (see Longuet-Higgins and Stewart, 1964), it has become possible to analytically predict the wave set-up, long-shore currents, and spacing of rip currents on beaches of simple planform. Recent strides have also been made towards predicting the dynamic response of the surf zone to fluctuating driving forces with time scales larger than that of the incident wind waves, such as surf beat (see, for example, Symonds, Huntley, and Bowen, 1982).

In general, however, the nearshore environment is a complex system which is not amenable to analytic treatment. Even in simple situations, the presence of a physical feature predicted by one mechanism, such as the longshore current, will greatly complicate the prediction of a separate feature, such as rip currents. In addition, the action of waves and currents on the bottom can create complex topographies, making a reduction of the analytic problems to one space dimension impossible.

This report represents a review and conclusion of several studies conducted at the University of Delaware with the aim of providing a numerical

model for calculating nearshore wave-induced currents and mean water level fluctuations. The purpose of constructing a numerical model rests on the need to extend our predictive capabilities into situations which lie beyond the scope of analytic methods. In the end, all numerical models, as well as analytic formulations, are limited in scope by the simplifying assumptions incorporated in their theoretical framework; in this regard, the present models represent an attempt to extend present analytic treatments to the case of a complex topography in two dimensions. The models do not consider the associated sediment transport problem, although this capability can be added (see McDougal, 1979, and Paddock and Ditmars, 1981). Also, the models require that the incident wave field be regarded as monochromatic, or, after some model modifications, narrow banded enough to be represented as a modulated wave train at a single carrier frequency.

The models described here utilize a wave refraction scheme developed by Noda et al. (1974). Using this scheme, Birkemeier and Dalrymple (1976) developed a circulation model, referred to here as the linear model, which neglected the effect of convective accelerations and lateral mixing. The model of Ebersole and Dalrymple (1979), referred to here as the nonlinear model, extended the treatment to include these effects.

In Chapter II, the theoretical framework for the two models is described, followed by an outline of the numerical formulations in Chapter III. In Chapter IV, we present a calibration of the models using field data from the NSTS Torrey Pines experiment (Gable, 1979). Chapter V gives a summary of applications of the models presented in Birkemeier and Dalrymple (1976) and Ebersole and Dalrymple (1979).

Chapter II

THEORETICAL DEVELOPMENT OF THE MODELS

1. INTRODUCTION

In this chapter the theoretical framework for the development of time averaged governing equations for the problem of waves and currents in the nearshore zone is outlined. The development of the numerical circulation models in either the "linear" or "nonlinear" form is then described in Chapter III based on the theoretical framework.

In general, the development of each model has been described in previous technical reports; the linear model in Birkemeier and Dalrymple (1976), and the nonlinear model in Ebersole and Dalrymple (1979). For this reason, some of the derivations and intermediate steps needed to develop the governing equations are not described in detail in the present report. The reader can refer to the previous work for missing details. However, both models now include the option of calculating wave energy decay due to interaction with the bottom, which has not been included in previous reports. The theory and implementation of this option is described in detail.

2. THEORETICAL FRAMEWORK FOR THE MODELS

The basis for any fluid dynamic model rests on the principle of conservation of mass, conservation of momentum (the Navier-Stokes equations),

and conservation of energy. The resulting system of equations, together with boundary conditions which quantify the interaction of the fluid continuum with its solid and free bounding surfaces, give a mathematical representation of the physical problem of interest. The problem may then be further simplified by assumptions which are consistent with the physical processes involved.

Here, we are interested in the effect of waves propagating towards shore over a complex bathymetry and breaking, and the mean currents driven by changes in the flux of wave momentum. The problem has two apparent time-scales; a fast time scale associated with the oscillation of the incident waves, and a slower time scale over which the characteristics of the incident wave, such as height and angle of incidence, may vary. The longer time scale may also include the effect of changes in wind, tidal oscillation, and, in models, which include sediment transport, gradual shift of the bottom. Since our attention here is towards mean quantities which are reasonably steady in time, the set of equations may be averaged over the faster time scale of the wave oscillation to remove the direct effect of the oscillation. The effect of the waves then is represented by a stress-like term acting on the slowly varying mean flow pattern. In addition, since we are mainly interested in net transport quantities rather than detailed structure of the velocity profiles over depth, the equations may be averaged over depth, reducing the entire problem to a two dimensional problem in the horizontal plane together with appropriate boundary conditions. This averaged model can then be solved using numerical procedures, as discussed in Chapter III. The quantities to be determined are: the horizontal components of mean wave-induced current,

the local wave height and angle of incidence, and the set-up, or wave-induced deviation of the mean water surface from its still-water level.

2.1 Specification of the Boundary Value Problem

A right-handed coordinate system is defined with x in the offshore direction, normal to the coastline, y in the longshore direction, and z vertically upward (see Figure 1). The continuity equation is

$$\frac{\partial \rho}{\partial t} + \frac{\partial(\rho u)}{\partial x} + \frac{\partial(\rho v)}{\partial y} + \frac{\partial(\rho w)}{\partial z} = 0 \quad (2.1)$$

where ρ is the water density and (u,v,w) are the (x,y,z) components of velocity, respectively. The continuity equation can be further reduced to the form

$$\frac{\partial u}{\partial x} + \frac{\partial v}{\partial y} + \frac{\partial w}{\partial z} = 0 \quad (2.2)$$

consistent with an assumption of constant water density ρ .

The momentum equations are, in the x direction

$$\frac{\partial u}{\partial t} + \frac{\partial u^2}{\partial x} + \frac{\partial uv}{\partial y} + \frac{\partial uw}{\partial z} = -\frac{1}{\rho} \frac{\partial P}{\partial x} + \frac{1}{\rho} \left\{ \frac{\partial \tau_{xx}}{\partial x} + \frac{\partial \tau_{yx}}{\partial y} + \frac{\partial \tau_{zx}}{\partial z} \right\}, \quad (2.3)$$

in the y direction,

$$\frac{\partial v}{\partial t} + \frac{\partial uv}{\partial x} + \frac{\partial v^2}{\partial y} + \frac{\partial vw}{\partial z} = -\frac{1}{\rho} \frac{\partial P}{\partial y} + \frac{1}{\rho} \left\{ \frac{\partial \tau_{xy}}{\partial x} + \frac{\partial \tau_{yy}}{\partial y} + \frac{\partial \tau_{zy}}{\partial z} \right\}, \quad (2.4)$$

and in the z direction,

$$\frac{\partial w}{\partial t} + \frac{\partial uw}{\partial x} + \frac{\partial vw}{\partial y} + \frac{\partial w^2}{\partial z} = -\frac{1}{\rho} \frac{\partial}{\partial z} (P + gz) + \frac{1}{\rho} \left\{ \frac{\partial \tau_{xz}}{\partial x} + \frac{\partial \tau_{yz}}{\partial y} + \frac{\partial \tau_{zz}}{\partial z} \right\}, \quad (2.5)$$

after substitution of the continuity equation into the convective acceleration terms.

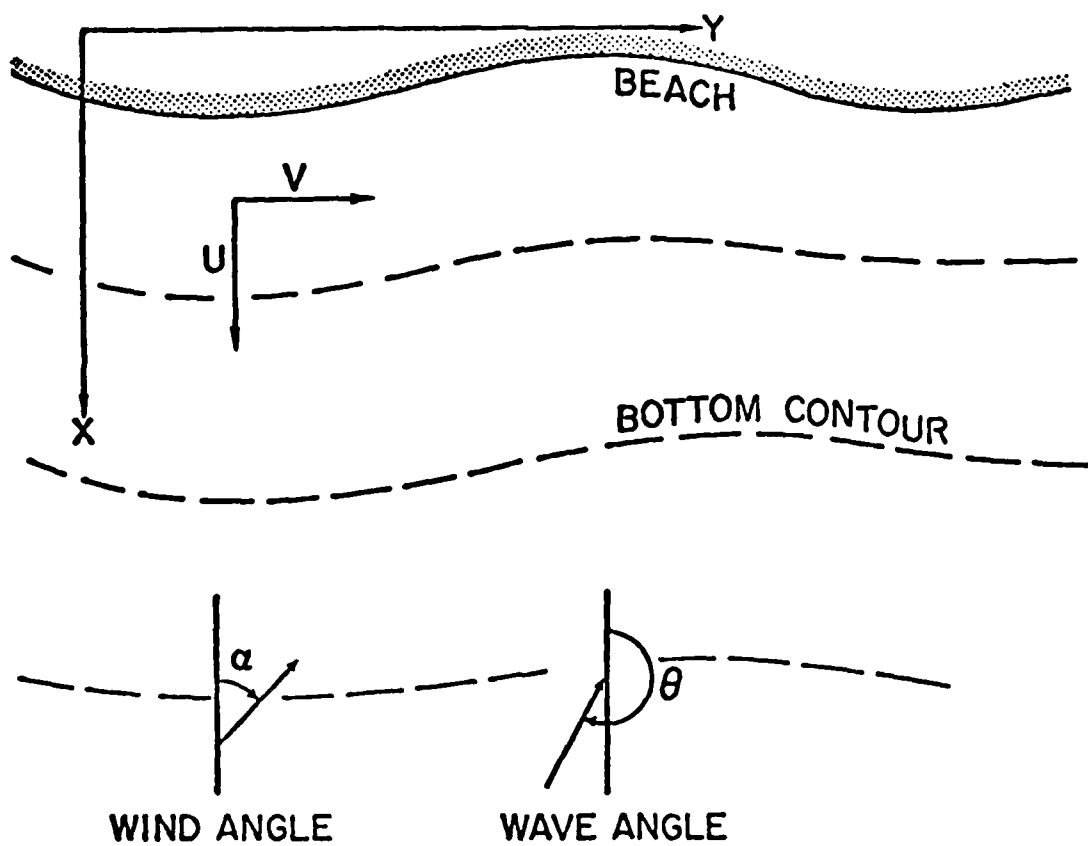


Figure 2-1. Plan Definition Sketch For Coordinate System.

Boundary Conditions

Certain boundary conditions are required at the physical boundary of the water body in question in order to correctly specify the problem. First, kinematic conditions are specified at the free surface and rigid bottom, which state that water particles may not cross the boundary surface, whether it be rigid or moving.

The equation of a surface of the fluid domain is given by

$$F(x,y,z,t) = 0 \quad .$$

A water particle cannot flow across the surface, otherwise the surface would cease to exist. Mathematically, this condition is expressed by the total time rate of change of the function $F(x,y,z,t)$ being equal to zero.

$$\frac{D}{Dt} (F(x,y,z,t)) = 0 \quad .$$

At the free surface the boundary is given by

$$F_1(x,y,z,t) = z - \eta(x,y,t) = 0$$

and at the bottom

$$F_2(x,y,z,t) = z + h(x,y,t) = 0 \quad .$$

Therefore, for the kinematic free surface boundary condition (KFSBC),

$$\frac{\partial F_1}{\partial t} + u \frac{\partial F_1}{\partial x} + v \frac{\partial F_1}{\partial y} + w \frac{\partial F_1}{\partial z} = 0 \quad z = \eta$$

or

$$\frac{\partial \eta}{\partial t} + u_\eta \frac{\partial \eta}{\partial x} + v_\eta \frac{\partial \eta}{\partial y} - w_\eta = 0 \quad . \quad (2.6)$$

For the bottom boundary condition (BBC) we get,

$$\frac{\partial h}{\partial t} + u_{-h} \frac{\partial h}{\partial x} + v_{-h} \frac{\partial h}{\partial y} + w_{-h} = 0 \quad (2.7)$$

where u, v, w are the velocity components in the x, y and z directions and the subscripts denote the evaluation of a specific term at the bottom, $z = -h$, or at the free surface, $z = \eta$.

In addition to the kinematic free surface boundary condition, a dynamic free surface boundary condition is required as well, which states that

$$P = \text{constant} \quad z = \eta$$

This condition is satisfactory if we neglect the local generation of waves by wind or the deformation of the free surface due to barotropic effects. Then, using Bernoulli's equation expanded to the free surface, we obtain

$$-\frac{\partial \phi_{\eta}}{\partial t} + \frac{(u_{\eta}^2 + v_{\eta}^2 + w_{\eta}^2)}{2} + g\eta = 0 \quad z = \eta \quad (2.8)$$

after setting $P = 0$, where $\phi(x, y, z, t)$ is the velocity potential for the wave motion.

The model also requires lateral boundary conditions. In the y (longshore) direction, the bathymetry, given by the surface $h(x, y)$ will be required to be periodic. Since the offshore wave conditions will be assumed uniform, lateral periodicity conditions for wave and currents are also assumed.

Offshore in the x direction, the usual boundary condition for a wave problem would be to assume that all waves at the boundary other than the

incident wave are propagating away from shore, the radiation condition (Sommerfeld (1949)). However, the circulation model does not directly calculate an actual wave field. Rather, a somewhat arbitrary condition,

$$u = 0 \quad ; \quad x = \text{furthest offshore grid}$$

is imposed, which serves to put a bound on the horizontal extent of the flow under consideration.

Specification of an onshore boundary condition is an uncertain task, due to the complexity of the surf zone. In general, it is likely that some wave energy survives the breaking process and reflects from the beach, leading to waves propagated back into the region of the model. However, it is assumed for the purpose of modelling that all wave energy decays in the surf zone, reducing the wave height to a value of zero at the shoreline. In addition, both u and v are set equal to zero at the shoreline.

2.2 Depth and Time Averaged Forms of the Equations

By integrating the equations of motion and continuity over depth and substituting the boundary conditions, the problem is reduced to equations in two horizontal dimensions, with lateral boundary conditions prescribed. Secondly, the quantities of principal interest are average in nature, i.e., mean currents, wave height and wave angle, and mean water level. The equations can then be time averaged over a wave period to remove consideration of instantaneous wave induced motions. The quantities remaining would be free to vary slowly in time in response to changing offshore conditions.

Integrating Eq. (2.2) over depth from $z = -h(x,y,t)$ to $z = \eta(x,y,t)$, using Leibnitz rule (Hildebrand (1976), p. 365) to remove partial derivatives from within the integrals, and substituting Eqs. (2.5) and (2.6), the continuity equation becomes

$$\frac{\partial}{\partial t} \int_{-h}^{\eta} \rho dz + \frac{\partial}{\partial x} \int_{-h}^{\eta} \rho u dz + \frac{\partial}{\partial y} \int_{-h}^{\eta} \rho v dz = 0 \quad (2.9)$$

Let both u and v be comprised of a time independent mean flow and a wave induced flow.

$$\begin{aligned} u &= \bar{U} + \hat{u} \\ v &= \bar{V} + \hat{v} \end{aligned}$$

By substituting the above expressions for u and v into Eq. (2.7) and time averaging over one wave period so as to eliminate the wave induced fluctuations, the continuity equation can be written as

$$\begin{aligned} \frac{\partial}{\partial t} \{ \rho(h + \bar{\eta}) \} + \frac{\partial}{\partial x} \{ \rho \bar{U}(h + \bar{\eta}) \} + \frac{\partial}{\partial x} \overline{\int_{-h}^{\eta} \rho \hat{u} dz} \\ + \frac{\partial}{\partial y} \{ \rho \bar{V}(h + \bar{\eta}) \} + \frac{\partial}{\partial y} \overline{\int_{-h}^{\eta} \rho \hat{v} dz} = 0 \end{aligned} \quad (2.10)$$

where the symbol "—" denotes the time average over one wave period and $\bar{\eta}$ the time independent mean free surface displacement. Note that the time averages of the vertically integrated wave induced velocities \hat{u} and \hat{v} are not zero.

$$\begin{aligned} \text{Defining} \quad U &\equiv \bar{U} + \bar{\hat{u}} \\ V &\equiv \bar{V} + \bar{\hat{v}} \end{aligned}$$

where $\bar{u} = \frac{\int_{-h}^{\bar{\eta}} \rho \bar{u} dz}{\rho (h + \bar{\eta})}$ and $\bar{v} = \frac{\int_{-h}^{\bar{\eta}} \rho \bar{v} dz}{\rho (h + \bar{\eta})}$

are the wave induced mass transport velocities, and substituting the total depth D for $(h + \bar{\eta})$, the time averaged, depth integrated continuity equation is, in its final form

$$\frac{\partial \bar{\eta}}{\partial t} + \frac{\partial}{\partial x} (UD) + \frac{\partial}{\partial y} (VD) = 0 \quad (2.11)$$

Inherent in the derivation are the assumptions that the bottom is constant with time and the density is constant in space and time.

Momentum Equations

The x and y momentum equations are manipulated in the same way as the continuity equation in order to achieve equations which are independent of wave induced oscillations, i.e., they are integrated over depth and time averaged over a wave period. Details of this derivation may be found in Ebersole and Dalrymple (1979). The resulting equations are equivalent to those given by Phillips (1977), but are written explicitly in terms of depth averaged mean velocities. The equations contain terms for mean bottom shear stress, mean surface shear stress due to wind, mean lateral friction (not used in the linear model), and excess mean momentum stress due to wave action (the radiation stress, see Longuet-Higgins and Stewart (1964)). The x momentum equation in its final form can be written as,

$$\begin{aligned} \frac{\partial}{\partial t} (UD) + \frac{\partial}{\partial x} (U^2 D) + \frac{\partial}{\partial y} (UVD) = -gD \frac{\partial \bar{\eta}}{\partial x} - \frac{D}{\rho} \frac{\partial \bar{\tau}_\ell}{\partial y} \\ - \frac{1}{\rho} \frac{\partial S_{xx}}{\partial x} - \frac{1}{\rho} \frac{\partial S_{xy}}{\partial y} + \frac{1}{\rho} \bar{\tau}_{sx} - \frac{1}{\rho} \bar{\tau}_{bx} \end{aligned} \quad (2.12)$$

and the final form of the y momentum equation can be written as

$$\begin{aligned} \frac{\partial}{\partial t} (VD) + \frac{\partial}{\partial x} (UVD) + \frac{\partial}{\partial y} (V^2D) = -gD \frac{\partial \bar{\eta}}{\partial y} - \frac{D}{\rho} \frac{\partial \bar{\tau}_x}{\partial x} \\ - \frac{1}{\rho} \frac{\partial S_{xy}}{\partial x} - \frac{1}{\rho} \frac{\partial S_{yy}}{\partial y} + \frac{1}{\rho} \bar{\tau}_{sy} - \frac{1}{\rho} \bar{\tau}_{by} \end{aligned} \quad (2.13)$$

Wave Energy Equation

Following Phillips (1977), an equation expressing the conservation of averaged wave energy may be written as

$$\begin{aligned} \frac{\partial E}{\partial t} + \frac{\partial}{\partial x} \{E(U + C_g \cos \theta)\} + \frac{\partial}{\partial y} \{E(V + C_g \sin \theta)\} \\ + S_{xx} \frac{\partial U}{\partial x} + S_{xy} \left(\frac{\partial V}{\partial x} + \frac{\partial U}{\partial y} \right) + S_{yy} \frac{\partial V}{\partial y} = \epsilon \end{aligned} \quad (2.14)$$

Here, C_g is the wave group velocity and θ is the local wave angle. The quantity ϵ represents the dissipation of wave energy, and is identically zero in a conservative wave field. It can be given a non-zero value to include the effect of wave damping, as described below.

2.3 Radiation Stresses

The radiation stresses included in Eqs. (2.12), (2.13) and (2.14) represent the stress on the water column induced by wave action. Neglecting the effects of small scale turbulent velocities, the stresses have been given in simple form by Longuet-Higgins and Stewart (1964) as

$$S_{xx} = E [(2n - 1/2)\cos^2 \theta + (n - 1/2)\sin^2 \theta] \quad (2.15)$$

$$S_{yy} = E [(2n - 1/2)\sin^2\theta + (n - 1/2)\cos^2\theta] \quad (2.16)$$

$$S_{xy} = S_{yx} = \frac{E}{2} n \sin (2\theta) \quad (2.17)$$

where E is the wave energy, θ is the wave angle, and n = ratio of group velocity (C_g), to wave celerity (C). To second order for a progressive small amplitude wave, E and n are given by

$$E = \frac{1}{8} \rho g H^2 \quad (2.18)$$

$$n = \frac{C_g}{C} = \frac{1}{2} \left[1 + \frac{2kh}{\sinh(2kh)} \right] \quad (2.19)$$

k = wave number ($= \frac{2\pi}{L}$)

h = depth

L = wave length

H = wave height.

2.4 Wind Stress

Although other methods exist for computing the surface stress due to the wind (see Wu (1968)), the one suggested in the Shore Protection Manual (1977) has been utilized. This form was first developed by Van Dorn (1953) and gives a fairly good fit to the existing experimental data. The form of the surface stress is quadratic in the wind speed and is given by

$$\overline{\tau}_{sx} = \rho K |W| W_x \quad (2.20)$$

$$\overline{\tau}_{sy} = \rho K |W| W_y \quad (2.21)$$

where W is the wind speed, and W_x , W_y are wind velocity components in the x and y directions, as determined by the wind angle, α .

The wind stress coefficient K is determined empirically to be dependent on the magnitude of the wind velocity such that

$$K = \begin{cases} K_1 & W \leq W_{cr} \\ K_1 + K_2 (1 + W_{cr}/W)^2 & W > W_{cr} \end{cases} \quad (2.22)$$

and $K_1 = 1.1 \times 10^{-6}$; $K_2 = 2.5 \times 10^{-6}$

$$W_{cr} = 7.2 \text{ meters/second}$$

A comparison of the wind stress coefficient given here with experimental data is given in Pearce (1972).

2.5 Bottom Stress

The correct method for specifying the effect of a rigid bottom on waves and currents is still a matter of lively debate. For the purpose of modelling hydrodynamics in the nearshore zone, the average bottom shear stress, τ_b , is generally taken to be of the form

$$\overline{\tau_b} = \rho \frac{f}{8} \overline{u_b |u_b|} \quad (2.23)$$

where f is a Darcy-Weisbach friction factor and u_b is the total instantaneous scalar velocity at the bottom (Longuet-Higgins (1970a)). This relation is known as a quadratic friction law. The components of shear stress in the x and y directions can be given quite generally by (Liu and Dalrymple (1978))

$$\overline{\tau_{bx}} = \frac{\rho f}{16\pi} \int_0^{2\pi} (U + u_m \cos \theta \cos \sigma t) \cdot |\vec{u}_b| d(\sigma t) \quad (2.24)$$

$$\overline{\tau_{by}} = \frac{\rho f}{16\pi} \int_0^{2\pi} (V + u_m \sin \theta \cos \sigma t) \cdot |\vec{u}_b| d(\sigma t) \quad (2.25)$$

where u_m is the maximum wave orbital velocity given by

$$u_m = \frac{gH}{2 \sinh kh} \quad (2.26)$$

and \vec{u}_b is the vector velocity at the bottom. The nonlinear model of Ebersole and Dalrymple (1979) retains these forms, where the integration is approximated by a 16 term Simpson's rule summation.

The linear model retains the form originally used by Birkemeier and Dalrymple (1976). For this form, the assumption that friction is primarily due to the influence of the wave orbital velocity is used. Making a small mean-current assumption, LeBlond and Tang (1974) show that the bottom stress is anisotropic, with

$$\overline{\tau_{bx}} = \frac{\rho f}{2\pi} u_m U \quad (2.27)$$

$$\overline{\tau_{by}} = \frac{\rho f}{4\pi} u_m V \quad , \quad (2.28)$$

with U , V , u_m , and f as previously defined. A derivation of these equations is given in Birkemeier and Dalrymple (1976), Appendix A.

2.6 Wave Refraction and Shoaling Including Wave-Current Interaction

The equations which govern both wave refraction and shoaling as a result of wave-current interaction used in the model are those of Noda et al. (1974). The advantage of Noda's method is that it can predict the wave angles and wave heights at certain points rather than along a wave ray. This procedure lends itself well to use in the finite difference model because calculations are performed at points which lie in the center of rectangular grid elements which are part of a larger grid mesh.

Starting with a progressive linear gravity wave, the free surface can be written as,

$$\eta(x,y,t) = a(x,y,t)\cos\{\phi(x,y,t)\}$$

where a is the wave amplitude and ϕ is a phase function. A wave number vector can be defined as

$$\vec{k} = \nabla\phi \quad (2.29)$$

and a wave scalar frequency can be defined as

$$\bar{\sigma} = - \frac{\partial\phi}{\partial t} \quad (2.30)$$

Using the mathematical property that the curl of a gradient is identically zero, it is shown that

$$\nabla \times \nabla\phi = 0$$

which implies that

$$\nabla \times \vec{k} = 0$$

This equality states that the wave number vector is irrotational. Assuming $\phi(x,y,t)$ is continuous, then

$$\frac{\partial}{\partial t} (\nabla\phi) = \nabla \frac{\partial\phi}{\partial t} \quad .$$

On substituting Eqs. (2.29) and (2.30) into the above expression, it is found that

$$\frac{\partial\vec{k}}{\partial t} + \nabla\bar{\sigma} = 0 \quad (2.31)$$

which is the classical conservation of waves equation.

For the case of a wave propagating on a current with velocity $\vec{u} = u\vec{i} + v\vec{j}$, it can be shown that the scalar frequency with respect to a stationary reference frame is

$$\sigma = \omega + \vec{k} \cdot \vec{U} \quad .$$

The wave frequency with respect to a moving reference frame is given by the dispersion relation,

$$\sigma^2 = gk \tanh kh \quad . \quad (2.32)$$

If it is also assumed that the wave number field is constant in time then, from Eq. (2.31),

$$\nabla(\sigma + \vec{k} \cdot \vec{U}) = 0$$

or

$$\sigma + \vec{k} \cdot \vec{U} = \text{constant} \quad . \quad (2.33)$$

This constant can be evaluated for the case where $\vec{U} = 0$ in which case $\sigma = \frac{2\pi}{T}$ where T is the wave period. Eq. (2.33) then becomes

$$\sigma + \vec{k} \cdot \vec{U} = \frac{2\pi}{T} \quad . \quad (2.34)$$

Using the coordinate system shown in Figure 1 and expanding Eqs. (2.29) and (2.34) into Cartesian coordinates and using the dispersion relation, the equations which govern wave refraction through wave-current interaction are given by

$$\cos \theta \left\{ \frac{\partial \theta}{\partial x} - \frac{1}{k} \frac{\partial k}{\partial y} \right\} + \sin \theta \left\{ \frac{\partial \theta}{\partial y} + \frac{1}{k} \frac{\partial k}{\partial x} \right\} = 0 \quad (2.35)$$

$$\{gk \tanh(kh)\}^{1/2} + Uk \cos \theta + Vk \sin \theta = \frac{2\pi}{T} \quad (2.36)$$

where θ , k , h , U and V are all functions that may vary in both the x and y directions.

The shoaling of waves is also affected by the interaction of waves and currents. The effect on the waves is determined by solving the energy equation. Dividing Eq. (2.14) by E and expanding in Cartesian coordinates, we get

$$\begin{aligned} & \frac{1}{E} \frac{\partial E}{\partial t} + (U + C_g \cos \theta) \frac{1}{E} \frac{\partial E}{\partial x} + (V + C_g \sin \theta) \frac{1}{E} \frac{\partial E}{\partial y} \\ & + \frac{\partial}{\partial x} (U + C_g \cos \theta) + \frac{\partial}{\partial y} (V + C_g \sin \theta) \\ & + \frac{1}{E} \{S_{xx} \frac{\partial U}{\partial x} + S_{xy} \frac{\partial U}{\partial y} + S_{yy} \frac{\partial V}{\partial y} + S_{xy} \frac{\partial V}{\partial x}\} = \frac{\epsilon}{E} \end{aligned}$$

Using this result, carrying out the differentiation, and letting a quantity Q be defined as

$$Q = \frac{1}{E} \{S_{xx} \frac{\partial U}{\partial x} + S_{xy} \frac{\partial U}{\partial y} + S_{xy} \frac{\partial V}{\partial x} + S_{yy} \frac{\partial V}{\partial y}\}$$

the energy equation becomes,

$$\begin{aligned} & \frac{2}{H} \frac{\partial H}{\partial t} + (U + C_g \cos \theta) \frac{2}{H} \frac{\partial H}{\partial x} + (V + C_g \sin \theta) \frac{2}{H} \frac{\partial H}{\partial y} + \frac{\partial U}{\partial x} + \frac{\partial V}{\partial y} \\ & - C_g \sin \theta \frac{\partial \theta}{\partial x} + \cos \theta \frac{\partial C_g}{\partial x} + C_g \cos \theta \frac{\partial \theta}{\partial y} + \sin \theta \frac{\partial C_g}{\partial y} + Q = \frac{\epsilon}{E} \end{aligned} \quad (2.37)$$

For all applications of the model the wave height H is assumed constant in time, so $\frac{\partial H}{\partial t} = 0$. From linear wave theory the group velocity C_g is given by

$$C_g = \frac{C}{2} \left\{ 1 + \frac{2kh}{\sinh(2kh)} \right\}$$

where

$$C = \left\{ \frac{g}{k} \tanh(kh) \right\}^{1/2}$$

is the wave speed or celerity, k is the wave number, and h is the water depth.

2.7 Wave Breaking Criteria

Since Eq. (2.37) is applicable only in determining the wave heights of nonbreaking waves, some method is needed to determine the point of breaking and the wave heights after breaking. Though a number of formulas for doing this have been developed, there is not as yet one which is universally applicable or accepted. The choice of a breaking criteria, although somewhat arbitrary, must be made with care since it determines the width of the surf zone and thus controls the set-up. The simplest breaking criteria is that predicted by solitary wave theory.

$$\left(\frac{H}{D} \right)_b = \text{constant} = .78 \quad (2.38)$$

where the subscript, b , denotes the value at breaking. There is, however, considerable evidence (Weggel, 1972) that this is an oversimplification.

Noda et al. (1974) used a modified version of the Miche formula

$$\left(\frac{H}{L} \right)_b = .12 \tanh \left(\frac{D}{L} \right)_b \quad (2.39)$$

both to predict the point of breaking and the decay of the wave after breaking. This was done by calculating both a wave height from Eq. (2.37) and a breaking height from Eq. (2.39). When the point was reached where the wave height was

equal to or greater than the breaking height, the wave was considered to have broken and the wave height from Eq. (2.39) was used. Eq. (2.39) is used in both models to determine broken wave heights.

2.8 Lateral Mixing

The non-linear model of Ebersole and Dalrymple (1979) includes the effect of the lateral shear stress terms

$$\frac{-D}{\rho} \frac{\partial \overline{\tau}_x}{\partial y}, \quad \frac{-D}{\rho} \frac{\partial \overline{\tau}_y}{\partial x}$$

in the x and y momentum equations (2.12) and (2.13) respectively. The need for these terms is pointed out by Longuet-Higgins (1970a) in his treatment of the longshore currents due to obliquely incident waves on a plane beach. Neglecting the effects of lateral shear stresses led to prediction of a longshore current distribution with a discontinuity at the breaker line and no current outside the surf zone. However, physical observation in both the laboratory and field indicate that mean longshore flows are present beyond the breaker line. Longuet-Higgins (1970b) presented a formulation which included the effect of lateral mixing as the means for handling the effect of lateral shear; the shear stresses are thus based on turbulent Reynolds stresses proportional to the local gradient of the mean velocity. The resulting velocity distributions have no discontinuity at the breaker line, and the peak velocities are shifted shoreward of the breaker line. Figure 2-2 shows a comparison of a theoretical velocity profile to one without lateral mixing included.

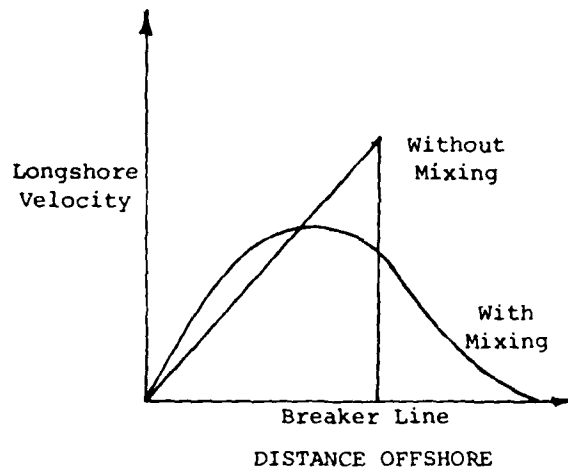


Figure 2-2 Longuet-Higgins' Analytical Solution for Oblique Wave Attack on a Plane Beach

Following the derivation of Longuet-Higgins (1970b), the lateral shear stress is written as

$$\tau_l = -\rho \left(c_y \frac{\partial U}{\partial y} + \epsilon_x \frac{\partial V}{\partial x} \right) \quad (2.40)$$

Longuet-Higgins argued that the mixing coefficient ϵ_x must tend to zero as the shoreline was approached since the turbulent eddies responsible for mixing cannot be of a scale greater than the distance to shore. He assumed that ϵ_x is proportional to the distance offshore, x , multiplied by some velocity scale which he chose to be \sqrt{gh} , the speed of a wave in shallow water where h is the local water depth. Therefore, ϵ_x can be written as

$$\epsilon_x = Nx \sqrt{gh}$$

where N is a dimensionless constant whose limits Longuet-Higgins gave as

$$0 \leq N \leq 0.016$$

In this model the coefficient, ϵ_x , was allowed to vary linearly with x to some value around the breaker line. From this point seaward the coefficient remained at this constant value. The reason for this approximation is that physically there must be some limit on the scale of these eddies. This limit is at present not known. The coefficient, ϵ_y , was chosen to be constant. The values of N and ϵ_y are chosen during the calibration of the model.

2.9 Wave Height Decay

In all applications of the circulation model to date, calculation of wave parameters has been confined to a region within several wavelengths of the shore. Over this distance, wave energy decay due to interaction with the bottom is not likely to be significant, except possibly in the case of waves propagating over a soft mud bottom (Dalrymple and Liu (1978)), which is not treated here. However, the circulation model could reasonably be used to model propagation over much longer offshore extents of shallow coastal waters. At some point, the accumulated effects of bottom interaction would result in wave height reductions of a significant degree. In order to accurately model the amount of wave energy available for driving currents and maintaining mean water level variations, it is necessary to include the effects of various dissipation mechanisms in the equation for calculating wave height (2.37).

Ebersole and Dalrymple (1979) included in the nonlinear computer model, but did not describe, the option to calculate wave energy dissipation due to viscous shear in the bottom boundary layer, and due to the effect of "pumping" of water through the permeable sand bottom due to wave induced pressure

gradients at the water-bottom interface. At present, the option of calculating wave energy decay due to both mechanisms is included in both the linear and nonlinear model.

The application of wave damping to the nearshore circulation model has been described by McDougal (1979), who included the energy dissipation rate ϵ in Eq. (2.14) in a sediment transport model based on the linear wave-current interaction model. The derivation of ϵ is based on Liu (1973). Let ϵ be given by

$$\epsilon = \epsilon_p + \epsilon_f \quad (2.41)$$

where ϵ_p is the dissipation rate due to the permeability of the bottom, and ϵ_f is the dissipation rate due to bottom friction. The two effects are treated separately.

Liu (1973) solved the linear problem for waves over a porous bed of infinite depth. If the wave amplitude $a(x,y,t) = \frac{H}{2}(x,y,t)$ is assumed to be a slowly varying function of the form

$$a(x,y,t) = a_0 e^{-\alpha t} \quad ,$$

Liu's solution leads to the following form for α ;

$$\alpha = \frac{kg}{2 \left| \cosh kh + \left(\frac{\sigma}{Q} \right) \sinh kh \right|^2} \left(\frac{\nu}{K_p} \frac{1}{|Q|^2} + \sqrt{\frac{\nu}{2\sigma}} \frac{k}{\sigma} \left| \frac{i\sigma}{Q} - 1 \right|^2 \right) \quad (2.42)$$

where Q is given by

$$Q = \frac{i\sigma}{p_0} - \frac{\nu}{K_p} \quad (2.43)$$

and

$$K_p = \text{bed permeability} \approx 10^{-10} \text{ M}^2$$

$$P_o = \text{bed porosity} \approx 0.6$$

$$\nu = \text{kinematic viscosity} \approx$$

For these values of K_p , P_o , and ν , the viscosity term in Q is dominant, and α may be reduced to the form

$$\alpha = \frac{gk}{2 \cosh^2 kh} \frac{K_p}{\nu} \quad (2.44)$$

The dissipation rate α is related to ϵ_p by

$$\epsilon_p \approx \frac{\partial E}{\partial t} = -2\alpha E$$

giving

$$\epsilon_p = - \frac{gkE}{\cosh^2 kh} \frac{K_p}{\nu} \quad (2.45)$$

The rate of energy dissipation due to bottom friction, ϵ_f , is given by

$$\epsilon_f = \overline{(\vec{\tau}_b \cdot \vec{U})} A_b \quad (2.46)$$

where A_b is the bed surface area.

Substituting for $\vec{\tau}_b$ and \vec{U} using results derived in the absence of a mean current, we obtain the form

$$\epsilon_f = - \frac{\rho f}{6\pi} (u_m)^3$$

where u_m is the maximum wave induced velocity at the bottom, given by (2.26).

After some manipulation, we obtain the form

$$\epsilon_f = - \frac{k}{6\pi} \frac{\sigma f H}{(\cosh^3 kh - \cosh kh)} \cdot E \quad (2.47)$$

The total energy dissipation including the effects of the porous bottom and friction is given by

$$\begin{aligned} \epsilon &= \epsilon_p + \epsilon_f \\ &= - \left\{ \frac{g k}{\cosh^2 kh} \frac{K_p}{v} + \frac{\sigma k f H}{6\pi (\cosh^3 kh - \cosh kh)} \right\} \cdot E \end{aligned} \quad (2.48)$$

The option of including these effects is available in both forms of the numerical model presented here.

3. AN OVERVIEW OF THE LINEAR AND NONLINEAR MODELS

While both of the numerical models described in Chapter III are based on the theory outlined in the previous section, each model contains a somewhat different subset of the overall development. In this section, we review the differences and similarities between the models before going on to their numerical formulation.

The intent of both of the models is to solve for the mean values U , V , and $\bar{\eta}$ at each grid point by solving the time and depth averaged equations of continuity (2.11) and momentum (2.12-13). Each model utilizes the refraction scheme of Noda et al. (1974), as represented by (2.35-37), to solve for wave angle and wave height. The model of Birkemeier and Dalrymple (1976) treats linearized forms of Eqs. (2.12-13), obtained by dropping the convective acceleration terms

$$\frac{\partial}{\partial x} (U^2 D) \quad ; \quad \frac{\partial}{\partial y} (U V D)$$

from the x-momentum equation, and the terms

$$\frac{\partial}{\partial x} (U V D) \quad ; \quad \frac{\partial}{\partial y} (V^2 D)$$

from the y-momentum equation. The model of Ebersole and Dalrymple (1979) retains the full nonlinear form of the momentum equations, leading to the principle theoretical difference between the models as well as explaining the distinction expressed by their names. The mathematical differences in the governing equations also lead to the requirement of significantly different numerical schemes, discussed in Chapter III.

The momentum equations contain various forcing terms which are formulated as stresses or stress gradients; these include radiation, surface and bottom stresses and a lateral stress representing the effect of turbulent mixing. The models treat radiation stresses and surface wind stresses identically. The linear model treats bottom stress according to a "weak current" formulation developed by LeBlond and Tang (1974), based on the assumption that the stress develops principally in response to the wave orbital motion. The nonlinear model uses a more exact bottom stress formulation, making no assumption as to the relative magnitude of wave orbital and mean current velocities. This distinction between the models is more historical than essential; the linear model can be updated to include the more exact relation given by Eqs. (2.24) and (2.25). This modification has been used by Allender et al. (1981) in a version of the linear model described here. A further possibility would be to represent the bottom friction using a "large-current"

formulation developed by Liu and Dalrymple (1978); this extension has not been investigated.

The remaining distinction between the models stems from the neglect of the "lateral mixing" terms Eqs. (2.12-13)

$$\frac{-D}{\rho} \frac{\overline{\gamma_1 \ell}}{\gamma_Y} \quad ; \quad \frac{-D}{\rho} \frac{\overline{\gamma_1 \ell}}{\gamma_X}$$

in the linear model, and their inclusion in the nonlinear model. This difference is again historical rather than essential; these terms could be included in a modified version of the linear model, although their inclusion would require more effort than the bottom friction modification discussed above. No investigation of the effect of including lateral mixing in the linear model has been made to date.

Chapter III

FORMULATION OF THE NUMERICAL MODELS

1. INTRODUCTION

In the previous chapter a mathematical formulation of the governing equations and associated boundary conditions for the problem of nearshore wave-induced circulation has been outlined. In this chapter, the numerical formulations of the mathematical model are reviewed, corresponding to the work of Birkemeier and Dalrymple (1976) and Ebersole and Dalrymple (1979).

The two models reviewed shall be referred to as the "linear model" and the "nonlinear model." The models contain significant differences as well as significant similarities in their numerical formulation as well as in their underlying mathematical formulation. Differences in the models will be discussed below following a review of the overall structure common to both models.

Both models reviewed here are finite-difference approximations to a set of three first order hyperbolic differential equations consisting of the continuity equation (2.11) and the x and y direction momentum equations (2.12, 2.13), with associated unknowns $U(x,y,t)$, $V(x,y,t)$ and $\bar{\eta}(x,y,t)$. The quantities of wave height $H(x,y,t)$ and wave angle $\theta(x,y,t)$ are solved for using the refraction scheme Eq. (2.35) and the wave energy equation (2.37). The models as developed contain the flexibility to handle unsteady response to

time varying incident wave conditions; however, we will be concerned exclusively with representing the response to a constant wave climate. In this guise, the models represent iterative schemes to determine the response to a steady state exciting force, and updated unknowns may be regarded as iterated values rather than advanced-in-time values.

Listings of the computer programs for the linear and nonlinear models are given in Appendix I together with some notes on running the programs.

2. THE GRID SCHEME AND LOCATION OF THE UNKNOWN QUANTITIES

The first step in constructing a finite difference model lies in choosing a network of discrete grids overlaying the physical domain of interest. The grid used by the present models is that of Noda et al. (1974), as illustrated in Figure 3-1. The physical domain is divided into regular grids of longshore extent Δy and offshore extent Δx . The topography is assumed to be periodic in the longshore y direction with a length λ given by

$$\lambda = (N - 1) \cdot \Delta y$$

Various requirements affecting the choice of grid are:

1. The grid must extend offshore far enough to remove the offshore region of the domain from the influence of currents driven by the surf zone, and to allow for the specification of a uniform longshore depth which will not significantly alter the wave refraction results in the nearshore.
2. The grid mesh must be fine enough to resolve the surf zone in a reasonable manner.

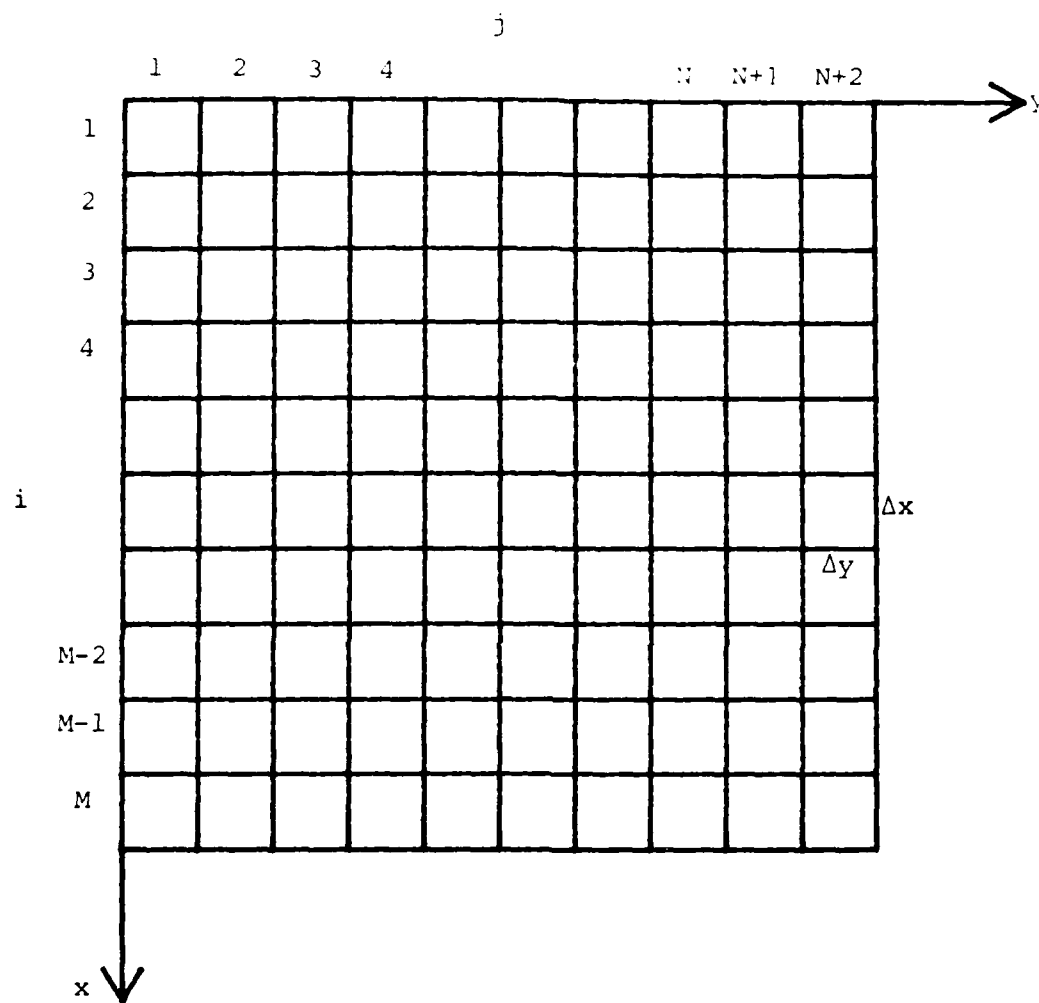


Figure 3-1. Grid Scheme [After Noda et. al. (1974)]

3. In the event that a single physical feature isolated in the longshore direction is to be modelled, the longshore extent of the grid must be sufficiently large to isolate the physical system from the effect of images created by the longshore periodicity requirement.

In the event that large, non-periodic physical features creating significant current patterns seaward of the breaker line are present, requirements (1) and (3) lead to the choice of a large grid, whereas requirement (2) can lead to choice of quite small offshore grid spacings on steep beaches. The resulting grid will often contain a large number of elements, leading to the requirement of large amounts of computer time to solve the complex set of governing equations.

The fixed and variable quantities are defined in relation to the grid structure as shown in Figure 3-2. The quantity $A_{i,j}$ is defined at the grid center and represents any of the set of quantities

$$A_{i,j} = \{H, \theta, k, \bar{\eta}, S, D, \tau_b, \tau_s\}_{i,j} \quad (3.1)$$

Velocities U and V are given at grid sides. This formulation relates naturally to the conservation law scheme of relating changes of a quantity in a bounded region to the fluxes of that quantity across the bounding surface, and is therefore physically correct in an heuristic sense, as well as possessing whatever degree of numerical accuracy consistent with the chosen difference schemes.

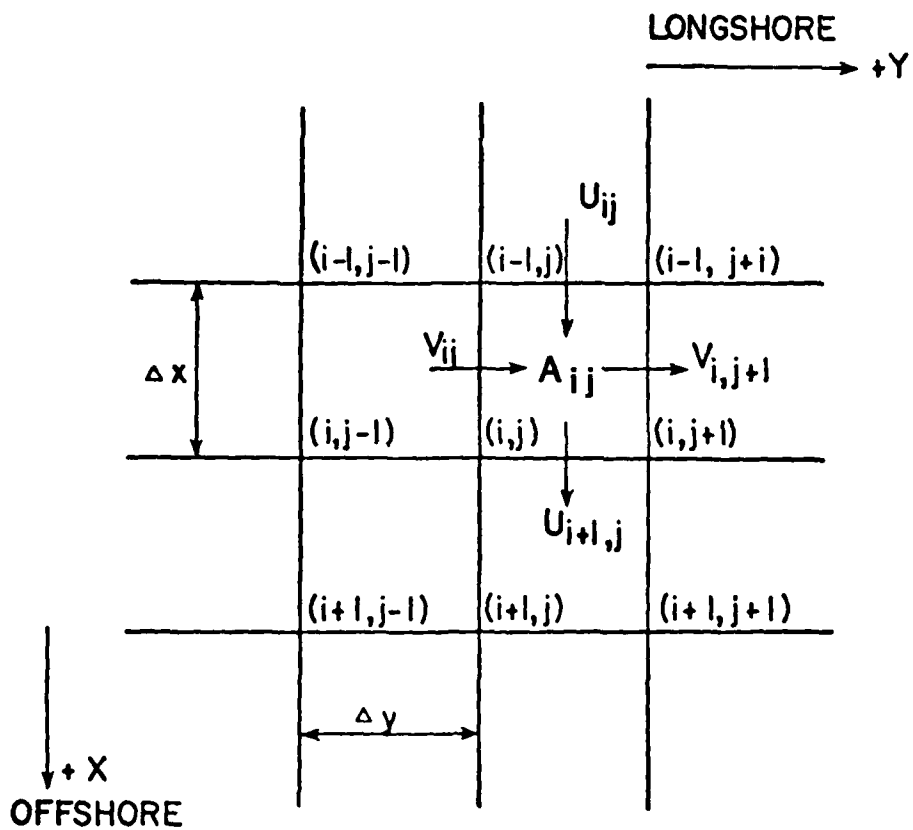


Figure 3-2. Velocity Components for Grid Block (i,j) . All Other Variables (D , S_{xx} , S_{xy} , H , etc.) Are Determined at Grid Center.

3. BOUNDARY CONDITIONS

In order to formulate the numerical models, a scheme was established which incorporated the lateral periodicity requirements mentioned above and the no-flow requirements at the shore and the offshore grid row, as mentioned in Chapter II.

The user defined depth grid is established for the M by N portion of the total grid shown in Figure 3.1, with the requirement that

$$D_{i,N} = D_{i,1} \quad (3.2)$$

to satisfy the periodicity requirement. The grid N then extended to the N + 1 and the N + 2 columns according to

$$D_{i,N+1} = D_{i,2} \quad (3.3)$$

$$D_{i,N+2} = D_{i,3} \quad .$$

Similar periodicity requirements are met by all calculated quantities (the A_{ij} in Eq. (3.1)). The models calculate values of the A_{ij} quantities from the j = 2 row to the j = N row. Periodicity is then established by setting

$$A_{i,1} = A_{i,N}$$

$$A_{i,N+1} = A_{i,2} \quad (3.4)$$

$$A_{i,N+2} = A_{i,3}$$

The velocities U and V are treated somewhat differently in that the calculations

are performed from the $j = 3$ to the $j = N+1$ grid rows, with periodicity established accordingly.

At the offshore grid row ($i = M$), a no-flow condition is applied for U and V . This condition serves to bound the calculated velocities during initial start-up of the model; however, the condition is artificial in that the offshore side of the modelled area becomes a solid vertical boundary. This treatment leads to potential seiching in the model. The presence of a seiching mode in the model calculations has been discussed thoroughly by Birkemeier and Dalrymple (1971) and Ebersole and Dalrymple (1979), who have shown that the period of seiching can be accurately predicted by the shallow water formulas for known topographies. For example, for a basin of triangular cross-section, Wilson (1966) predicts the period of the first mode oscillation by

$$T = \frac{3.28L}{\sqrt{gh_{\max}}} \quad (3.5)$$

where

- T = period of oscillation in the basin
- L = length of the basin = $(M - 1) \cdot \Delta x$
- h_{\max} = maximum still water depth in the basin.

Similarly, a no flow condition for the shore-normal velocity U is applied at the onshore grid row, whose position remains fixed during a model run. The linear model originally described by Birkemeier and Dalrymple (1976) included a provision for flooding shoreward dry grids in order to model the effect of wave set-up; model results have been seen to be somewhat insensitive to the correction provided by this provision. Flooding is not included in the nonlinear model of Ebersole and Dalrymple or in the present version of the linear model.

In addition to the lateral boundary conditions, the system of hyperbolic equations requires initial conditions for a complete solution. The models are started from a state of rest with no wave field present. In order to reduce the effect of seiching, the wave height H at the offshore grid is brought up to its full value gradually according to

$$H = H_0 \tanh \left(\frac{2t}{T} \right) , \quad (3.6)$$

where

t = model time

T = arbitrary fixed time period.

Wave height is typically allowed to build up for 400 model iterations. It is also noted that, in principal, the seiching effect could be removed by setting $\bar{\eta}$ to zero at the offshore boundary, rather than U .

4. FINITE DIFFERENCE OPERATORS AND NOTATIONS

The derivations of the numerical models given by Birkemeier and Dalrymple (1976) and Ebersole and Dalrymple (1979) differ significantly in notation. For this reason, a standardized notation is presented here. We retain as far as possible the terminology of Ebersole and Dalrymple (1979) in describing both the linear and nonlinear models.

The numerical formulations require both averaging and differencing operations. Let $F(x,y,t)$ be an arbitrary function varying in space and time. The average of the function over one grid spacing is given by

$$\overline{F(x,y,t)}^x \equiv \frac{1}{2} \{ F(x + \frac{\Delta x}{2}, y, t) + F(x - \frac{\Delta x}{2}, y, t) \} \quad (3.7)$$

for an average in the x -direction. Successive averaging is given by

$$\overline{F(x,y,t)}^{xy} \equiv \overline{F(x,y,t)}^x{}^y \quad (3.8)$$

First derivatives can be given in terms of forward and backward differences over a single grid space, or as central differences over two grid spaces. We define the forward and backward difference operators, respectively, as

$$\delta_x\{F(x,y,t)\} = \frac{1}{\Delta x} \{F(x + \Delta x, y, t) - F(x, y, t)\} \quad (3.9)$$

$$\delta_{-x}\{F(x,y,t)\} = \frac{1}{\Delta x} \{F(x, y, t) - F(x - \Delta x, y, t)\} \quad (3.10)$$

and the central difference operator as

$$\delta_{\hat{x}}\{F(x,y,t)\} = \frac{1}{2\Delta x} \{F(x + \Delta x, y, t) - F(x - \Delta x, y, t)\} \quad (3.11)$$

We also define an auxiliary operator which represents the central difference at a grid center based on values at the grid sides

$$\delta_{\tilde{x}}\{F(x,y,t)\} = \frac{1}{\Delta x} \{F(x + \frac{\Delta x}{2}, y, t) - F(x - \frac{\Delta x}{2}, y, t)\} \quad (3.12)$$

It is easily shown by direct substitution that the $\delta_{\tilde{x}}$ operator is related to $\delta_{\hat{x}}$ through the relation

$$\delta_{\tilde{x}}\{\overline{F(x,y,t)}^x\} = \delta_{\hat{x}}\{F(x,y,t)\} \quad (3.13)$$

The nonlinear model makes extensive use of the $\delta_{\tilde{x}}$ operator, while the linear model is formulated more conventionally in terms of the standard forward and backward differences given by Eqs. (3.9) and (3.10).

5. FINITE DIFFERENCE FORMS OF THE GOVERNING EQUATIONS - LINEAR MODEL

Before applying the finite difference scheme to the linear formulation, we rewrite the equations here for clarity. The equations of continuity and

x- and y-momentum are given respectively by

$$\frac{\partial \bar{\eta}}{\partial t} = - \frac{\partial}{\partial x} (\bar{U}D) - \frac{\partial}{\partial y} (\bar{V}D) \quad (3.14)$$

$$\frac{\partial \bar{U}}{\partial t} = - g \frac{\partial \bar{\eta}}{\partial x} - \frac{1}{\rho D} \left\{ \frac{\partial S_{xx}}{\partial x} + \frac{\partial S_{xy}}{\partial y} - \overline{\tau_{sx}} + \overline{\tau_{bx}} \right\} \quad (3.15)$$

$$\frac{\partial \bar{V}}{\partial t} = - g \frac{\partial \bar{\eta}}{\partial y} - \frac{1}{\rho D} \left\{ \frac{\partial S_{xy}}{\partial x} + \frac{\partial S_{yy}}{\partial y} - \overline{\tau_{sy}} + \overline{\tau_{by}} \right\} \quad (3.16)$$

In deriving this set of equations, we have tacitly assumed that variations of $\bar{\eta}$ with respect to time are small in comparison to variations in \bar{U} and \bar{V} . As we are striving for a steady state solution, the model results should not be sensitive to this assumption. Care should be taken, however, in removing time derivatives of D in cases where time dependent results are desired.

In keeping with standard techniques for treating first order linear hyperbolic equations, difference equations are formulated using a forward time-forward space (FTFS) scheme for the continuity equation (3.14), and forward time-backward space (FTBS) formulation for the momentum equations (3.15) and (3.16). Recalling that depths and set-up are known at grid centers, while velocities are given at grid boundaries, equations (3.14) - (3.16) are written in finite difference form as:

$$\delta_t \{\bar{\eta}\} = - \delta_x \{\bar{U}D^x\} - \delta_y \{\bar{V}D^y\} \quad (3.17)$$

$$\begin{aligned} \delta_t \{\bar{U}\} = & - g \delta_x \{\bar{\eta}\} - \frac{1}{\rho D} \left\{ \delta_x \{S_{xx}\} + \delta_y \{S_{xy}\}^x \right. \\ & \left. - \overline{\tau_{sx}}^x + \overline{\tau_{bx}}^x \right\} \end{aligned} \quad (3.18)$$

$$\begin{aligned} \delta_t(V) = & -g \delta_y(\bar{\eta}) - \frac{1}{\rho D} \frac{1}{y} \left\{ \delta_x(S_{xy})^y + \delta_y(S_{yy})^y \right. \\ & \left. - \tau_{sy}^y + \tau_{by}^y \right\} \end{aligned} \quad (3.19)$$

Note that $\delta_t(F)$ yields the forward difference

$$\delta_t(F) = \frac{F^{k+1} - F^k}{\Delta t} \quad (3.20)$$

where k and $k+1$ are successive time levels. Expanded forms of the equations (3.17) - (3.19) can be found in Birkemeier and Dalrymple (1976). At each iteration, the values of U and V are updated to time level $k+1$ using $\bar{\eta}$ and forcing terms evaluated at time level k . Then $\bar{\eta}$ is updated using the newly evaluated values of U and V at time level $k+1$. The method thus requires only one time level of storage for each of the unknown quantities.

Difference forms of the type used here have been discussed extensively by a number of authors (see, for example, Roache (1976)). The explicit method is subject to certain stability conditions. The problem of obtaining stability criteria for equations with non-constant coefficients is in general unsolved to date; however, we can make a reasonable guess based on constant-coefficient forms of the governing equations. If we drop the forcing terms, assume $D \approx h$, and hold h constant, we obtain

$$\begin{aligned} \frac{\partial \bar{\eta}}{\partial t} &= -h \left\{ \frac{\partial U}{\partial x} + \frac{\partial V}{\partial y} \right\} \\ \frac{\partial U}{\partial t} &= -g \frac{\partial \bar{\eta}}{\partial x} \\ \frac{\partial V}{\partial t} &= -g \frac{\partial \bar{\eta}}{\partial y} \end{aligned} \quad (3.21)$$

Cross-differentiating to eliminate U and V, we obtain the second-order hyperbolic equation for $\bar{\eta}$:

$$\frac{\partial^2 \bar{\eta}}{\partial t^2} = gh \left\{ \frac{\partial^2 \bar{\eta}}{\partial x^2} + \frac{\partial^2 \bar{\eta}}{\partial y^2} \right\} \quad (3.22)$$

The stability criterion corresponding to this reduced equation is given by the Courant condition:

$$\Delta t \leq \frac{\Delta x}{\sqrt{2gh}}, \quad (3.23)$$

assuming that $\Delta y = \Delta x$. Generalizing to the full model, the stability criterion (3.23) can be extended to include the effect of rectangular grids and the advection of disturbances by the mean currents.

$$\Delta t \leq \frac{\sqrt{(\Delta x)^2 + (\Delta y)^2}}{\sqrt{2gh} + |\vec{U}|} \quad (3.24)$$

The stability criterion basically states that time steps in the model may not be so large as to allow long wave disturbances to pass completely through a grid in one iteration. Violation of the criterion leads to rapidly growing instability of the numerical solution. In practice, time steps on the order of 0.25 times the maximum Δt are used.

6. FINITE DIFFERENCE FORMS OF THE GOVERNING EQUATIONS - NONLINEAR MODEL

The set of nonlinear momentum equations (2.12) - (2.13), together with the continuity equation (2.11), require a more careful development in difference form than the previously described linear model. Nonlinear formulations are in a practical sense subject to a number of instability mechanisms which are

not strictly related to stability criteria for the corresponding linear formulations, as discussed by Roache (1976).

The nonlinear model has been formulated using a method which has been applied successfully to geophysical and tidal models by Lilly (1965) and Blumberg (1977). Using the difference and average operators defined in section 4, the equations (2.11-13) are rewritten as

Continuity:

$$\delta_t \{\bar{\eta}^t\} + \delta_x \{\bar{D}^x U\} + \delta_y \{\bar{D}^y V\} = 0 \quad (3.25)$$

X-Momentum

$$\begin{aligned} \delta_t \{\bar{D}^x U^t\} + \delta_x \{\bar{D}^x U^x \bar{U}^x\} + \delta_y \{\bar{D}^y V^x \bar{U}^y\} = \\ = -g \bar{D}^x \delta_x \{\bar{\eta}\} + \frac{1}{\rho} \{\bar{\tau}_{sx}^x - \bar{\tau}_{bx}^x - \delta_y \{\bar{S}_{xy}^{xy}\} - \\ - \delta_x \{\bar{S}_{xx}\}\} + \bar{D}^x \delta_y \{\bar{\epsilon}_y \delta_y \{U\} + \bar{\epsilon}_x^{xy} \delta_x \{V\}\} \end{aligned} \quad (3.26)$$

Y-Momentum

$$\begin{aligned} \delta_t \{\bar{D}^y V^t\} + \delta_x \{\bar{D}^x U^y \bar{V}^y\} + \delta_y \{\bar{D}^y V^y \bar{V}^y\} = \\ = -g \bar{D}^y \delta_y \{\bar{\eta}\} + \frac{1}{\rho} \{\bar{\tau}_{sy}^y - \bar{\tau}_{by}^y - \delta_x \{\bar{S}_{xy}\} - \\ - \delta_y \{\bar{S}_{yy}\}\} + \bar{D}^y \delta_x \{\bar{\epsilon}_x \delta_x \{U\} + \bar{\epsilon}_y^{xy} \delta_y \{V\}\} \end{aligned} \quad (3.27)$$

The formula for lateral mixing given by Eq. (2.46) has been substituted into Eqs. (3.26-27). Note that, following Eq. (3.13), the central difference on the time averaged water set-up in Eq. (3.25) leads to

$$\delta_t^{\frac{-}{\eta}} \approx \delta_t^{\frac{-}{\eta}} = \frac{\eta_{i,j}^{k+1} - \eta_{i,j}^{k-1}}{2\Delta t} \quad (3.28)$$

The governing equations in this case then contain function values at three times levels, given by $k+1$, k , and $k-1$. The equations (3.25-27) can be found written out with respect to the i,j grid in Ebersole and Dalrymple (1979). These three equations can also be written in the following abbreviated form,

$$\eta_{i,j}^{k+1} = \eta_{i,j}^{k-1} + 2\Delta t F_1 \quad (3.29)$$

$$U_{i,j}^{k+1} = A U_{i,j}^{k-1} + 2\Delta t F_2 \quad (3.30)$$

$$V_{i,j}^{k+1} = B V_{i,j}^{k-1} + 2\Delta t F_3 \quad (3.31)$$

where A and B are functions of the depth alone and F_1 , F_2 , and F_3 are functions of all the variables in the problem. The quantities F_1 , F_2 , and F_3 contain quantities evaluated at time level k and $k-1$.

The method of solution for Eqs. (3.29-31) is based on a leapfrog scheme, and thus requires the storage of three time levels of values for all the calculated variables. In order to select the model, a single step is taken based on a forward difference formulation similar to that described in conjunction with the linear model. The forward difference formulation can be indicated schematically by

$$\eta_{i,j}^{k+1} = \eta_{i,j}^k + \Delta t F_1 \quad (3.32)$$

$$U_{i,j}^{k+1} = C U_{i,j}^k + \Delta t F_4 \quad (3.33)$$

$$V_{i,j}^{k+1} = D V_{i,j}^k + \Delta t F_5 \quad (3.34)$$

The computational method is schematized in Figure 3-3.

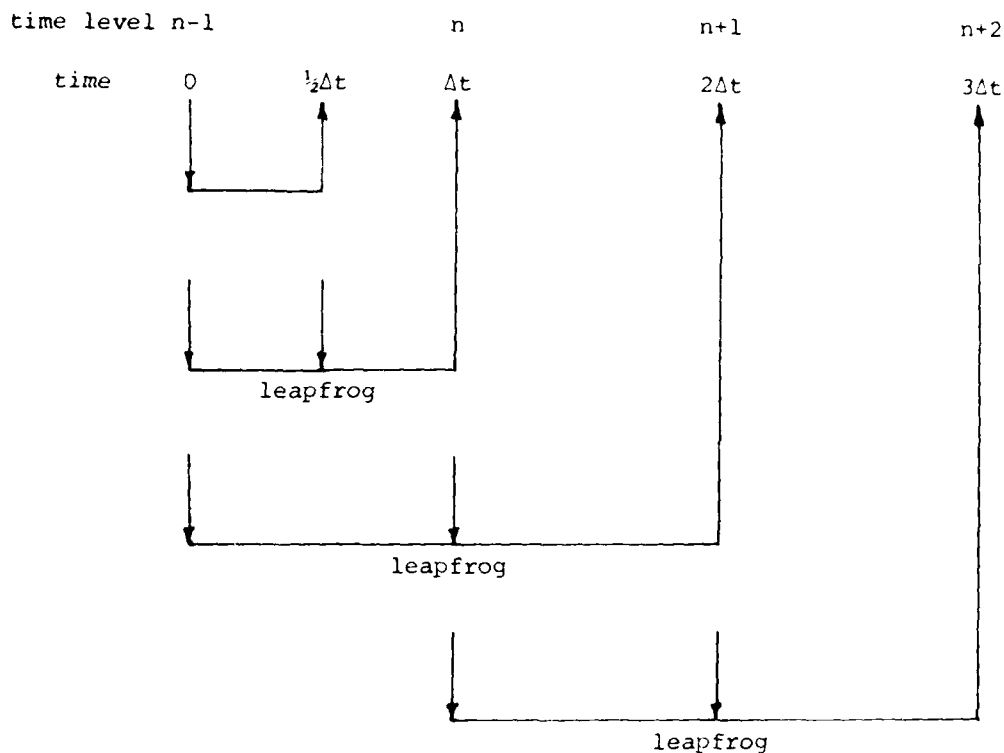


Figure 3-3. General Leapfrog Solution Scheme

The stability criterion for the present scheme was assumed to be given by Eq. (3.24), which has physical if not mathematical significance in the present situation. In practice, as is the case of the linear model, it was necessary to reduce the maximum allowable time step to a value significantly below the one predicted by the stability criterion.

The nonlinear model was also subject to a second computational stability problem. In general, computational schemes for first order equations which are

centered in space and time (CSCT) exhibit forms of unstable behavior. In particular, in the context of the first order parabolic diffusion equation, such explicit CSCT schemes can be shown to be unconditionally unstable. In the present case, as the model approached a steady state, the solution diverged into two disjoint solutions; one associated with the even time steps and the other the odd steps. These solutions oscillated with growing amplitudes about the steady state solution. In Roache (1976), the author referred to this as time splitting.

To alleviate the problem, a leapfrog-backward correction scheme, Kurihara (1965), was initiated every tenth time step. The scheme is shown below as,

$$h^* = h^{k-1} + 2\Delta t G^k \quad (3.35)$$

$$h^{k+1} = h^k + \Delta t G^* \quad (3.36)$$

where h may be U , V or $\bar{\eta}$. Equation (3.35) is simply the leapfrog calculation done by the Eqs. (3.29-31) where $*$ denotes the new or "interim" time level. Using the new values U , V , $\bar{\eta}$ at time $*$, the functions G^* , like the functions F_1 , F_2 , and F_3 from Eqs. (3.29-31) are calculated and used in Eq. (3.36) which is merely a backwards difference in time to the level k .

This scheme was chosen because it damps the computational mode of the solution while leaving the physical mode relatively unaffected. For a more in-depth discussion the reader is referred to the work by Kurihara. With this correction scheme included, which essentially "ties" the solutions together every tenth iteration, the model proceeded to reach a steady state without any further time-splitting instability.

7. THE NUMERICAL SCHEME FOR REFRACTION AND THE WAVE HEIGHT FIELD

The equations governing wave refraction, wave height, and wave number are given by Eqs. (2.35), (2.37), and (2.36) respectively. The method of solving these equations for the unknown $\theta_{i,j}$, $H_{i,j}$ and $k_{i,j}$ is identical in both the linear and nonlinear models. The method was given originally by Noda et al. (1974).

If Eq. (2.36) is differentiated with respect to x to get $\frac{\partial k}{\partial x}$ and with respect to y to get $\frac{\partial k}{\partial y}$, these quantities can be substituted into Eq. (2.35), which can then be written in the following form:

$$A \frac{\partial \theta}{\partial x} = B \frac{\partial \theta}{\partial y} = C \quad (3.37)$$

where A , B and C are functions of the quantities $\sin \theta$, $\cos \theta$, k , h , u and v . By taking a forward difference in x to approximate $\frac{\partial \theta}{\partial x}$ and a backwards difference in y to approximate $\frac{\partial \theta}{\partial y}$, Eq. (3.37) becomes:

$$\theta_{i,j} = D + E \theta_{i,j-1} - F \theta_{i+1,j} \quad (3.38)$$

where D , E and F are now functions of the quantities $\sin \theta_{i,j}$, $\cos \theta_{i,j}$, $k_{i,j}$, $h_{i,j}$, $u_{i,j}$, $v_{i,j}$. To evaluate $\sin \theta_{i,j}$ and $\cos \theta_{i,j}$ Noda used a first order Taylor series expansion to the four neighboring grids $(i+1,j)$, $(i-1,j)$, $(i,j+1)$ and $(i,j-1)$, summed the results and took an average value.

The theta field $\theta_{i,j}$ is solved for in the following way. Snell's Law is used to approximate the angles at the offshore row. Working shoreward Eq. (3.38) is solved for in a row-by-row relaxation until the angles converge to their correct values with wave-current interaction included. After each updated value of theta, a new wave number must be solved for.

Eq. (2.36) can be written as

$$E(k) = \{gk \tanh(kh)\}^{1/2} + uk \cos \theta + vk \sin \theta - \frac{2\pi}{T} = 0 \quad (3.39)$$

To solve for the wave number, k , after each updated angle is found, the Newton-Raphson Method, or "method of tangents", is used. This method states that

$$k_{\text{new}} = k_{\text{old}} - \frac{E(k_{\text{old}})}{E'(k_{\text{old}})}$$

Differentiating Eq. (3.39), k_{new} is iteratively solved for until

$$|k_{\text{new}} - k_{\text{old}}| \leq .001 |k_{\text{new}}|$$

The wave height field is calculated in much the same way as the wave angle field. Multiplying Eq. (2.37) by $\frac{H}{2}$ and letting $\frac{\partial H}{\partial t} = 0$, the energy equation can now be written in the form

$$A \frac{\partial H}{\partial x} + B \frac{\partial H}{\partial y} = C H \quad (3.40)$$

where A , B and C are functions of u , $v \cos \theta$, $\sin \theta$, C_g , Δx , Δy and the radiation stresses. Taking a forward difference in x to approximate $\frac{\partial H}{\partial x}$ and a backward difference in y to approximate $\frac{\partial H}{\partial y}$ and solving for $H_{i,j}$, it can be shown that

$$H_{i,j} = D H_{i,j-1} - E H_{i+1,j}$$

where D and E are functions of the same quantities as A , B and C . Again the offshore row of wave heights are obtained from shoaling and refraction due to Snell's Law and the wave height field is determined by relaxing row by row in the shoreward direction. On each row a solution for the wave height is reached when $|H_{\text{new}} - H_{\text{old}}| \leq .01 H_{\text{new}}$. After each updated value of $H_{i,j}$, a breaking wave height is also calculated from the breaking criteria given by the Miche

formula

$$\left(\frac{H}{L}\right)_b = .12 \tanh(kh)_b \quad .$$

If the calculated $H_{i,j}$ is larger than the allowable breaking height, the height $H_{i,j}$ was set equal to the breaking height.

CHAPTER IV

CALIBRATION OF THE NEARSHORE CIRCULATION MODELS

In order to make the circulation model more generally applicable to prediction of field conditions, both versions of the model were calibrated using field data. The calibrations consisted of determining a monochromatic deepwater wave condition and a uniform wind condition, and then running the models using the field conditions and measured bathymetry. Adjustable coefficients were then tuned to obtain the best possible qualitative and quantitative fit between the currents predicted by the model and those measured in the field.

In this chapter, the field data set used for calibration is described. Results for the circulation models are then shown for a range of coefficient values.

1. FIELD DATA USED FOR CALIBRATION

Field data used during calibration of the nearshore circulation models was obtained from the results of the Nearshore Sediment Transport Study (NSTS) experiment conducted at Torrey Pines beach, near La Jolla, Ca., (see Figure 4-1) in November - December 1978. The results of this study were chosen as being applicable to calibration of the models for several reasons. Torrey Pines beach is a long, straight beach with fairly uniform and parallel offshore contours. The field bathymetry was thus easily adapted into the model's scheme of longshore periodicity.

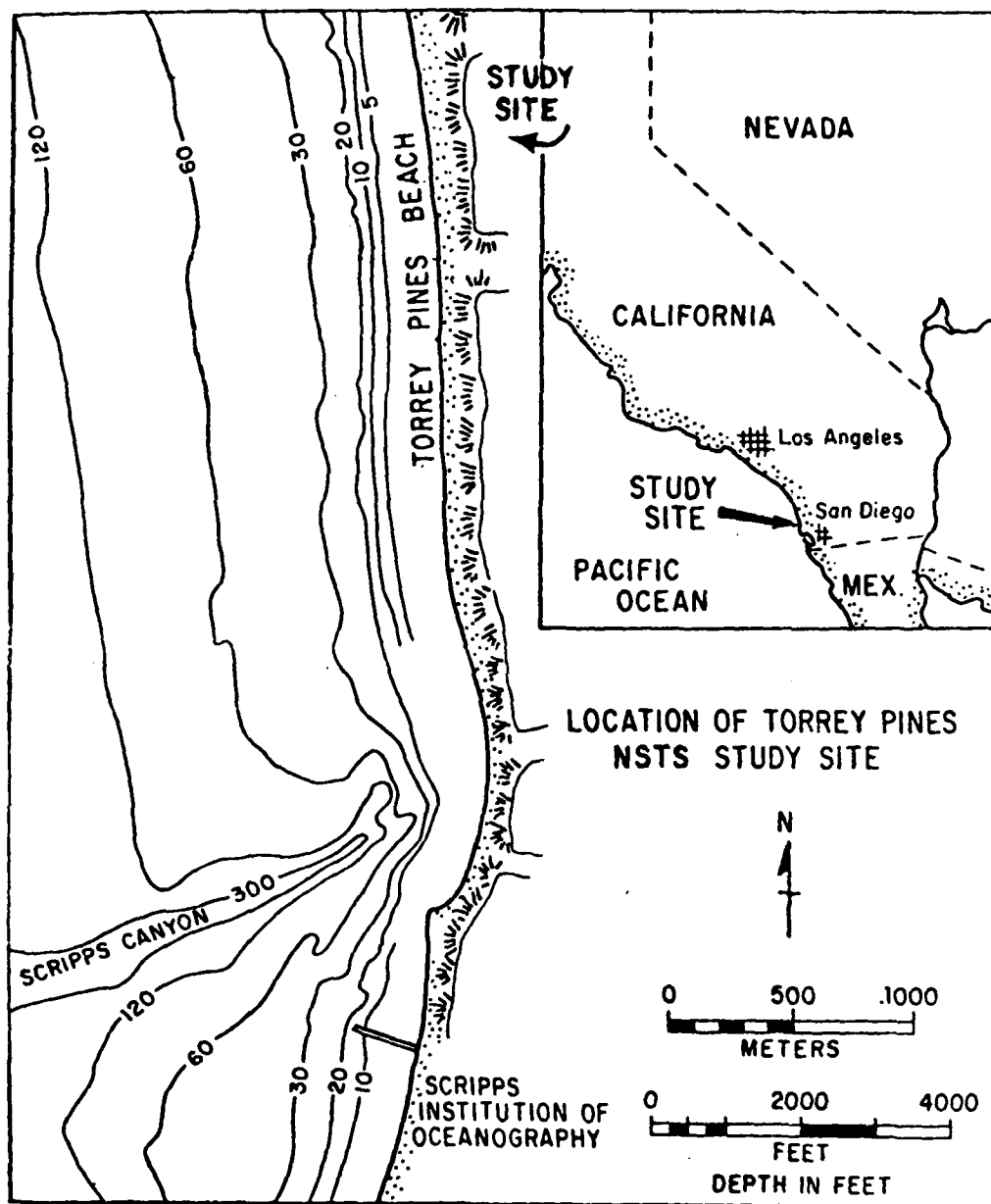


Figure 4-1. Location of NSTS Torrey Pines Experiment.
(From Gable, 1979)

The experiment itself produced a detailed picture of nearshore currents and waves, with up to 22 current meters, 10 pressure gages, and 7 wave staffs being operated simultaneously. Thus the resolution needed to accurately fit the model predictions was present in the field data. Gable (1979) gives a detailed description of the site, instrumentation, and conduct of the NSTS experiment. The arrangement of fixed instruments used in the experiment is shown in Figure 4-2. Angles and distances used in this report will be with respect to the baseline (0 offshore distance) in Figure 4-2. Two separate bathymetry maps are shown in Figures 4-3 and 4-4. It is noted that the survey of Nov. 9, 1978 indicates the presence of a shallow channel oriented almost perpendicular to the baseline at about 40 m left of the main range (0 m alongshore). This feature is not present in the Nov. 18, 1978 survey, which, on the whole, exhibits greater random fluctuation in the location of the contours. Both the channel in the Nov. 9 bathymetry data and the unevenness in the Nov. 18 data appear to be transient features, as will be discussed below.

1.1 Choice of Field Data for Calibration

Several requirements were chosen in order to determine a valid set of field data for comparison to the numerical model. First, the numerical models in their basic state are designed to be run with a monochromatic deepwater wave condition. It was therefore required that the wave field for the chosen data be narrow banded both in a frequency and directional sense. The presence of a second wave component at a different direction than the primary component introduces a forcing mechanism

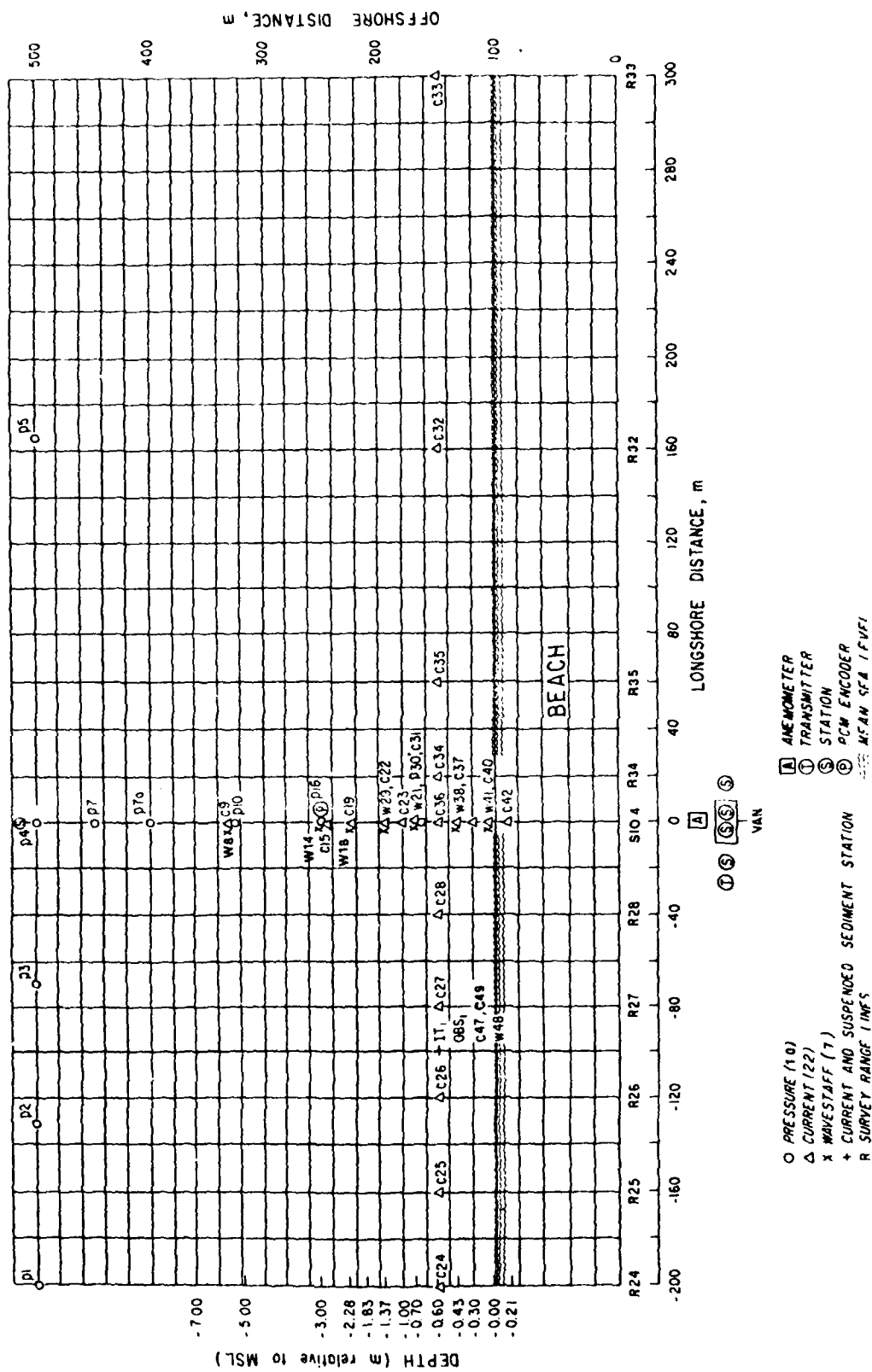


Figure 4-2. Instrumentation for NSTS Torrey Pines Experiment.
(1968-1969, 1970)

NEARSHORE BATHYMETRY-TORREY PINES BEACH
 SURVEY OF 9 NOVEMBER 1978
 (CONTOURS RELATIVE TO MEAN SEA LEVEL)

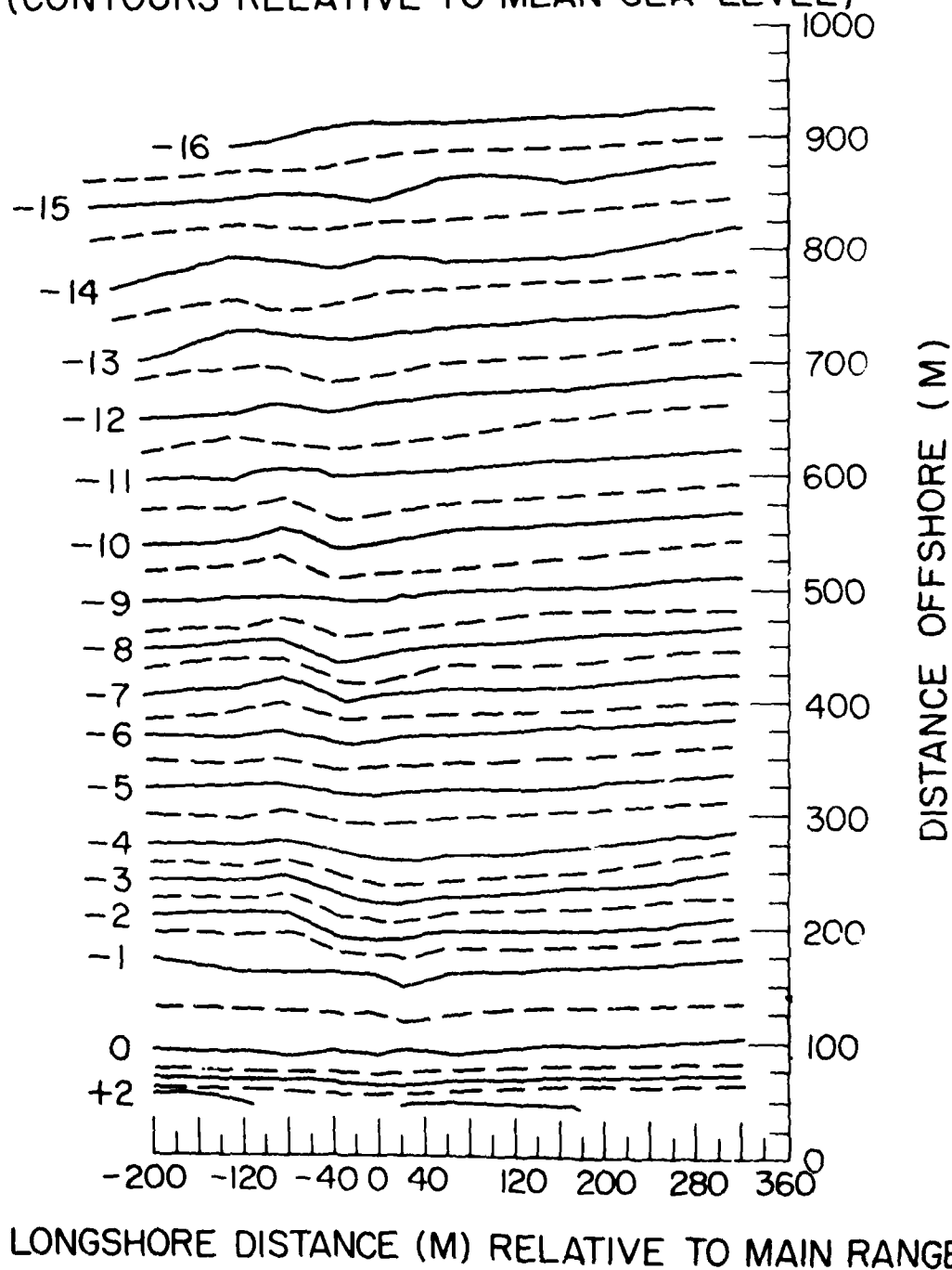


Figure 4-3. Nearshore Bathymetry, Nov. 9, 1978
 (from Gable 1979)

NEARSHORE BATHYMETRY-TORREY PINES BEACH
 SURVEY OF 18 NOVEMBER 1978
 (CONTOURS RELATIVE TO MEAN SEA LEVEL)

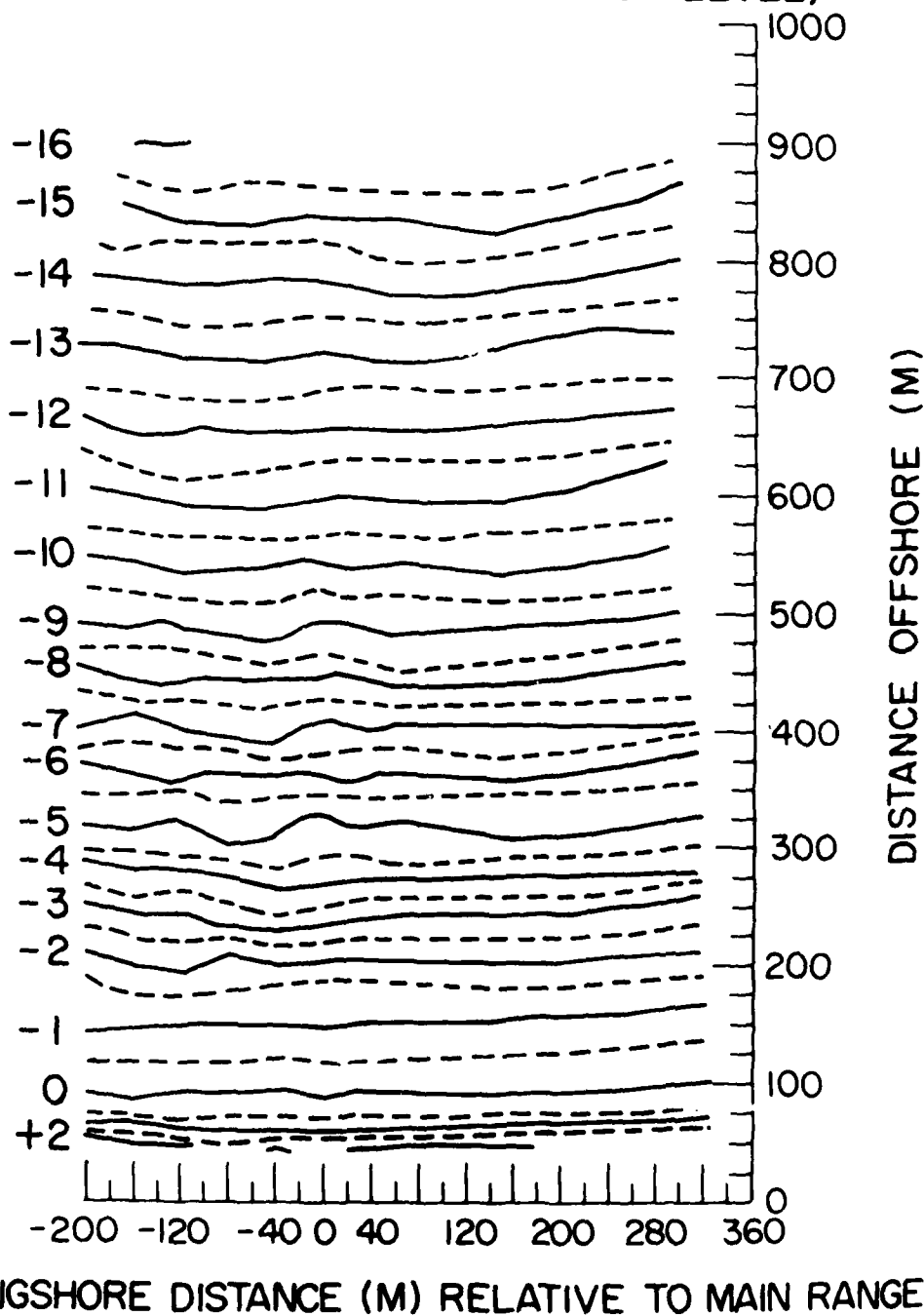


Figure 4-4. Nearshore Bathymetry, Nov. 18, 1978
 (from Gable 1979)

which would tend to produce rip cells on a plane beach, as shown by Dalrymple (1975). Just such a case was treated by a simplified refraction model in Ebersole and Dalrymple (1979), but the capability to handle the condition has not been retained in the final model versions since the refraction scheme used does not model the interaction of different waves. In addition, the use of a 17 minute average of the field measured currents in order to obtain fairly steady conditions precluded the modelling of essentially transient circulation phenomenon.

Secondly, since it was desired to calculate a steady state wave and current field, it was required that wave and wind conditions be nearly steady over the interval of averaged field measurements. This required either a quiet or unidirectional wind field as well as fairly steady wave direction, height and period.

The field data set available from the NSTS results was roughly screened on the basis of the beach observations given in Gable (1979). In particular, observation of long crested waves indicated the presence of narrow banded directional spectra. It was found that the NSTS data presented a problem, in that almost all data sets exhibited at least some degree of bi-directionality, with waves approaching from both the north and south. The data chosen for initial calibration has a somewhat smaller wave component from the north than other records, but is still suspect as a valid calibration standard.

Data Set Number 1

The NSTS data tapes divide the current and pressure records into 17 minute segments. The first data set chosen for use in calibration,

and subsequently used for the majority of calibration runs, was taken from the second 17 minute segment of the test of Nov. 10, 1978. The 17 minute segments were further subdivided into four 4.25 minute segments, and averaged current fields were plotted for each 4.25 minute segment. Two representative plots for the first data set are shown in Figure 4-5a and b.

Based on an average of the 4.25 minute average velocity profiles, an average 17 minute velocity profile was constructed for data values on the main range (offshore array of meters) and is shown in Figure 4-6. The resulting velocity profile indicates a longshore current of about 8 cm/sec magnitude offshore of the surf zone. This current is too far outside the breaker line to be surf driven, and may be due to the presence of a tidal or seasonal current. The effect of this current on the model results is discussed below.

The monochromatic deepwater wave conditions determined for data set No. 1 were as follows:

Wave period	T	:	14.52 seconds
Wave height	H ₀	:	0.62 meters
Wave angle	A	:	165.7° measured clockwise from +x (offshore direction).

The uniform wind conditions were:

Wind speed	W	:	7.2 meters/second
Wind angle	α	:	294.5° measured clockwise from -x (onshore) direction.

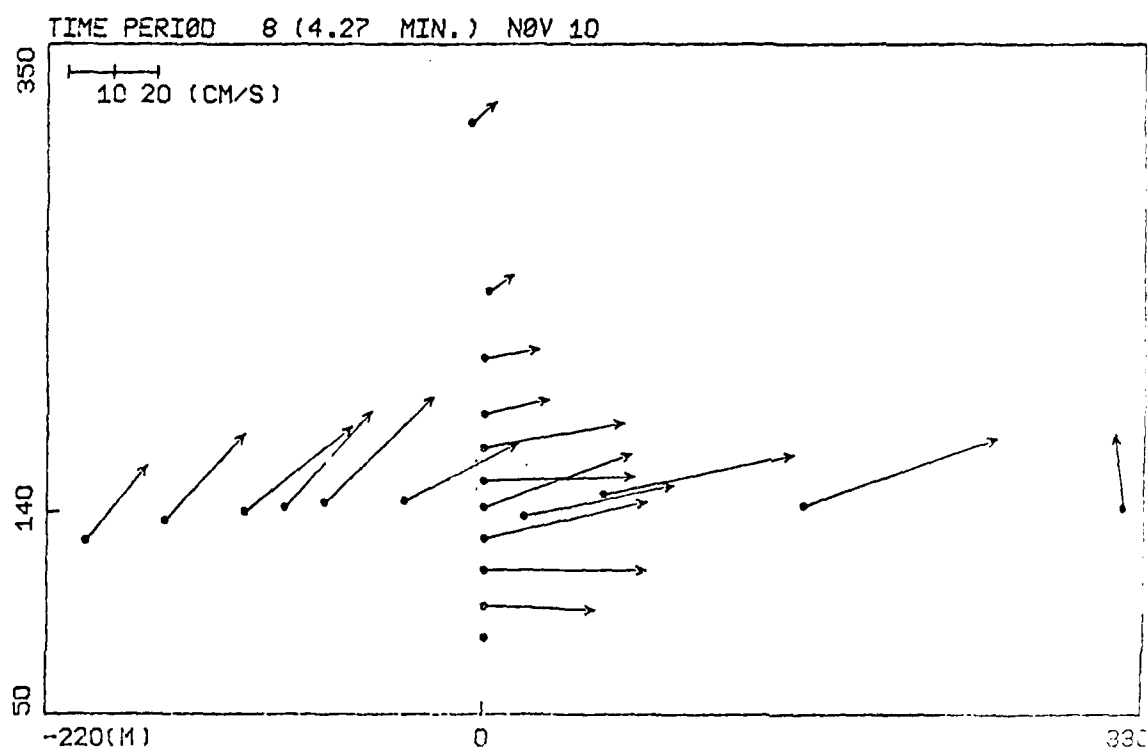
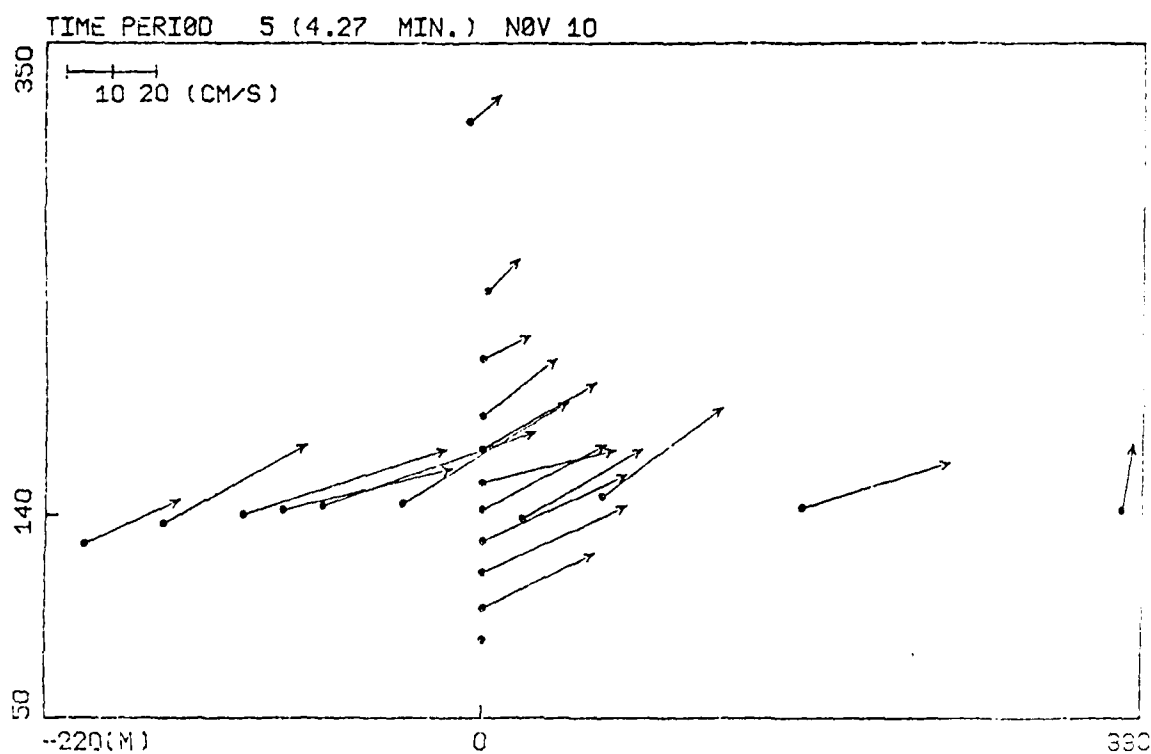


Figure 4-5. 4.27 Minute Average Current Vectors, Nov. 10, 1978.

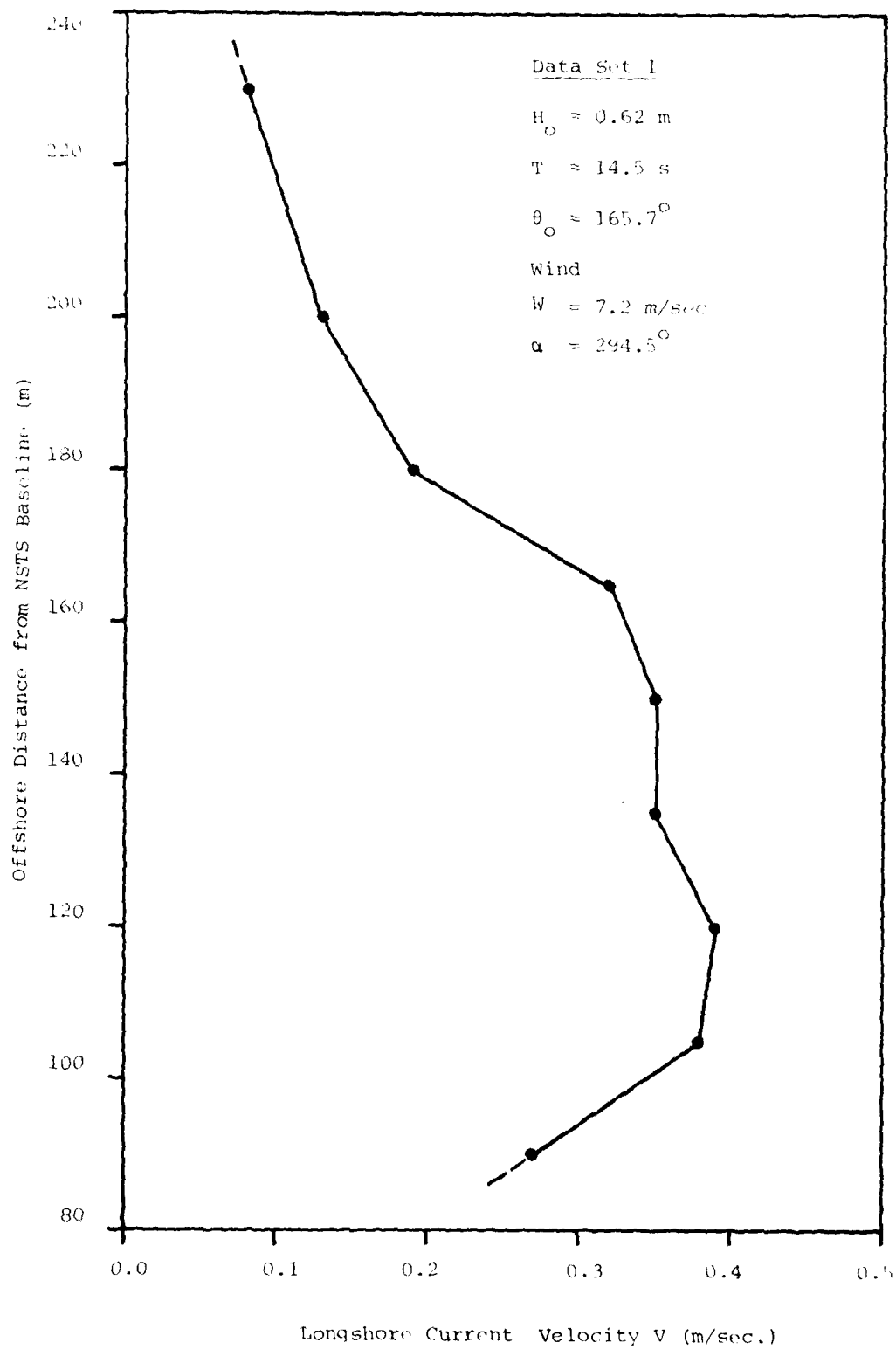


Figure 4.6 Average Field Velocity Profile
Data Set 1.

Data Set Number 2

Data Set Number 1 represented the only strongly unidirectional, narrow banded wave spectrum contained in the Torrey Pines data. The remaining data sets, even in the absence of locally generated short wind waves, exhibited at least a strong tendency towards bidirectionality, with spectral peaks nearly symmetrically placed about the shore-normal axis. Since it is anticipated that measured wave fields in general would seldom exhibit the narrow banded, unidirectionality required as input into the model, a data set was constructed based on averaging over the parameters of the measured wave field in order to test the response of the model using a "best guess" for the desired input parameters.

The data chosen for this test was from the eighth 17-minute time period of the November 15 data. Wave energy was contained in two directional peaks in a narrow frequency band (Figure 4-7). Using directional spectra supplied by Pawka (1980), the data set was constructed by summing the mean energy density over all frequencies in the dominant spectral peak. The wave angle was chosen as the average of the dominant angle at each frequency weighted by the energy densities. The peak energy containing frequency was taken as the dominant frequency. The resulting data set follows:

Wave Period	T	:	14.71 seconds
Wave Height	H_o	:	0.43 meters
Wave Angle	A	:	168° measured clockwise from +x (offshore direction)

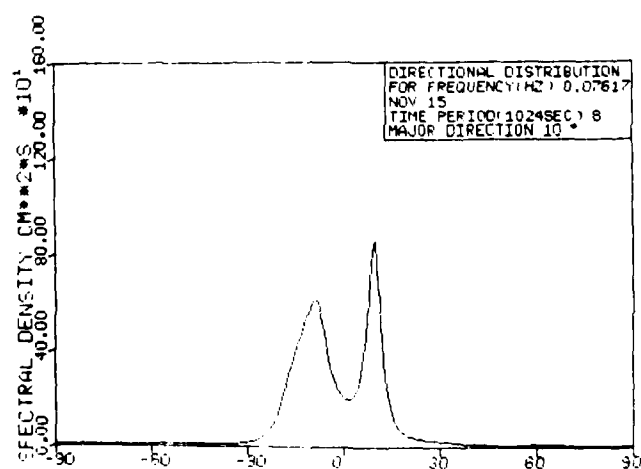
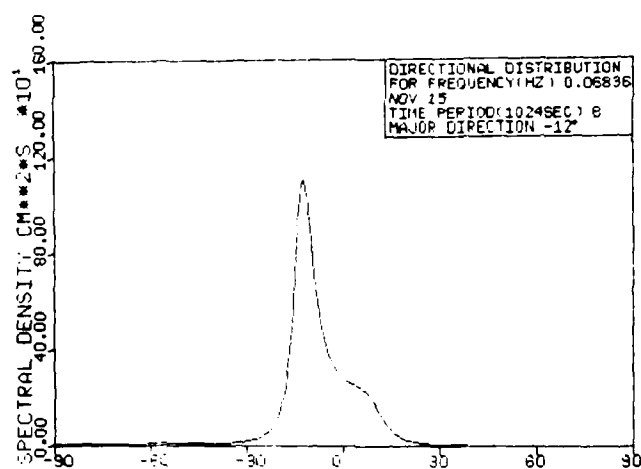
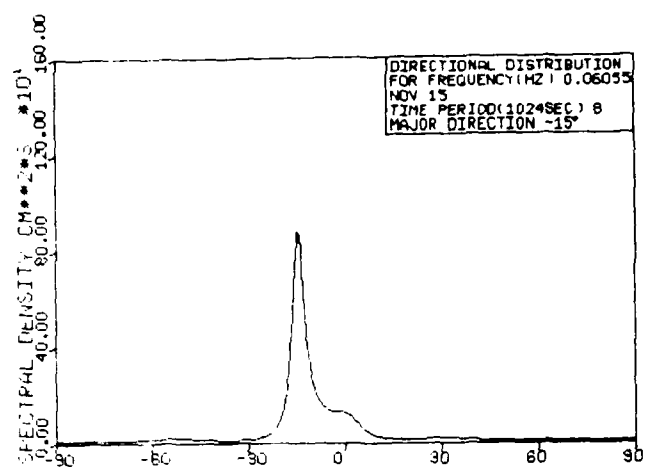


Figure 4-7. Directional Distribution of Wave Energy at Peak Frequencies,
Nov. 15, 1978 (supplied by S. Pawka, 1980)

There was no significant steady wind component.

Wind speed W : 0.0 meters/second

Wind angle α : not applicable.

The resulting data set has an indeterminant connection with the measured field data, and at best the model could be expected to exhibit results in qualitative agreement with the field data.

Figure 4-8 shows a plot of average longshore current over the 17 minute period of data collection. Individual plots (not shown) of 4.25 minute averages show a great deal of scatter in peak velocities and shape of the profile, indicating some unsteadiness in the current field, as would be expected due to the bi-directional wave field.

2. CALIBRATION OF THE MODELS

Both the linear and nonlinear models have a bottom friction factor f and the Van Dorn coefficients K_1 and K_2 as adjustable parameters. In addition, the nonlinear model has adjustable coefficients of lateral eddy mixing in both the longshore and offshore directions.

The Van Dorn wind stress formulation used in the models is intended to represent the transfer of momentum from a wind field to the water column, leading to a wind-induced longshore current for wind stress applied in the long shore direction, and wind set up for wind blowing towards shore. Wind set up cannot currently be accurately calibrated in the present models due to the artificial barrier at the offshore grid row; no additional water can

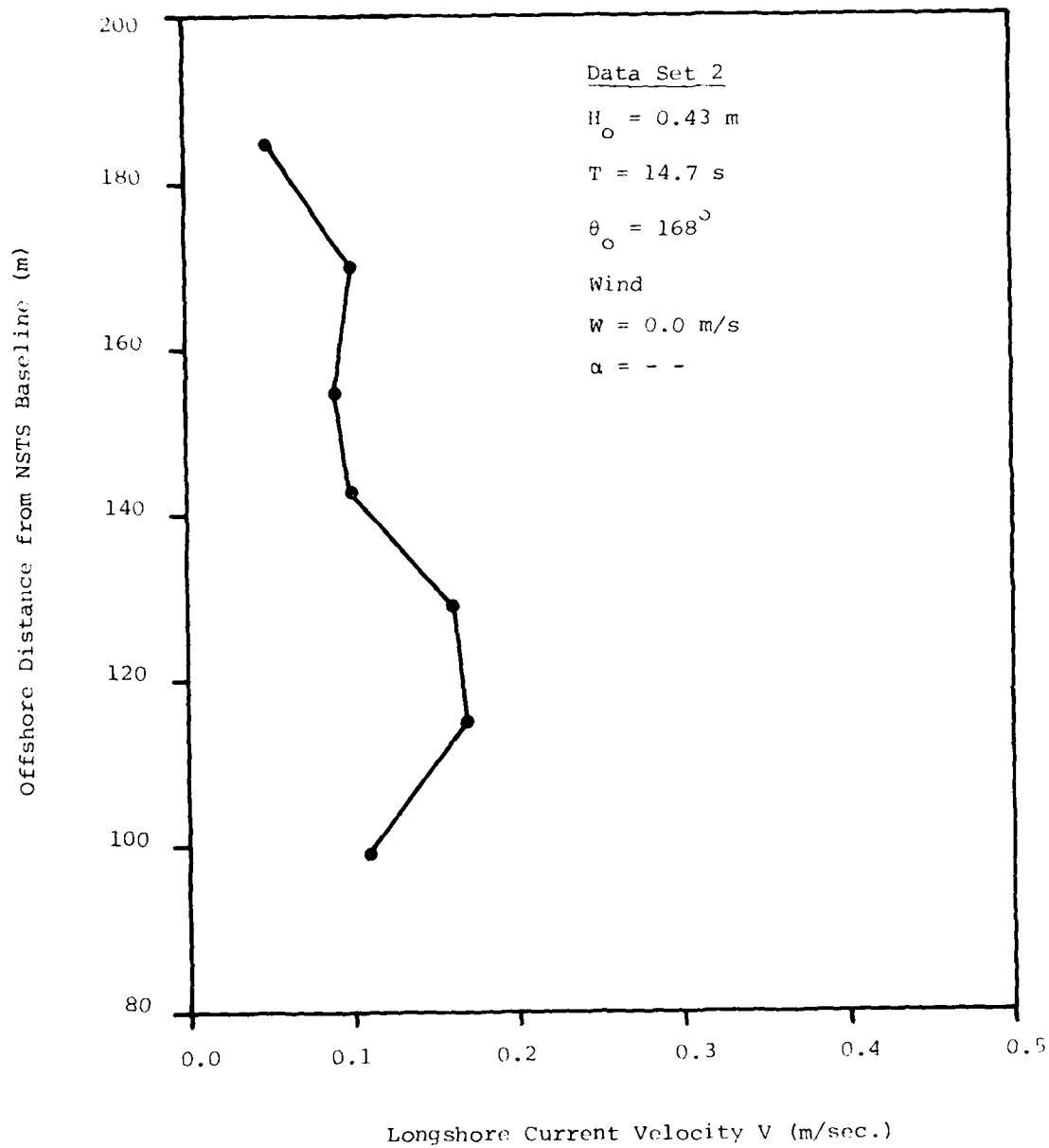


Figure 4-8 Average Field Velocity Profile
Data Set 2

enter the model after the start of the run with a given depth grid. The parameters used in the Van Dorn formula have been tested in previous large scale models (Pearce, 1972), and have been found to be satisfactory.

With the elimination of the wind stress coefficients, only the bottom friction coefficient, f , remained to be calibrated in the linear model. The procedure used was to choose a value of f for both models based on a comparison of field data with the linear model. The value of f chosen was then used in the nonlinear model as a first approximation, and values of the eddy mixing coefficients were adjusted to again obtain a best fit between the results of the nonlinear model and the field data. It should be noted, however, that there is no a priori reason that both models should behave optimally with the same value of f .

2.1 Linear Model Calibration

Runs of the linear model were conducted using the deepwater wave conditions of Data Set 1 and the measured bathymetry of Nov. 9, 1978. For all values of f chosen, rip currents formed near the shallow channel seen in the Nov. 9 bathymetry. These rip currents were not apparent in the Nov. 10 currents (Figure 4-5), where they would affect the main range velocity profile. An example of the current field calculated using the Nov. 9 bathymetry is shown in Figure (4-9). The value of f for the run shown was 0.01.

It was tentatively concluded at this point that the shallow channel seen in the Nov. 9 data was a transient feature and was not present on Nov. 10, judging from the uniformity of the measured currents. It was decided to run a model using a bathymetry based on a longshore average of the Nov. 9 bathymetry

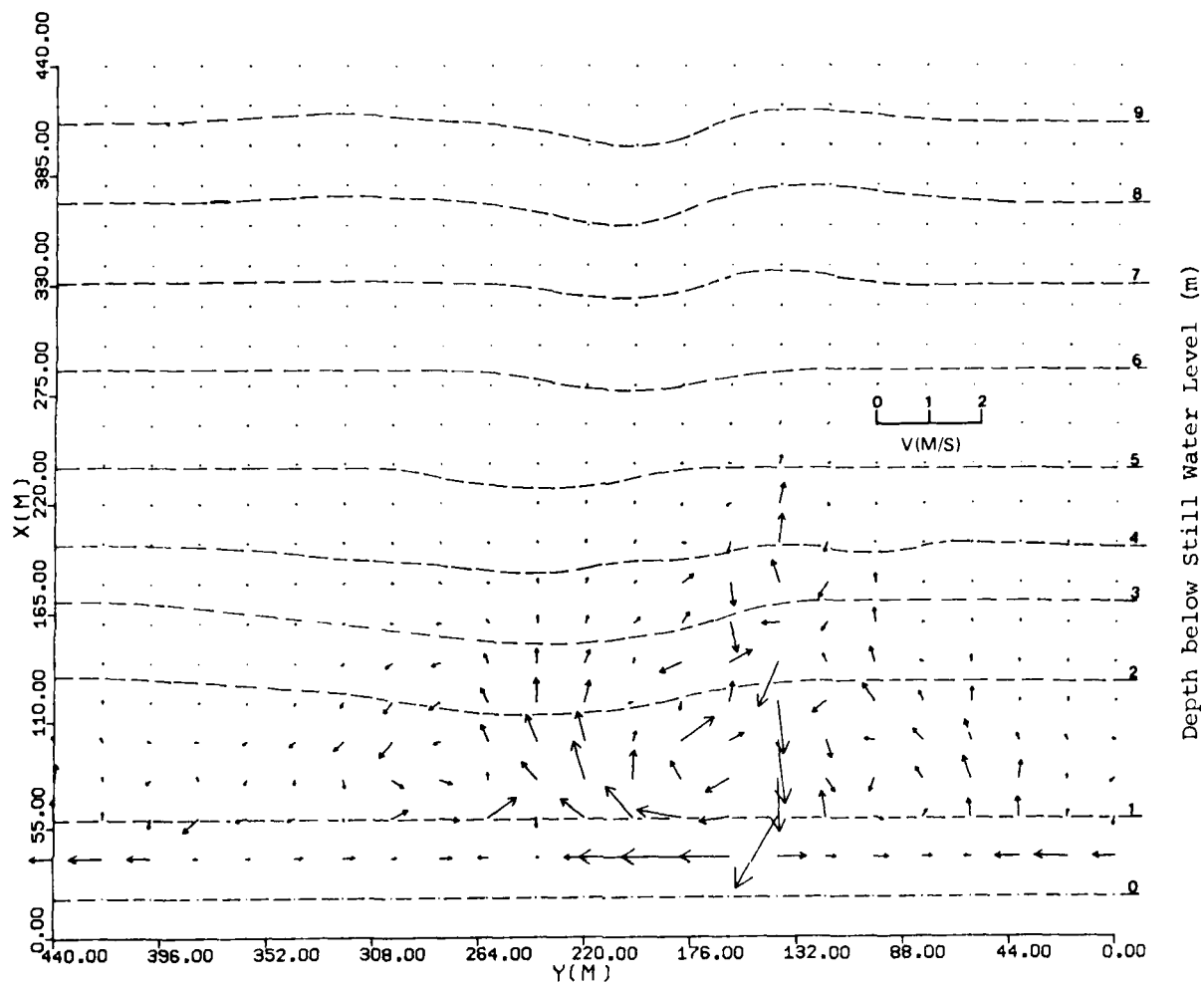


Figure 4-9 Currents Induced in Field Using Nov. 9 Bathymetry
Nonlinear Model: Data Set 1.

data. The longshore extent of the beach was arbitrarily chosen as 200 meters. The profile is shown in Figure 4-10.

Using the longshore averaged bathymetry, model runs were conducted for a range of f values. Velocity profiles for values of f of 0.01, 0.015 and 0.02 are shown in Figure 4-11, in comparison to the current distribution measured in the field. In addition, a "corrected" field current distribution constructed by subtracting the 0.08 m/sec offshore current is shown as the dashed line.

Figure 4-11 shows that, by using a value of f equal to 0.015, the linear model closely predicts the maximum velocities and the general velocity distribution in the surf zone. The longshore current predicted by the model dies off more quickly offshore due to the absence of lateral mixing effects in the linear model.

2.2 Nonlinear Model Calibration

The nonlinear model was run using Data Set 1 and the value of $f = 0.015$ obtained from the linear model calibration. Three sets of mixing coefficients ϵ_x (or N) and ϵ_y were used (see Equation (2.40)).

\underline{N}	$\underline{\epsilon_y}$	
0.000	0.00	no mixing
0.0025	0.25	
0.005	0.50	

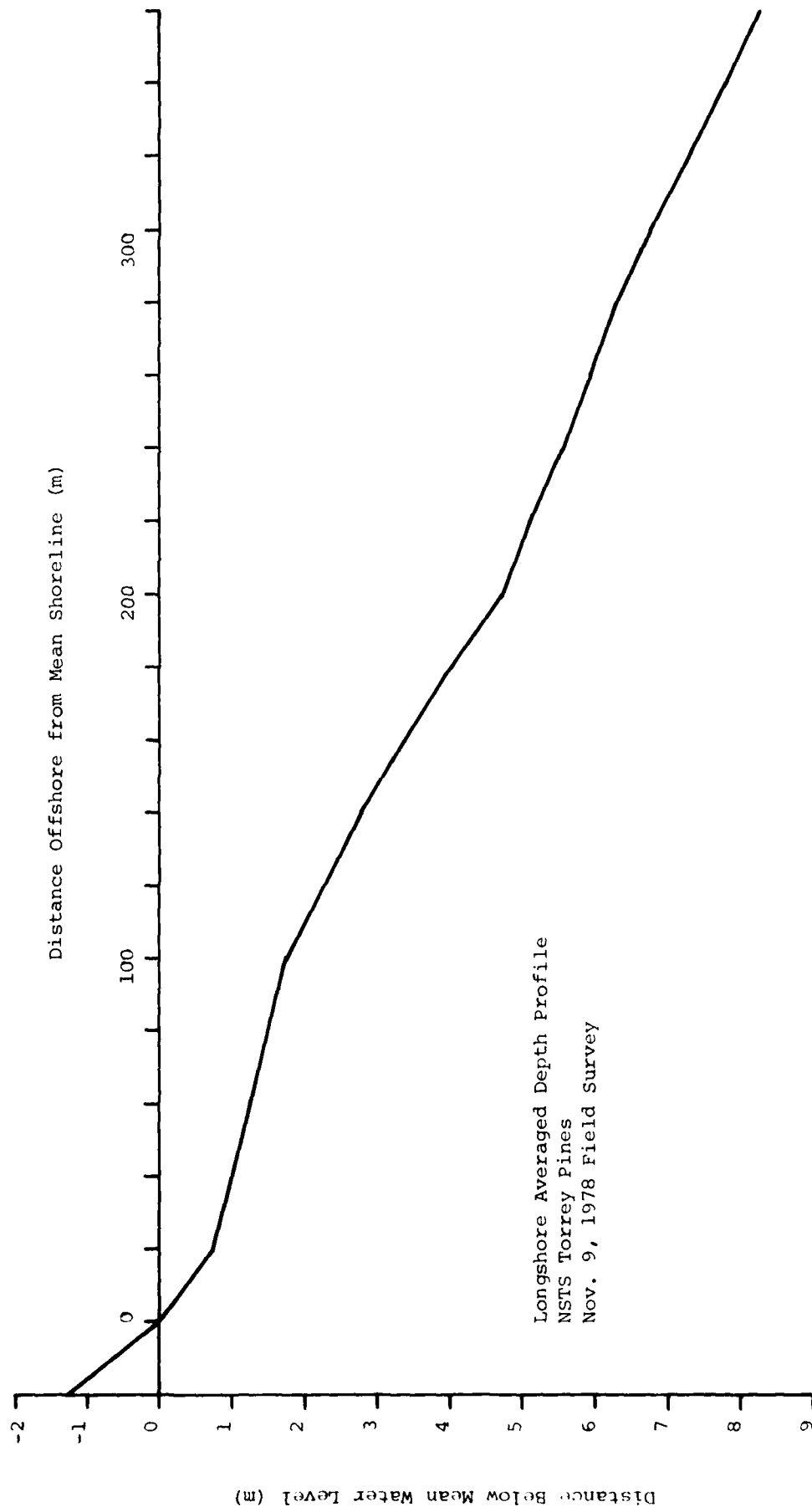


Figure 4-19 Longshore Average Depth Profile, Torrey Pines, November 9, 1978.

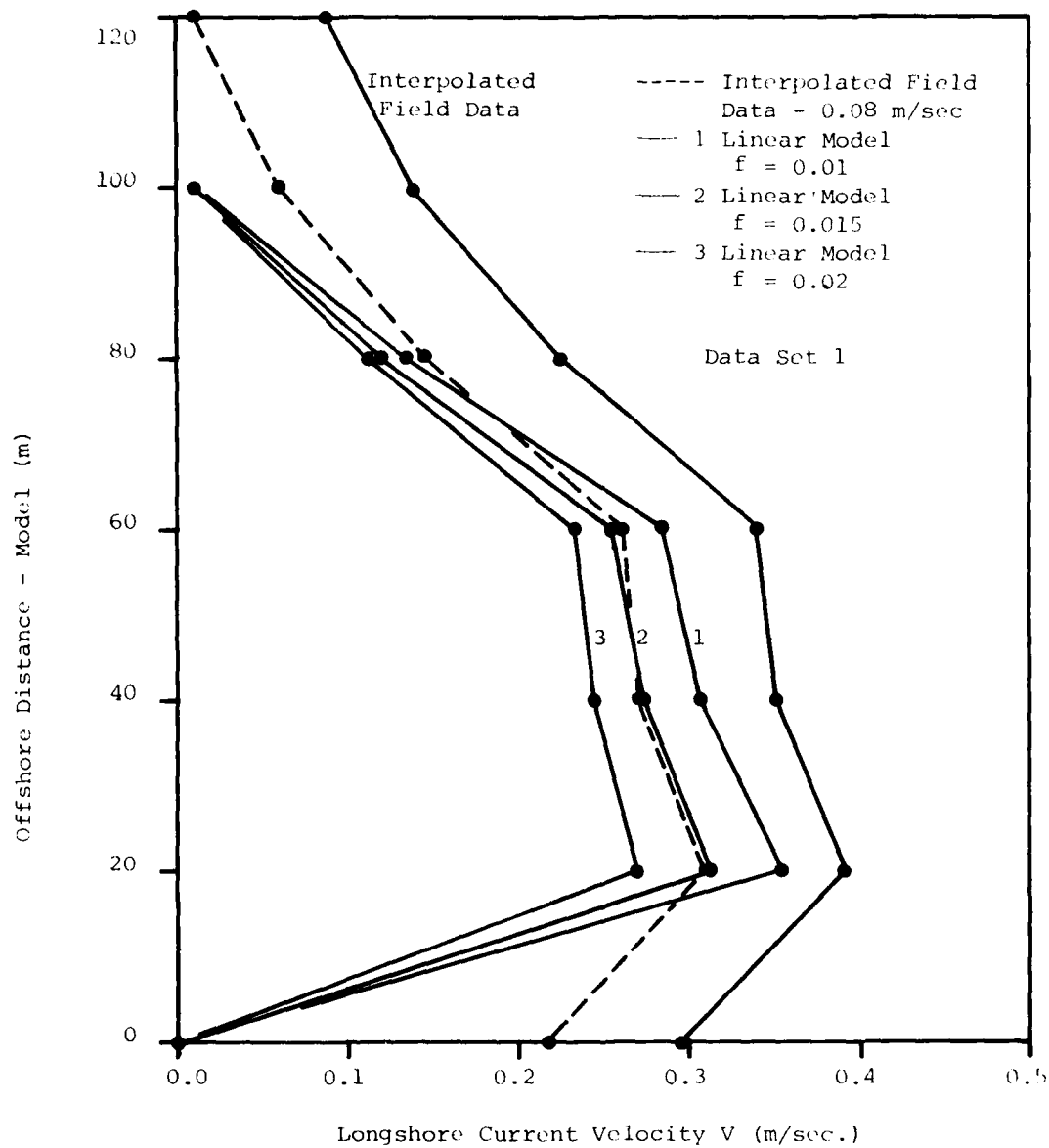


Figure 4-11 Variation of Longshore Current with Friction Factor in the Linear Model.

Results for $f = 0.015$ are shown in Figure 4-12. It was found that the inclusion of mixing satisfactorily extended the velocity profile in the offshore direction, but in both cases, including mixing, the current magnitudes in the surf zone were underpredicted. The model was therefore retested using a smaller value for the friction coefficient, $f = 0.01$. Results are shown in Figure 4-13. The smaller value of f is seen to correct for the underprediction of longshore current. Coefficient values for the nonlinear model were chosen based on the second set of results,

$$f = 0.01$$

$$N = 0.0025$$

$$\epsilon_y = 0.25 \quad .$$

2.3 Response of Both Models Using Data Set 2

The linear and nonlinear models were run using Data Set 2 and the calibrated coefficients obtained above. Results for the linear model are shown in Figure 4-14. Nonlinear model results were similar to the linear model results. Both models were seen to overpredict the maximum longshore current in comparison to the averaged field data, and to underpredict the offshore extent of the longshore current. It is likely that a better fit to the field data could be obtained by artificially increasing the lateral mixing in the nonlinear model. However, the field data represents the average of a complex flow pattern, where the effect of mixing in the averaged data is induced by large scale phenomenon not likely to be found in the steady current fields induced by a unidirectional wave field. Since it is likely that the magnitude of artificial mixing would vary greatly as a function of

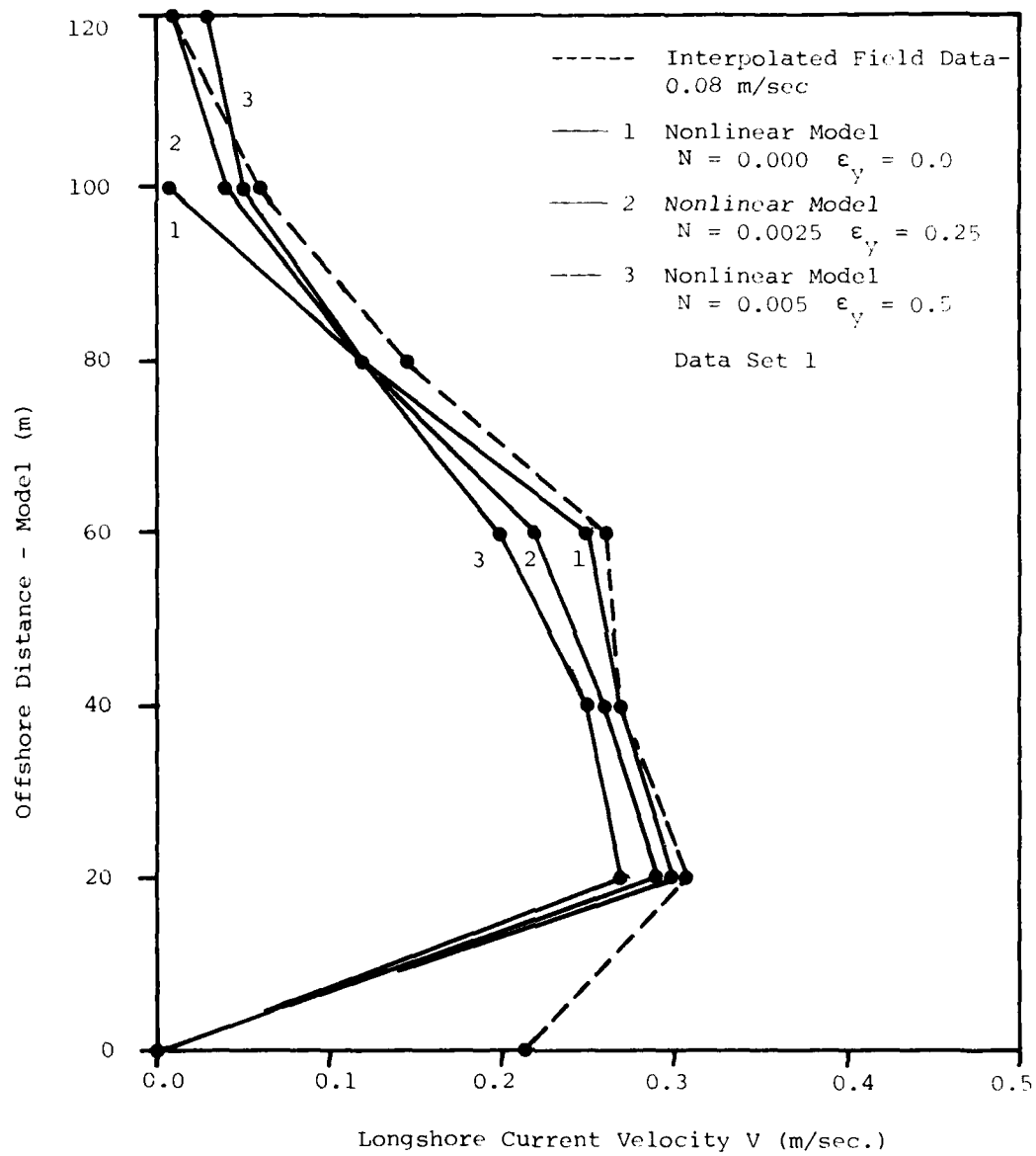


Figure 4-12 Variation of Longshore Current with Lateral Mixing in the Nonlinear Model.
f = 0.015

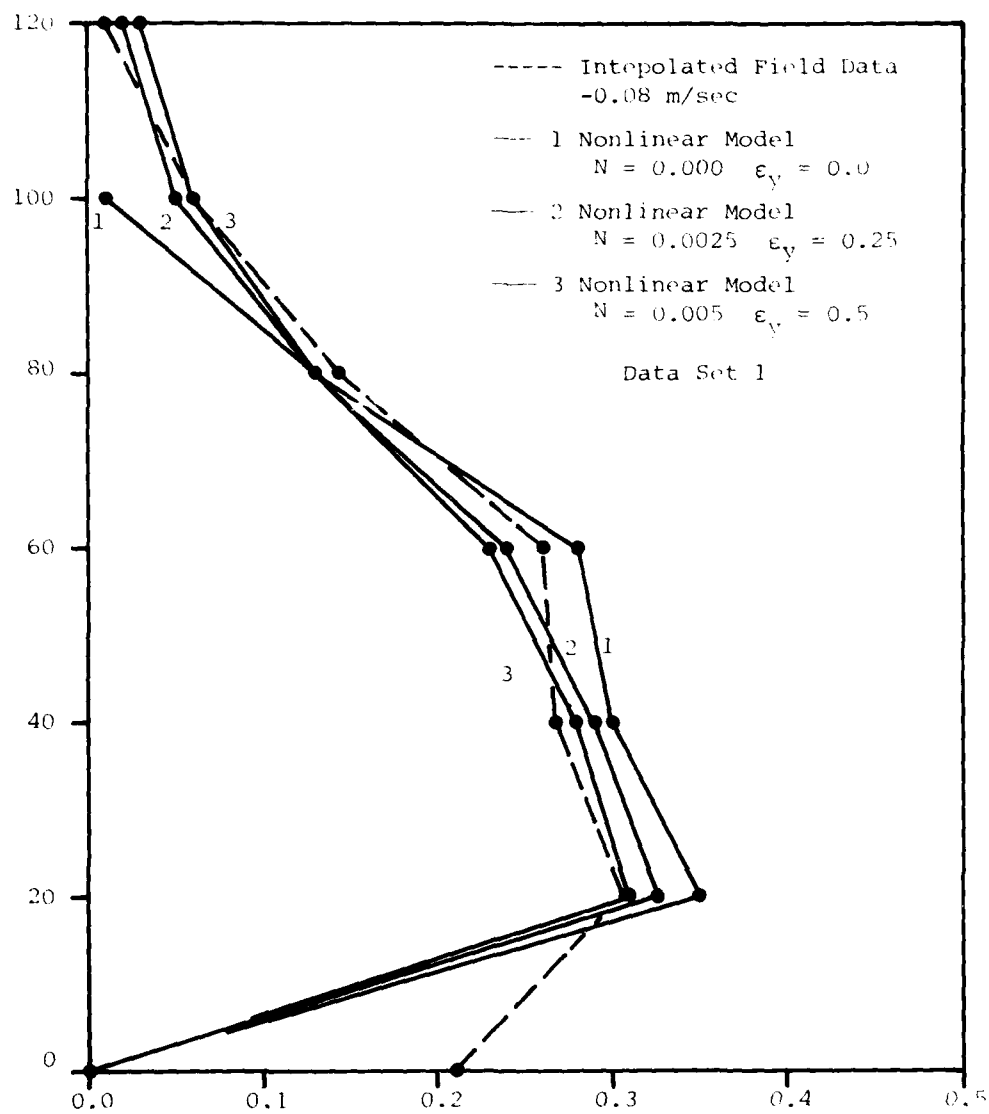


Figure 4-10 Variation of Longshore Current with Lateral Mixing in the Nonlinear Model.
 $f = 0.010$

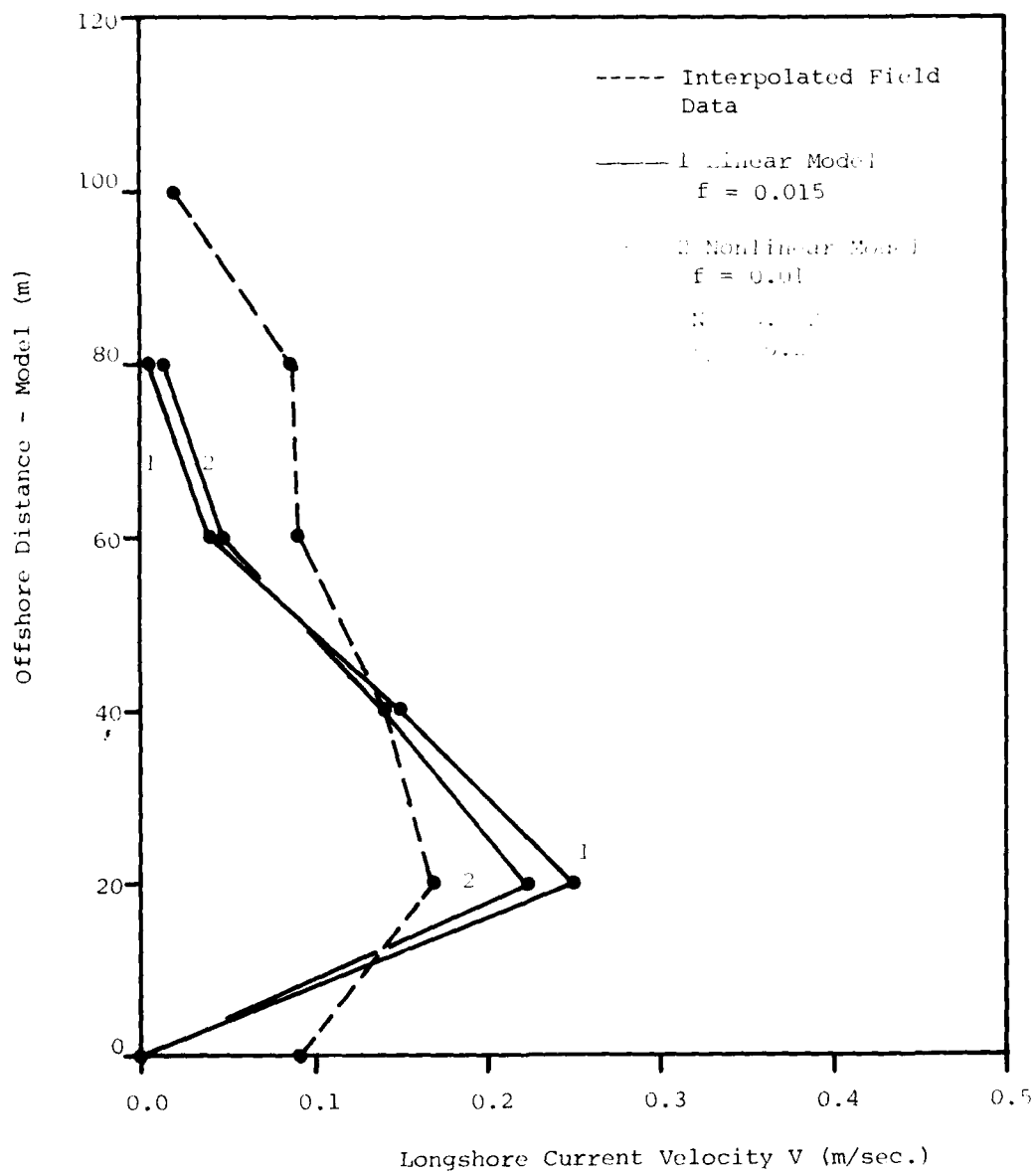


Figure 4-14 Longshore Current in the Linear and Nonlinear Models. Data Set 2

wave directionality and spatial complexity, it would be unjustified to alter the parameters of the model to fit a single case. It may become possible at some future date to estimate mixing parameters based on the characteristics of the random wave field.

A plot of the velocity vectors for data set 2 obtained using the calibrated model and the November 18 bathymetry is shown in Figure 4-15. As in the November 10 case, the circulation pattern is seen to be sensitive to the bottom variations. This result is probably due to the low values obtained for the friction coefficient f .

3. DISCUSSION OF THE CALIBRATED COEFFICIENTS

The value of the friction factor f obtained in this study differs significantly from the value used in previous work and retained by Allender *et al.* (1981). Based on a bottom shear stress relation given by Eqs. (2.27-2.28), Birkemeier and Dalrymple (1976) chose a value of $C_f = 0.01$, which corresponds to a choice of $f = 0.08$. This value of f is carried over into the results discussed in the next chapter. However, model calibration has indicated that the value of f is more of the order 0.01-0.02, with values of 0.015 and 0.01 chosen for the linear and nonlinear models respectively. It is felt that this alteration in choice of the friction factor requires some discussion.

Many formulae exist to calculate the bottom friction factor under waves, the most successful being those of Jonsson (1966) and Kajiura (1968). Writing Kajiura's formula in a form given by Dalrymple and Lozano (1978), we obtain

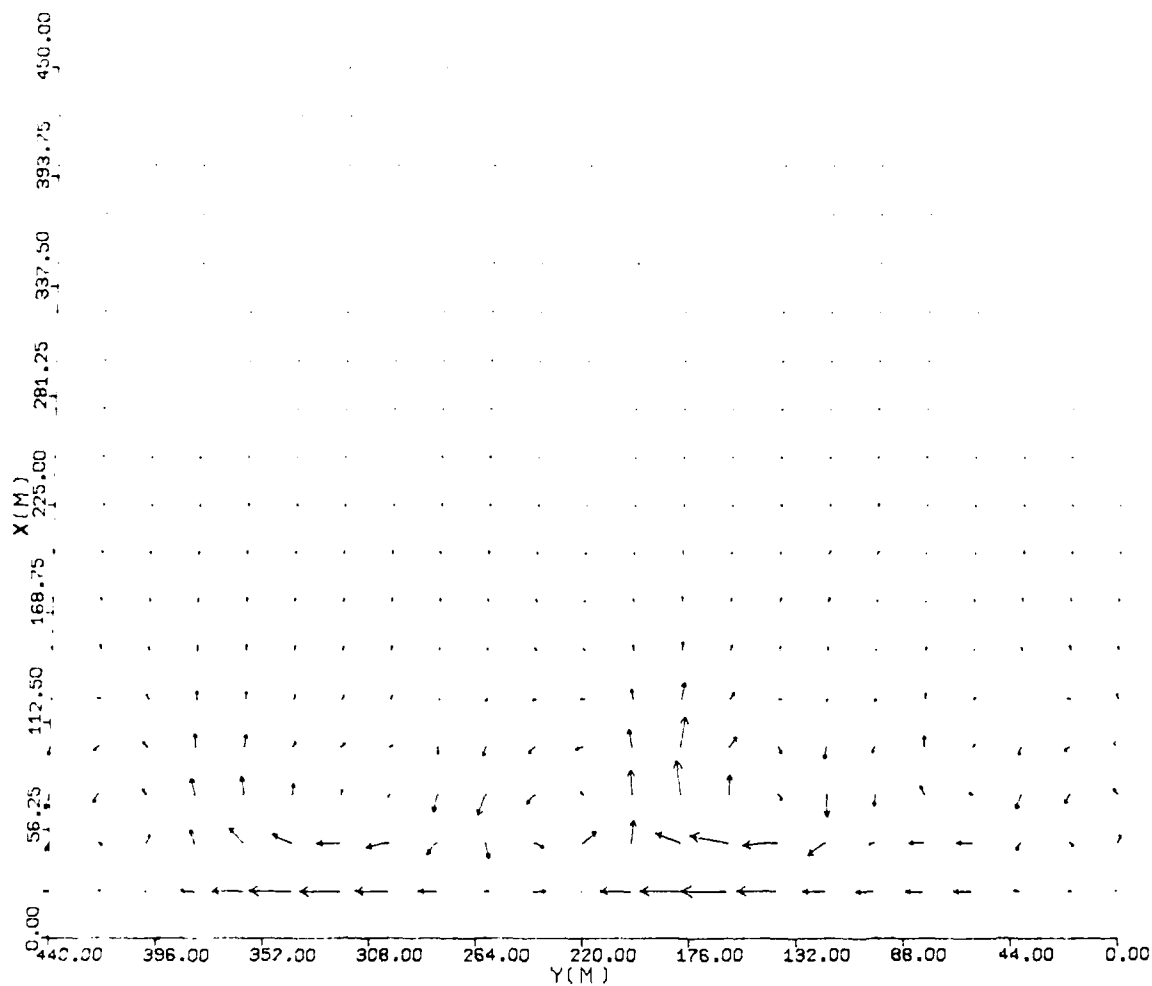


Figure 4-15. Currents Induced on Nov. 18, 1978 Bathymetry
Using Data Set 2: Nonlinear Model.

$$C_f = \frac{f}{8} = 1.41 \left\{ \frac{4\pi d}{T(g h_b \kappa^2)^{1/2}} \right\}^{2/3}$$

where d is the median sand grain diameter and κ is the breaking index. The value of f at the breaker line represents a reasonable choice for an average value over the surf zone region. For Torrey Pines Beach, d is approximately given by

$$d \sim d_{50} = 0.27 \text{ mm}$$

For the field data used, h_b is taken as approximately 1.5 m. This yields a value of

$$C_f = .0025 \text{ or } f = 0.02$$

The values of f obtained during calibration are thus of the correct order of magnitude for flows over a planar bed with no ripples. However, the real physical bottom being studied should exhibit a higher roughness, with length scales based on ripple geometry rather than the sand grain diameter, indicating that the initially chosen value of $C_f = 0.01$ is probably more correct on physical grounds.

In this regard, we note the questionable practice of using distinctly bi-directional wave data to generate monochromatic input wave conditions for calibration purposes. The calibration obtained here possibly constitutes a valid site specific calibration for the Torrey Pines beach, since it was found to be possible to predict net longshore flows resulting from wave fields with several components. In a practical sense, few data sets exist which are strictly useful for calibration purposes.

The values of the offshore mixing coefficient N chosen in this study are approximately one order of magnitude smaller than the corresponding value suggested by Bowen and Inman (1974), who investigated a group of dye dispersion studies performed by various investigators. Some indication that a larger value of N may be desirable is given by Figure (4-9): however, the validity of the field bathymetry is suspect in this case. It should be noted that the model exhibits a certain degree of numerical diffusion when large grid spacings are used, indicating that the value of N chosen should be less than the corresponding physically realistic value in any case.

Chapter V

EXAMPLES OF NUMERICAL RESULTS USING THE NEARSHORE CIRCULATION MODELS

1. INTRODUCTION

Various results of calculations using the linear and nonlinear models have been described in detail in Birkemeier and Dalrymple (1976) and Ebersole and Dalrymple (1979). Results pertaining to the questions of model stability and convergence have been mentioned in the previous chapters, with special attention to the seiching mode of oscillation generated at model start-up. In this chapter, results of model calculations in specific situations will be discussed, with emphasis on comparison to analytic models, and to bottom topographies which reproduce earlier efforts.

In addition to the general facilities for user-defined input, each of the models described in the two previous studies contained specialized facilities for the purpose of illustrating specific situations not covered by the basic model structures. These special cases are discussed here for completeness, although in most cases the final model versions may not retain the corresponding capability.

2. SPECIFIC APPLICATIONS OF THE LINEAR AND NONLINEAR MODELS

In this section, we review results presented by Birkemeier and Dalrymple (1976) and Ebersole and Dalrymple (1979). In addition, we present results for an additional form of generalized topography.

2.1 Plane Beach Applications

Historically, the first application of the averaged momentum flux formulation presented in Chapter II to nearshore dynamics was made in an attempt to explain the phenomenon of wave set-up and longshore wave-induced currents in the surf zone. In the simplest formulation, the equation lead to a linear longshore current profile as shown in Figure 2-2 (Longuet-Higgins, 1970a). The addition of a turbulent stress term representing the effect of lateral mixing leads to a smoothed profile which is more representative of observed current distributions, as discussed by Longuet-Higgins (1970b). In the development in Chapter II, a lateral mixing model in the x and y directions was outlined based on the model used by Longuet-Higgins. Here, we review results calculated both with and without the lateral mixing effects.

Birkemeier and Dalrymple (1976) presented results for set-up resulting from normally incident waves on a plane slope, as shown in Figure 5-1 in comparison with the laboratory measurements of Bowen et al. (1968). Since, for this case, no currents are generated, the distinction between the linear and nonlinear models are inapplicable. The model is seen to accurately reproduce aspects of the solution based on linear incident waves, including the sharp drop in the mean water level just outside of the breaker line. It is noted that this drop can be eliminated, and a more realistic solution obtained, by the use of radiation stress terms derived from cnoidal wave theory (James 1974)). This possible refinement has not been included in the models.

Birkemeier and Dalrymple also investigated the dynamic set-up resulting from a time varying incident wave height given by

$$H_o = H_s + A \sin \left(2\pi n \frac{\Delta t}{T_g} \right) \quad (5.1)$$

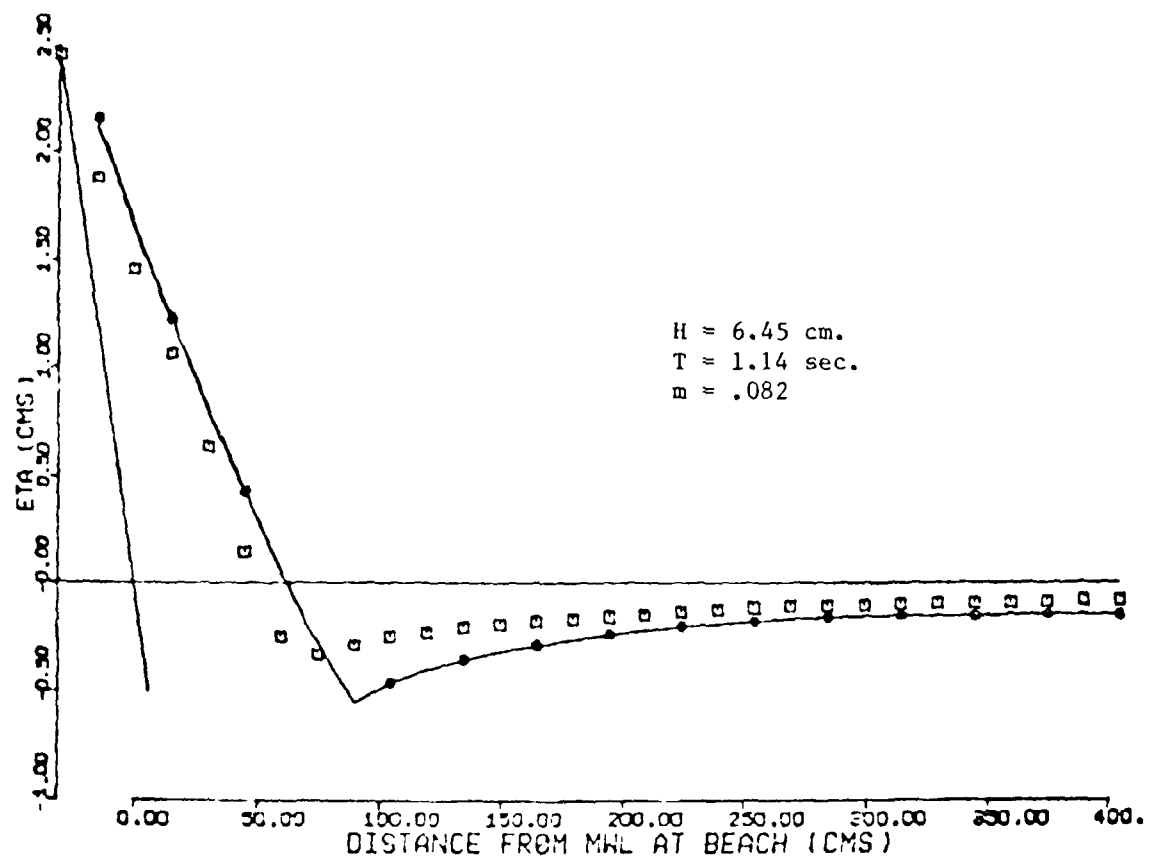


Figure 5-1. Set-up on a Plane Beach

- - Bowen et. al. (1968) experiment
- - Linear Model

where

H_s = starting wave height

A = amplitude of variation

n = iteration index

T_g = group period.

Results for dynamic set-up in comparison to incident wave height are shown in Figure 5-2. As an example of the seiching response of the model, a case was also run where the group period corresponded to the seiche period of the model as given by Eq. (3.5). Figure 5-3 indicates the resulting instability in the set-up which represents the growth of the seiche.

In the previous example, a model seiche appeared as a forced response to the applied wave-induced stress. Figure 5-4 indicates a more typical result of a seiching response to the transient model start-up. In this case, the oscillation is a free motion which gradually dies away due to the effect of bottom friction (as well as numerical dispersion). As mentioned in section 3.4, this type of response can be reduced by a gradual build-up of the incident wave height.

Results for a longshore current on a plane beach are shown in Figure 5-5, for the linear model and no lateral mixing, and in Figure 5-6, for the nonlinear model with mixing. The two solutions clearly represent the behavior predicted by the theoretical solutions, with the exception that the sharp decay in velocity at the breaker line predicted by the solution with no mixing is spread over several grid spaces in the linear model due to the use of finite grid squares. This effect can be reduced by the use of a finer grid spacing.

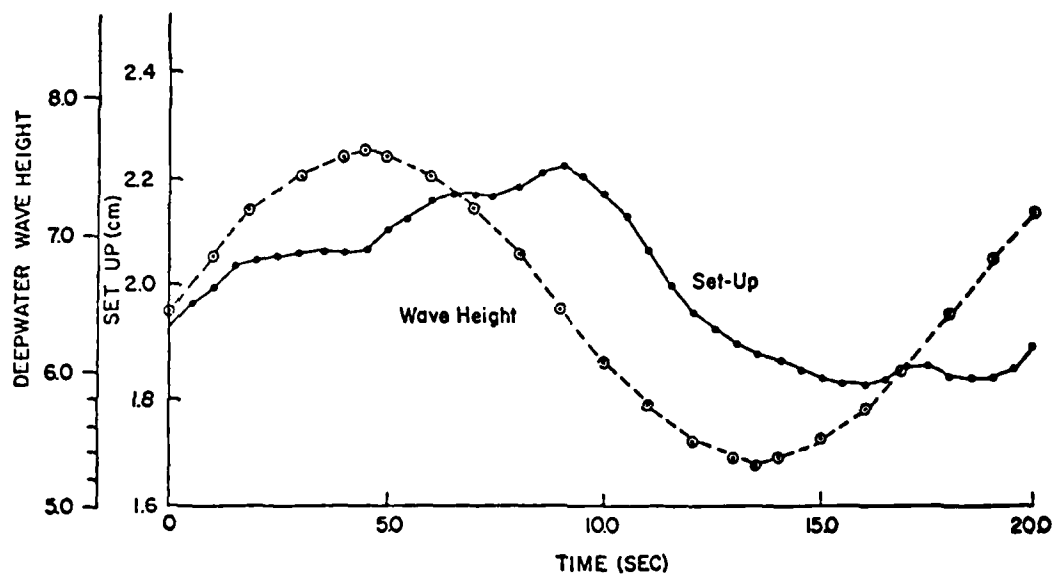


Figure 5-2. Set-up at Shoreline due to a Wave Group
with 18 second period.
Linear Model

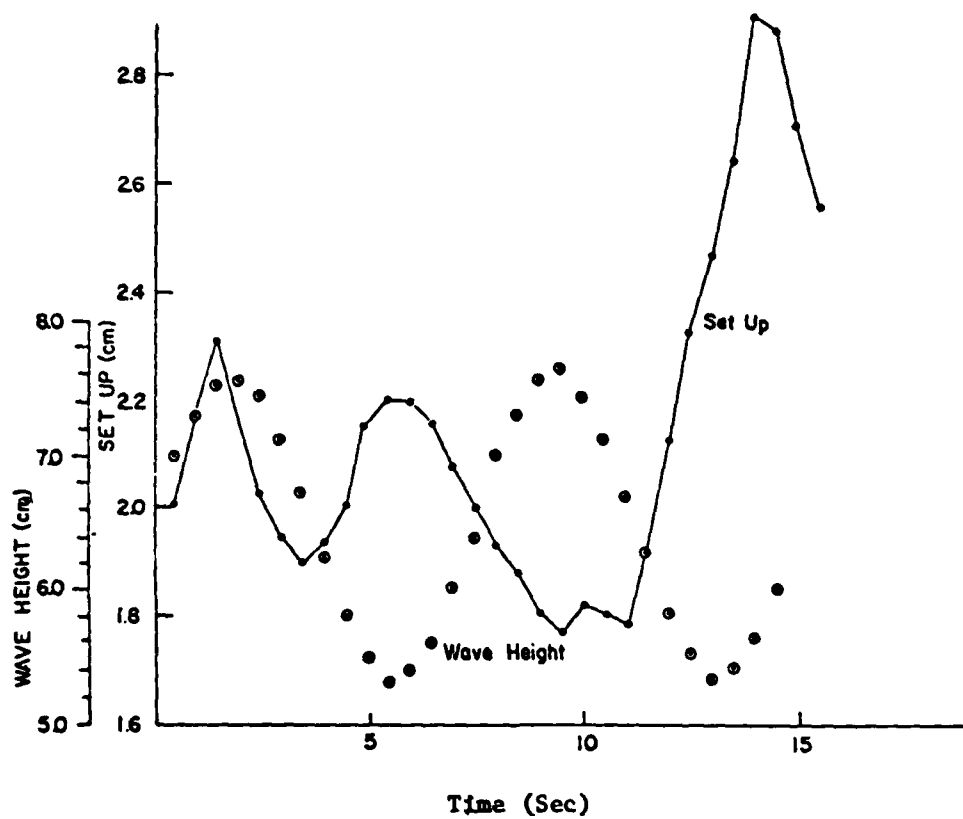


Figure 5-3. Resonance of Wave Channel Due to Forcing at Seiche Period

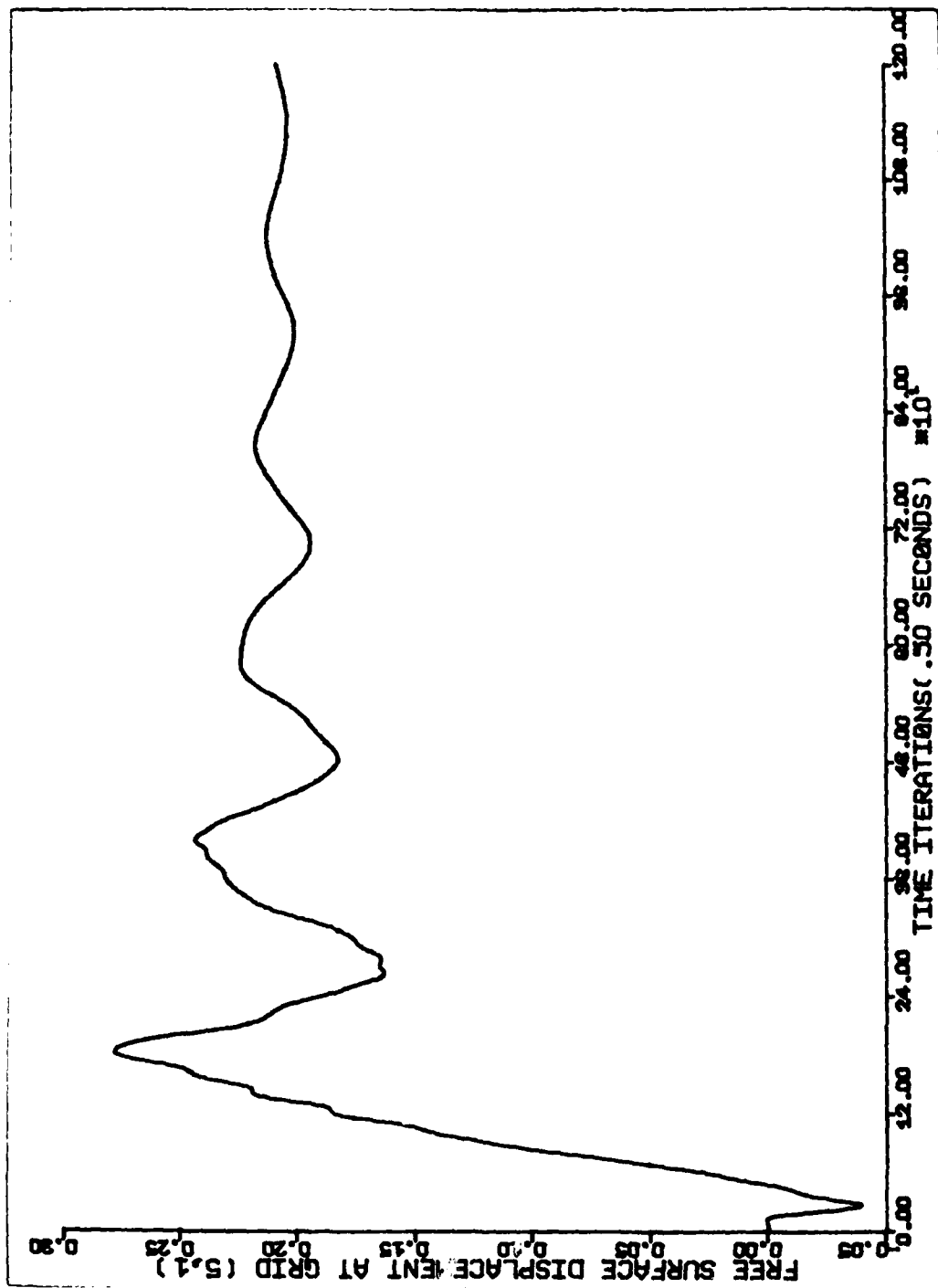


Figure 5-4. Inshore Mean Free Surface Displacement Versus Time for the Non-Linear Model Application to a Plane Beach

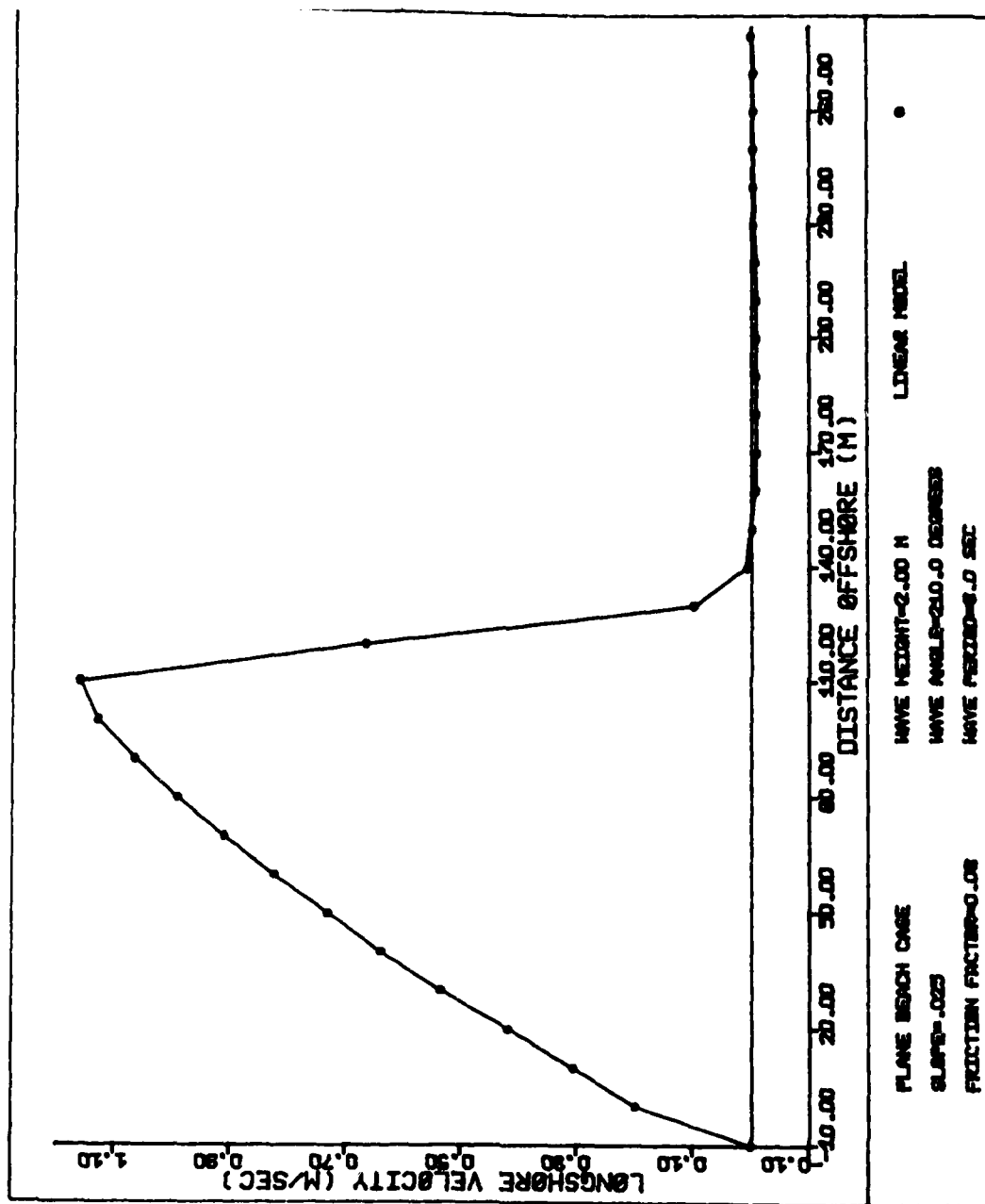


Figure 5-5. Longshore Current Profile for Plane Beach
Linear Model

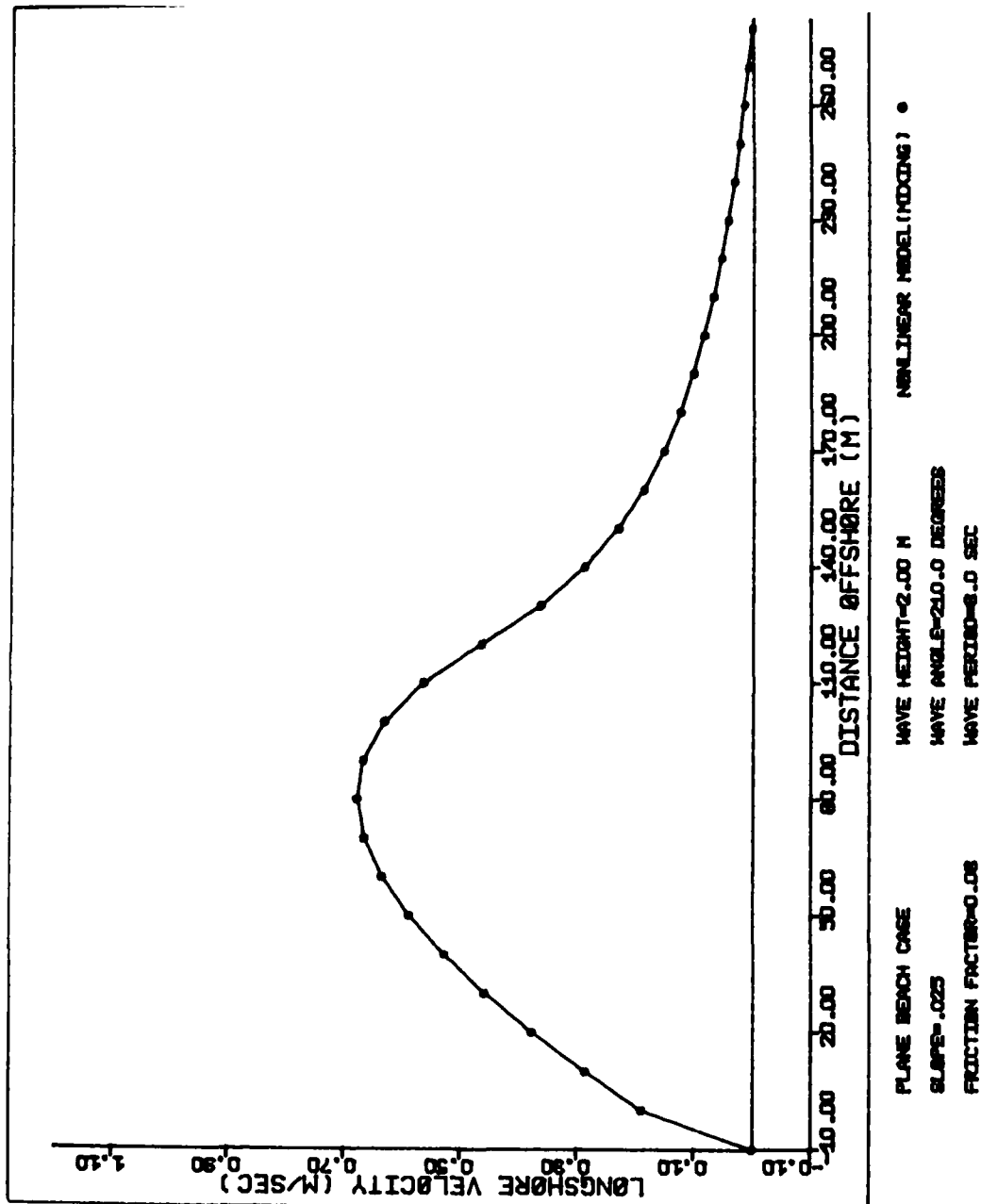


Figure 5-6. Longshore Current Profile for Plane Beach including
Lateral Mixing
Nonlinear Model

The applications discussed here indicate that the model accurately reproduces the available analytic solutions for simplified physical situations.

2.2 Barred Profile Applications

In nature, beaches are often fronted by continuous or fragmented longshore bars. In order to model this situation, the nonlinear model was run using a barred profile (Figure 5-7) for the same wave conditions used to generate the plane beach results described above. For this case, the model was run neglecting the effect of lateral mixing, and including the effect; results are shown in Figures 5-8 and 5-9 respectively. The solution without lateral mixing demonstrates the major discrepancy found between theoretical solution and field data for the special case. As the model wave passes the crest of the offshore bar, it stops breaking since it responds instantaneously to the local bottom. In the absence of lateral mixing, no currents are generated in the trough between shore and bar. This result is in disagreement with field observation as shown recently by Allender et al. (1981) as well as other investigators. The inclusion of lateral mixing effects partially alleviates this discrepancy.

Two factors may contribute to the observations that currents in natural surf zones tend to be strongest in the trough between bar and shore. First, fragmented bars tend naturally to induce two dimensional flow patterns characterized by rip currents flowing seaward at the gaps in the bar system. These currents are driven by longshore variations in the set-up resulting from interaction between the incident waves and the non-uniform topography.

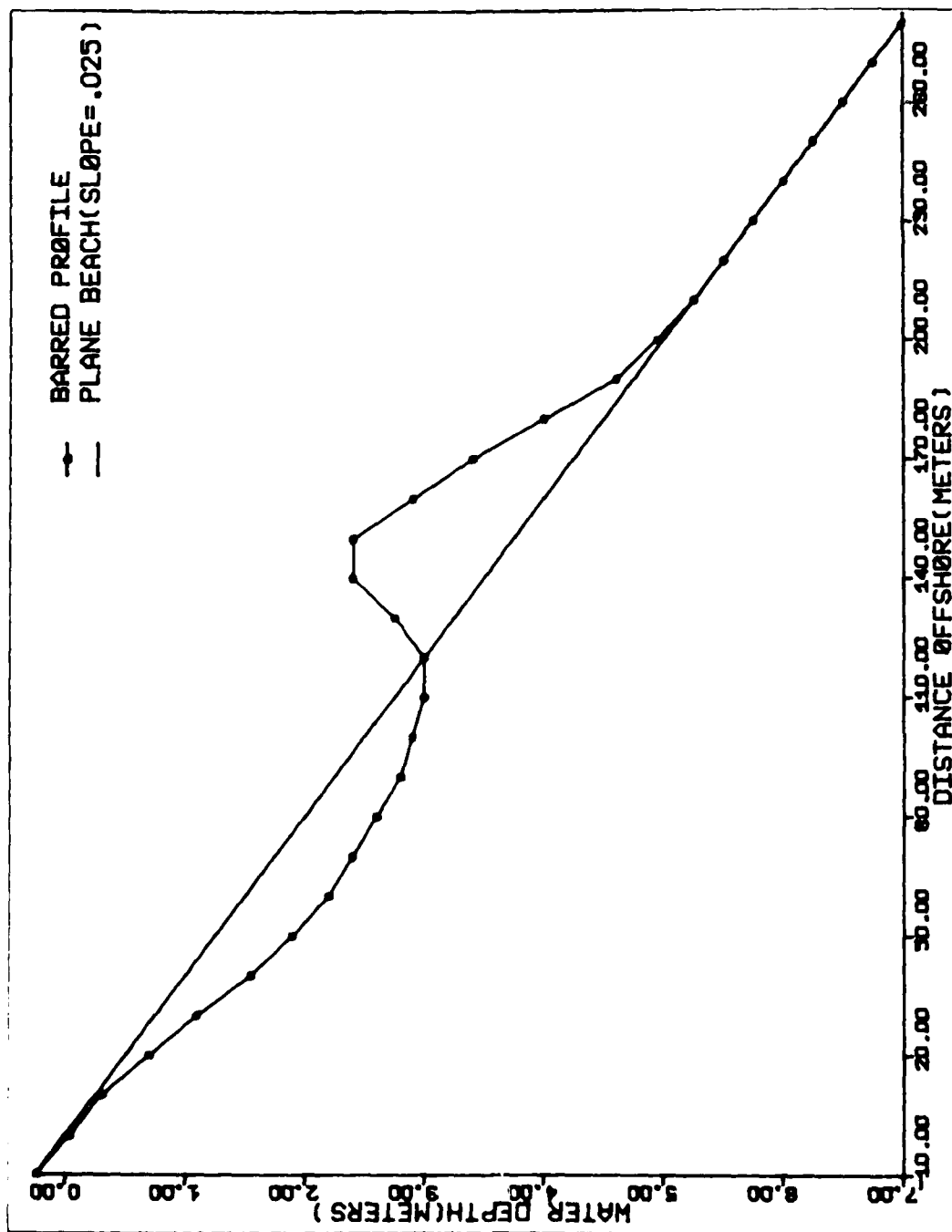


Figure 5-7. Barred Profile used for Results in Figures 5-8, 5-9.

AD-A118 518

DELAWARE UNIV NEWARK DEPT OF CIVIL ENGINEERING
NUMERICAL MODELING OF THE NEARSHORE REGION.(U)
JUN 82 J T KIRBY, R A DALRYMPLE

F/G 8/3

N00014-81-K-0297

NL

UNCLASSIFIED

CE-82-24

2 of 2

40 A
118518

END
DATE
FILMED
10-82
DTIC

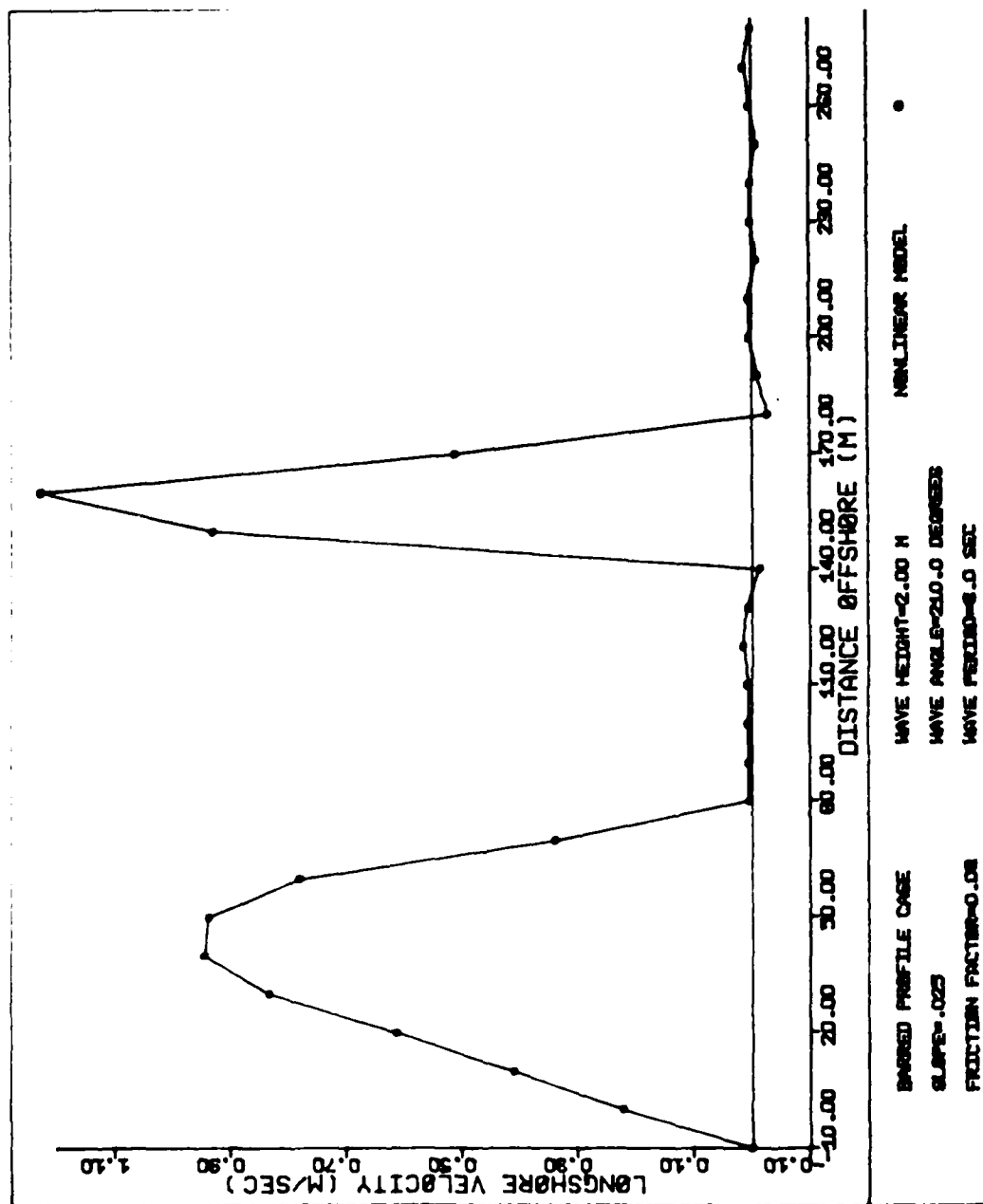


Figure 5-8. Longshore Current for Barred Profile
Nonlinear Model, No Lateral Mixing

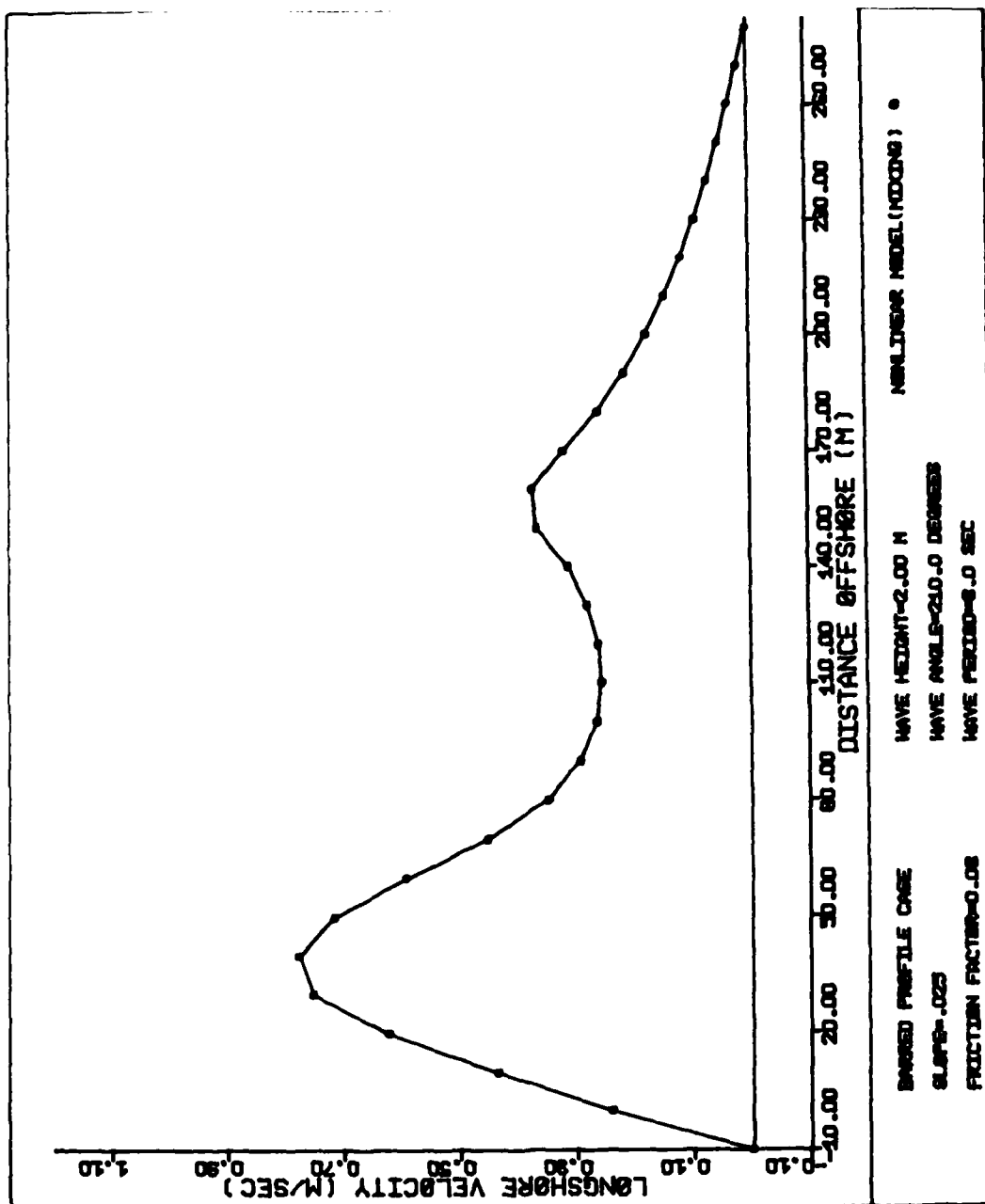


Figure 5-9. Longshore Current for Barred Profile
Nonlinear Model, Lateral Mixing Included

In these situations, currents flowing along the beach are driven by gradients in the mean water surface; the flow is naturally higher in the trough, where hydraulic resistance is lower. This mechanism for rip current maintenance has been discussed by Dalrymple (1978). It is possible that this mechanism will always bias the currents observed on real beaches.

The second possibility perhaps lies in the standard treatment of surf zone wave height as a function only of the local depth. The process of wave breaking initiates a turbulent flow pattern which is certain to have some time dependence, at least in its decay. A model for spilling breakers including this effect has been discussed by Longuet-Higgins and Turner (1974). It is possible, then, that an accurate picture of currents on a barred profile would require the inclusion of a continuation of wave energy decay in a time dependent manner past the point where the wave stops shoaling. Wave energy decay models have been used successfully by Divoky, LeMehaute and Lin (1970) in a study of wave height decay in the surf zone, and by Miller and Barcilon (1978) in a study of rip currents. However, present models do not allow for the cessation of breaking, which is required if the process of wave breaking and reformation is to be successfully treated.

2.3 Applications to the Laboratory Wave Basin

In order to model currents in a laboratory wave basin, the linear model described here was modified to include no flow boundary conditions at the longshore boundaries. (This option is not included in the present model.) Model tests were conducted to numerically approximate the experimental set-up and analytic theory of Dalrymple et al. (1977). In the physical experiment,

a plane beach was established at an angle of 15° to a flap-type wavemaker. Waves approached the beach over a flat bottom until they reached the front of the beach slope, where refraction effects began. Three cases were tested experimentally and theoretically; here, we restrict our attention to the case where the surf zone is bounded laterally by walls extending to infinity in the offshore direction. Experimentally determined streamlines are shown in Figure (5-10), in comparison to the analytic solution. In the numerical model, the physical situation was altered by extending impermeable walls in a direction normal to the beach; the waves, however, are allowed to propagate freely according to refraction governed by an infinite beach. The numerical model corresponded to the conditions used to develop the analytic solution. Velocity vectors calculated by the linear model are shown in Figure (5-11), in mirror image to the geometry in Figure (5-10). Longshore current velocities calculated by the linear model are compared to experimental values in Figure (5-12). The model is seen to underpredict currents in comparison to the analytic and experimental results.

2.4 Periodic Bottom Topography

In a study of rip currents caused by submerged on-offshore channels, Noda (1970) developed an equation for the depth which produces a channel oriented at an angle to the beach. The present models were tested using Noda's periodic bottom, given by

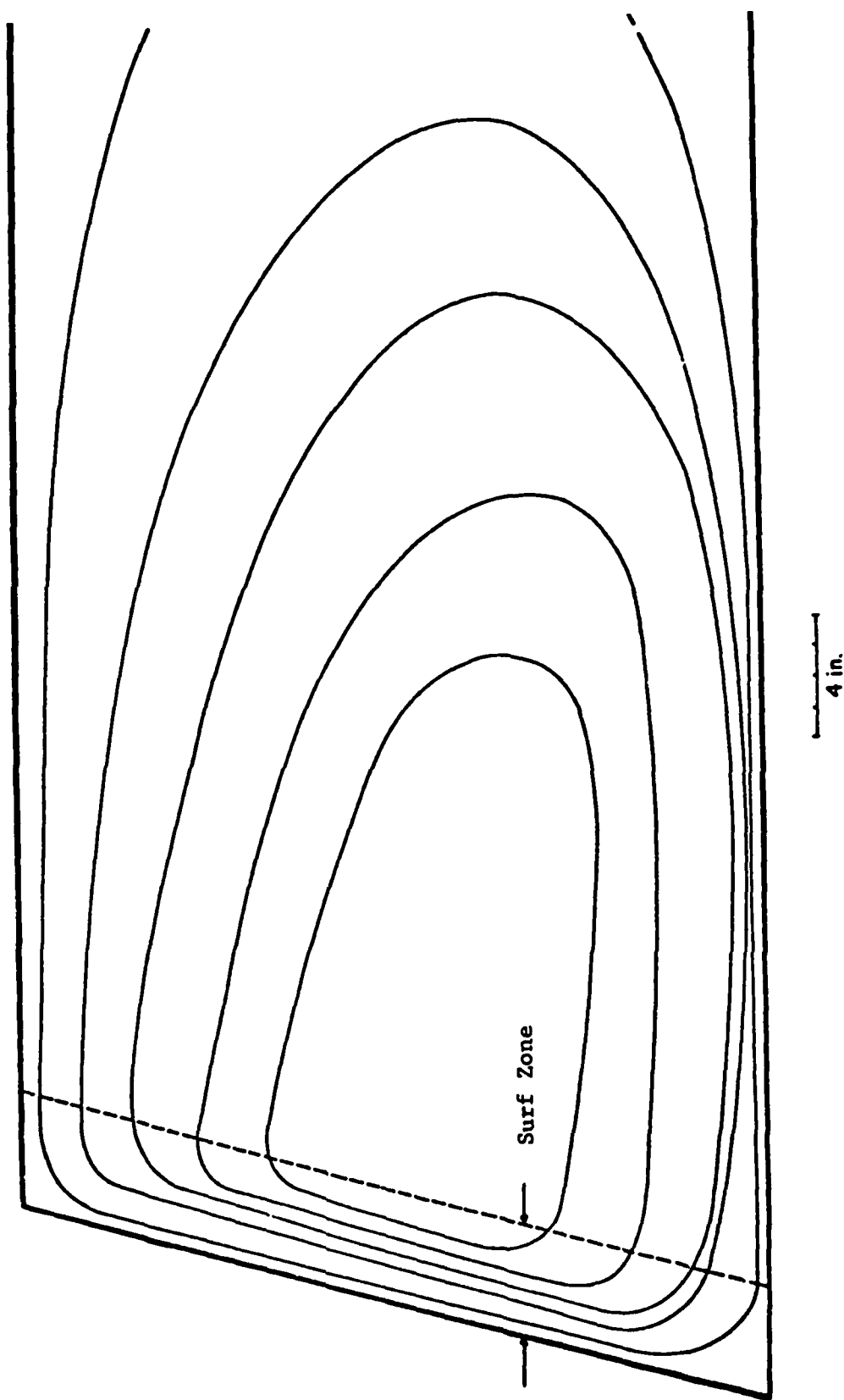


Figure 5-10. Experimental Streamlines in the Wave Basin [From Dalrymple et al. (1977)].

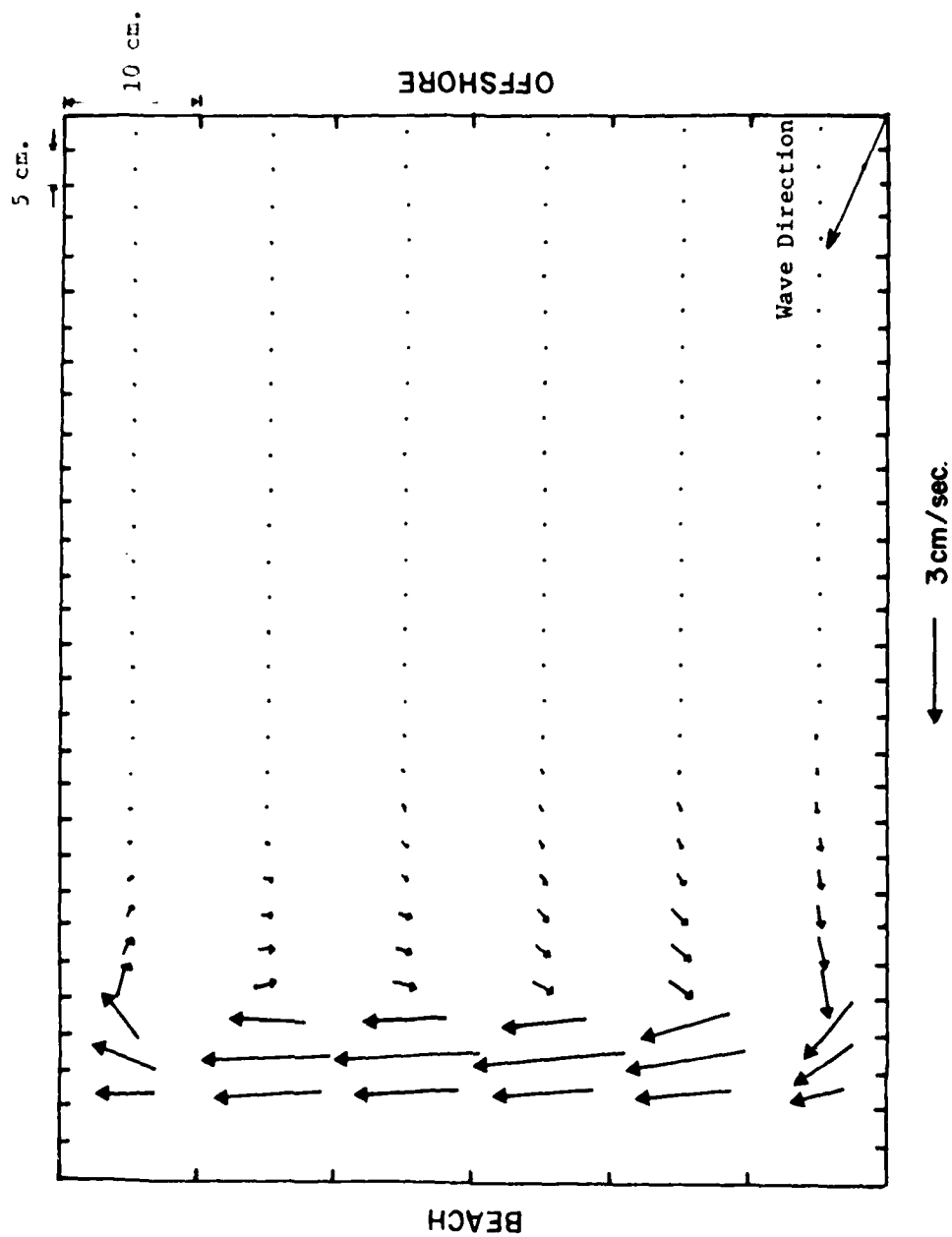


Figure 5-11. Calculated Velocity Vectors for Closed Basin Corresponding to Experimental Results of Figure 5-10

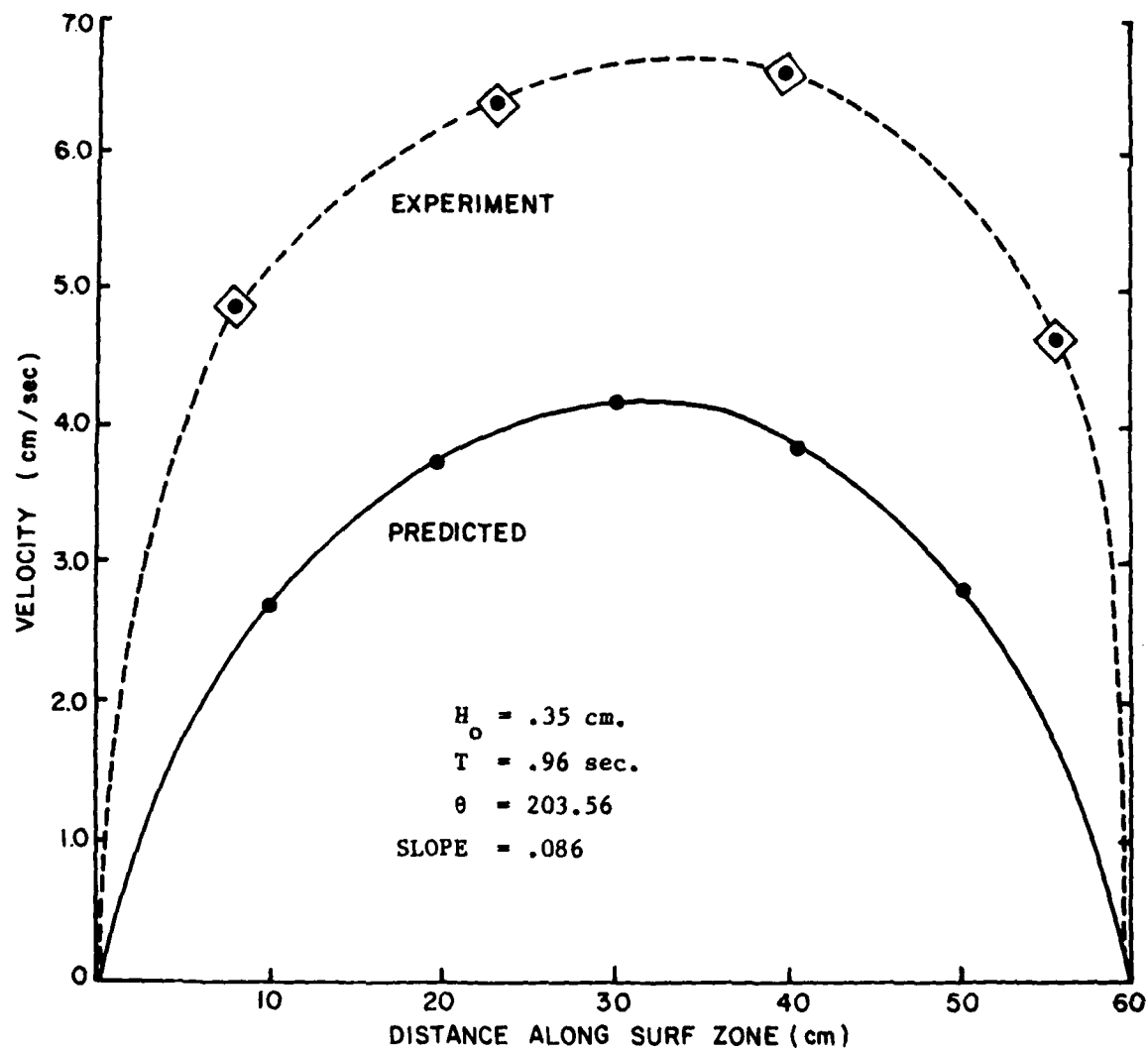


Figure 5-12. Predicted and Measured Longshore Velocities
for the Closed Basin Test Case.
Linear Model.

$$D_{i,j} = \begin{cases} -m(4 - i)\Delta x & i = 1, 2, 3, 4 \\ m\Delta x \{1 + A \exp[-3(\frac{x}{20})^{1/3}] \sin^{10} \frac{\pi}{\lambda} (y - x \tan \beta)\} & i > 4 \end{cases}$$

where

- x, y are coordinates of grid (i, j)
- m = average beach slope = 0.025
- λ = length of periodicity = 70 m
- A = amplitude of bottom variation = 20
- β = angle of rip channel to beach normal = 30°

The test contours are shown in Figure 5-13. The bottom topography was intended to model a field case studied by Sonu (1972). Current vectors calculated using the linear model are shown in Figure 5-14; current magnitude agree well with the field data reported in Noda et al. (1974), and are higher than the currents calculated in Noda et al.'s model, in which only 50% of the calculated current is used in determining the wave number due to numerical instability problems.

The Noda profile was also tested using the nonlinear model with lateral mixing (Figure 5-15). The effect of the extra terms modelled is to largely drop out the rip current clearly seen in the linear model results. Similar results have been obtained by Liu (1982), using a finite element approach, but the absence of a rip current under the given conditions is clearly at odds with the field data of Sonu (1972).

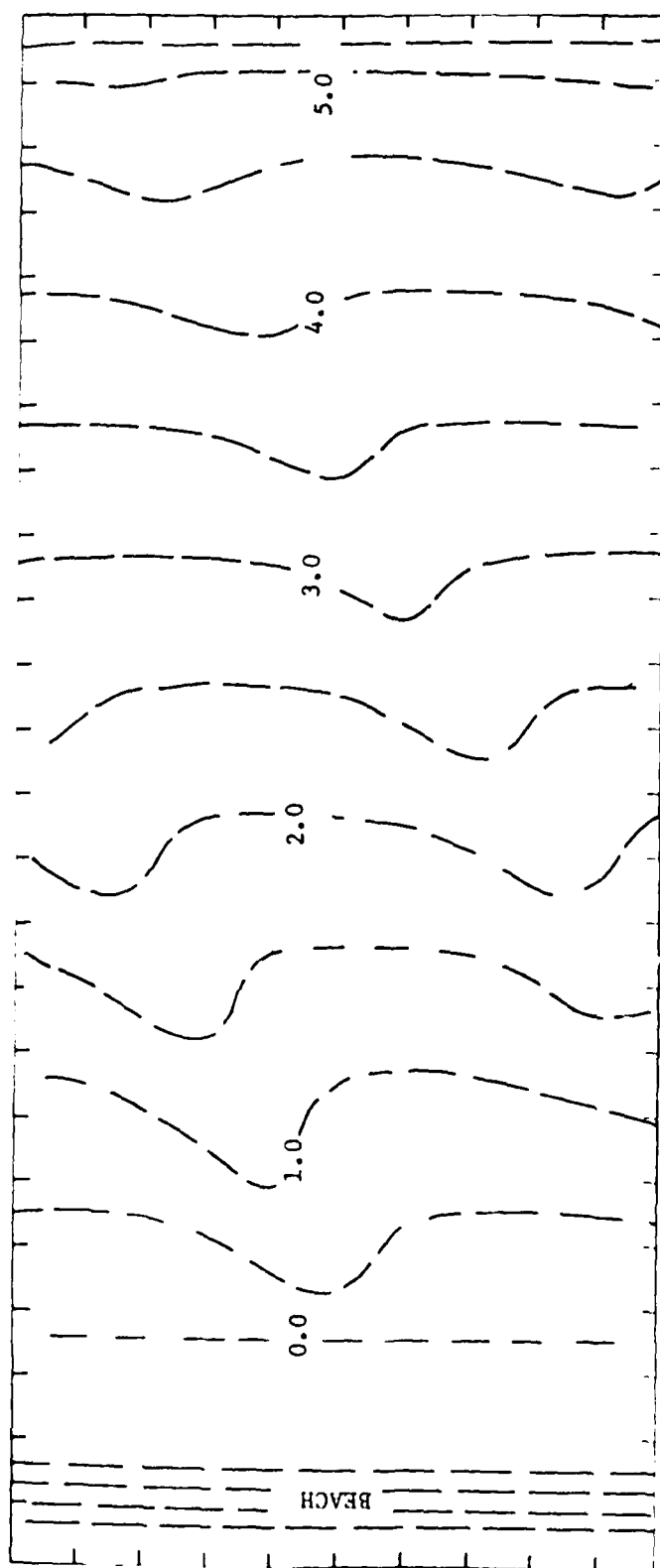


Figure 5-13. Depth Contours for the Periodic Bottom Due to Noda (1973).

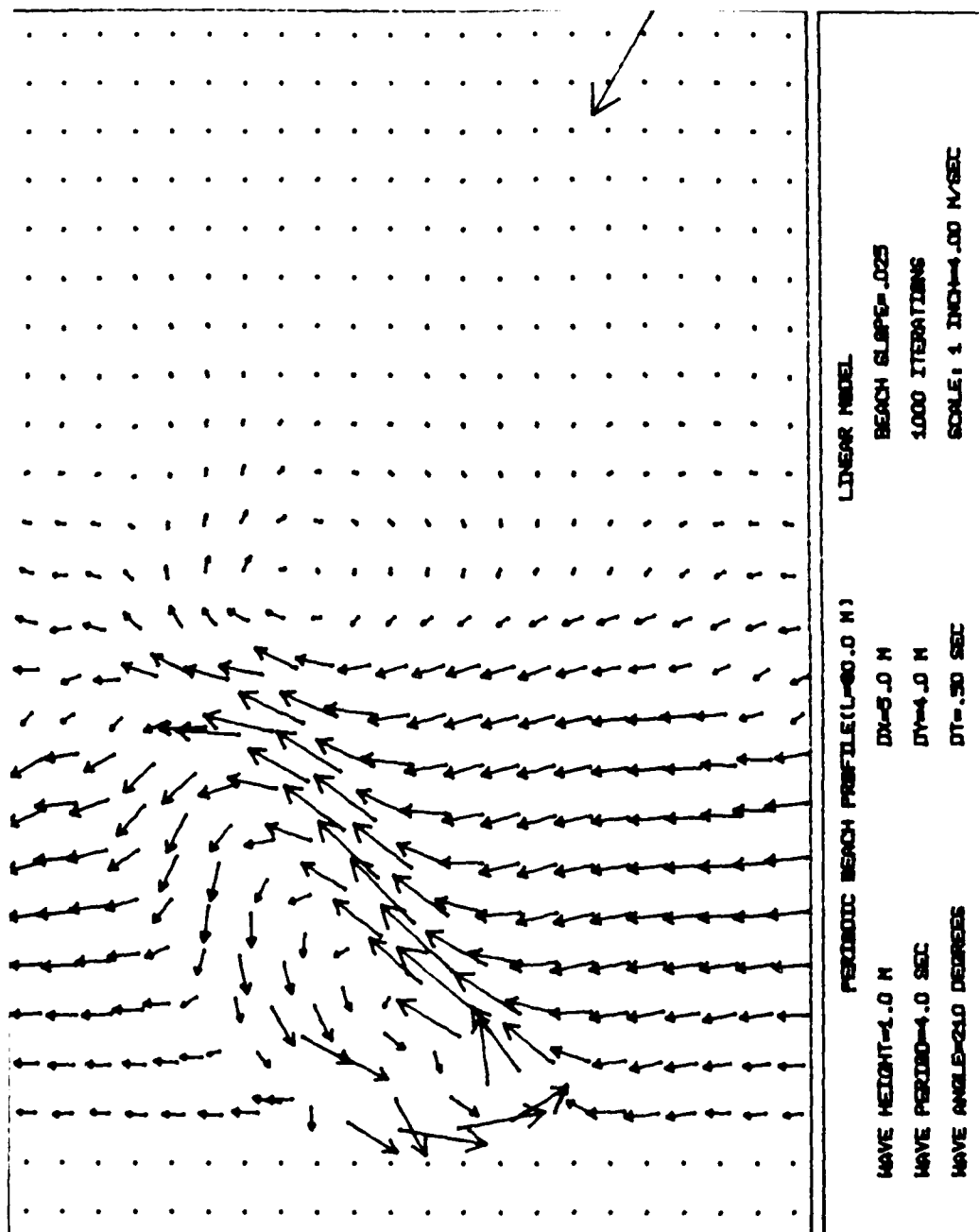


Figure 5-14. Current Vector Plot for Bottom Topography of Noda.
Linear Model, No Lateral Mixing.

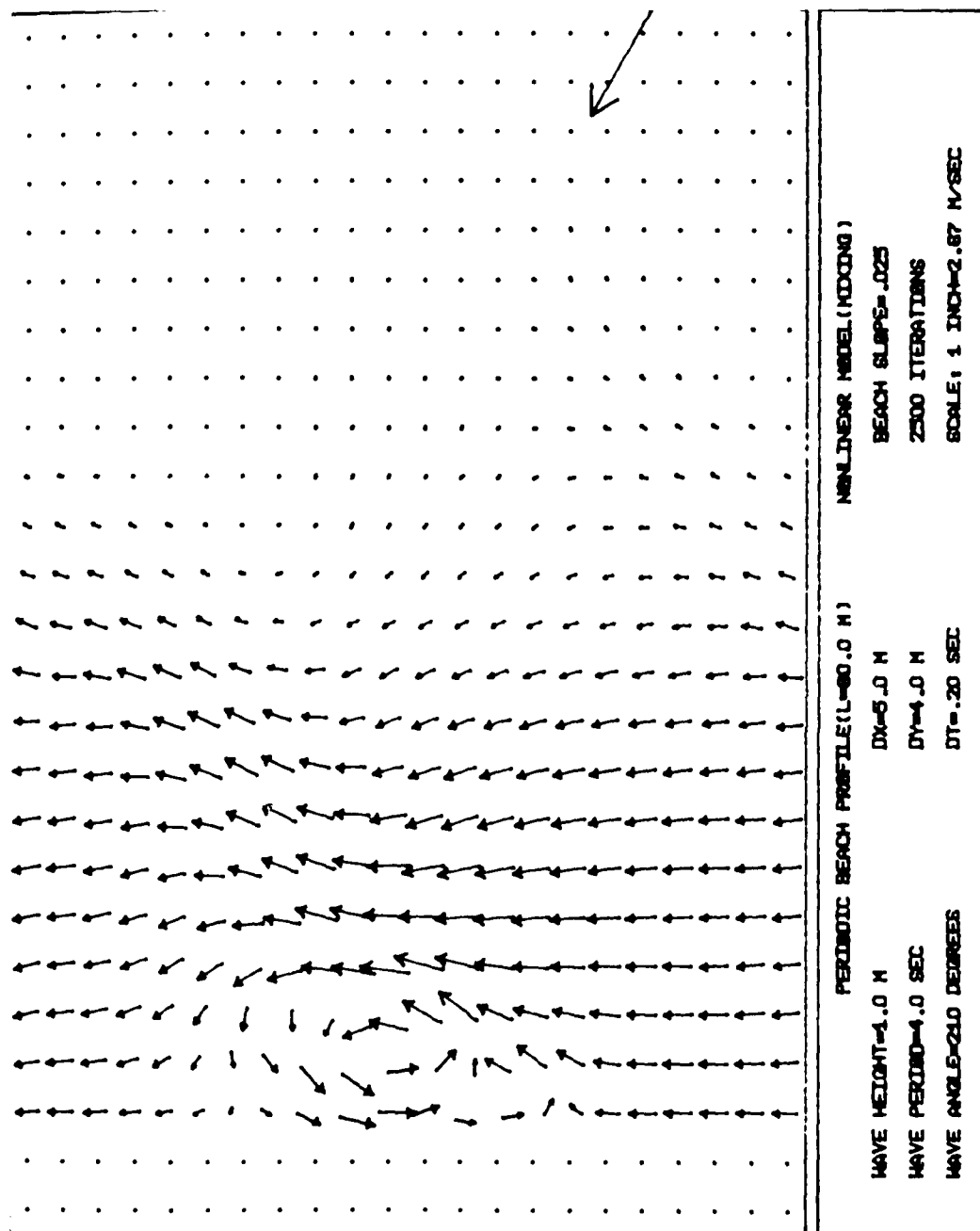


Figure 5-15. Current Vector Plot for Bottom Topography of Noda.
Nonlinear Model, Lateral Mixing Included.

A second periodic topography has been investigated for the present study. It is well established that the presence of a nearly shore-normal channel deeper than the surrounding beach slope will tend to induce a rip current, with flow directed offshore in the channel. For the present case, a longshore-periodic perturbation consisting of a localized bulge, or relatively shallow region, has been added to an otherwise planar beach profile. The bottom is given by the relation

$$D_{i,j} = \begin{cases} -m(2-i)\Delta x & i = 1 \\ m(i\Delta x)(1 - 0.9 \cos^6 \left\{ \frac{j}{(N-1)} \pi \right\}) \exp(-0.015 i\Delta x) & i > 1 \end{cases}$$

where

m = average beach slope = 0.02

i, j = grid coordinates

$(N-1)\Delta y$ = longshore periodicity

Results using both models are shown in Figures 5-16 and 5-17. The effect of the inclusion of convective acceleration terms in the nonlinear model is not apparent in the results, which may be a result of the counterbalancing effect of lateral mixing. The lateral mixing effect can be seen in the shoremost grid row. The overall effect modelled here can be explained most simply in terms of a longshore imbalance in the steady state set-up. As the bulge concentrates wave energy by refraction, a region of relatively high breaking waves is created. As water is pumped on shore by the gradient of the onshore radiation stress, a localized region of high set-up is created; this region in turn pumps the onshore-flowing water alongshore into the regions of low set-up. The waves over the region of the bulge then must continuously pump water onshore in an attempt to fill the surf zone up to the

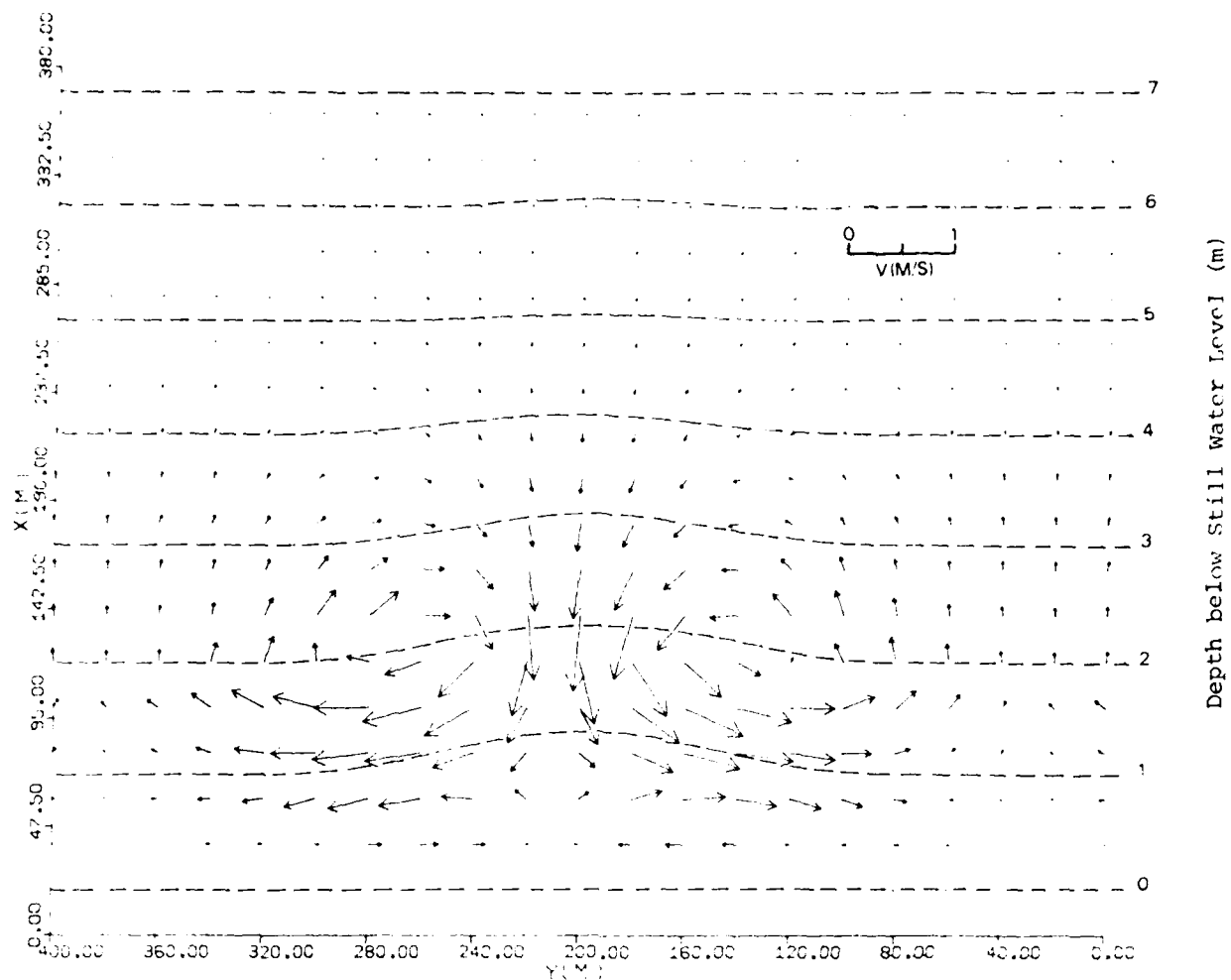


Figure 5-16. Currents Induced by Bulge on a Plane Beach Linear Model:
 $T = 10.0 \text{ s}$, $H_o = 1.0 \text{ m}$, $\theta_o = 180^\circ$.

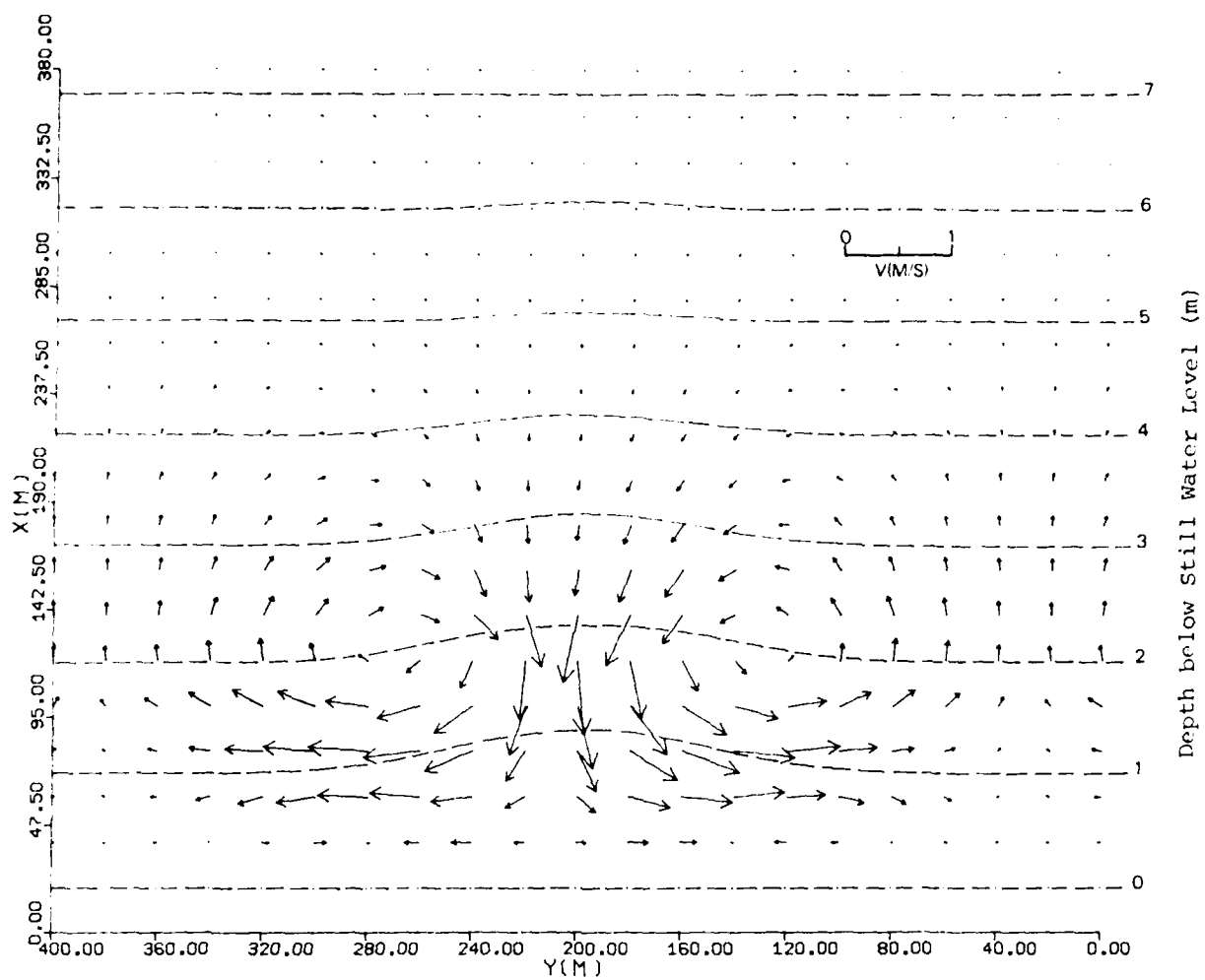


Figure 5-17. Currents Induced by Bulge on a Plane Beach Nonlinear Model:
 $T = 10.0$ s, $H_0 = 1.0$ m, $\theta_0 = 180^\circ$.

level determined by the decay of wave energy, leading to a steady state circulation pattern.

2.5 Intersecting Waves Application

Ebersole and Dalrymple have discussed the application of the model to the case of intersecting wave trains of the same frequency on a plane beach, which provides a mechanism for generating rip currents, as shown by Dalrymple (1975). The purpose of this application was to investigate the effect of the convective acceleration terms in the model. The following derivation closely follows the work of Dalrymple.

Given two intersecting wave trains A and B with amplitudes a and b and a common frequency, σ , in terms of the coordinate system shown in Figure 5-18, the free surface displacements for the two wave trains can be written as,

$$\eta_A = a \cos(k \cos \alpha x + k \sin \alpha y + \sigma t)$$

$$\eta_B = b \cos(k \cos \beta x + k \sin \beta y + \sigma t) \quad .$$

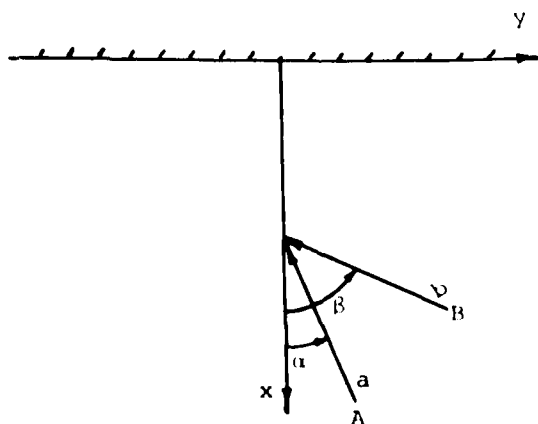


Figure 5-18. Wave Angles for Intersecting Waves.

The total free surface $\eta_T = \eta_1 + \eta_2$ can then be written as,

$$\begin{aligned} \eta_T = & 2a \cos \left\{ \frac{k}{2}(\cos \alpha + \cos \beta)x + \frac{k}{2}(\sin \alpha + \sin \beta)y + \sigma t \right\} \cdot \\ & \cos \left\{ \frac{k}{2}(\cos \alpha - \cos \beta)x + \frac{k}{2}(\sin \alpha - \sin \beta)y \right\} \\ & + (b-a) \cos \{k \cos \beta x + k \sin \beta y + \sigma t\} \quad . \end{aligned} \quad (5.2)$$

Using the linearized dynamic free surface boundary condition the velocity potential ϕ_T can be shown to equal,

$$\begin{aligned} \phi_T = & \frac{2ag}{\sigma} \frac{\cosh k(h+z)}{\cosh kh} \sin \left\{ \frac{k}{2}(\cos \alpha + \cos \beta)x + \frac{k}{2}(\sin \alpha + \sin \beta)y + \sigma t \right\} \cdot \\ & \cos \left\{ \frac{k}{2}(\cos \alpha - \cos \beta)x + \frac{k}{2}(\sin \alpha - \sin \beta)y \right\} \\ & + \frac{(b-a)}{\sigma} \frac{\cosh k(h+z)}{\cosh kh} \sin \{k \cos \beta x + k \sin \beta y + \sigma t\} \quad . \end{aligned}$$

From the velocity potential the total orbital velocities can be found from,

$$u = - \frac{\partial \phi}{\partial x} \quad , \quad v = - \frac{\partial \phi}{\partial y} \quad , \quad w = - \frac{\partial \phi}{\partial z} \quad .$$

The radiation stresses, which are essentially the forcing terms, are defined as,

$$\begin{aligned} S_{xx} &= \int_{-h}^0 \overline{\rho u^2} dz + \int_{-h}^{\eta} \bar{P} dz - \frac{1}{2} \rho g (h + \bar{\eta})^2 + \frac{1}{2} \rho g \bar{\eta}^2 \\ S_{yy} &= \int_{-h}^0 \overline{\rho v^2} dz + \int_{-h}^{\eta} \bar{P} dz - \frac{1}{2} \rho g (h + \bar{\eta})^2 + \frac{1}{2} \rho g \bar{\eta}^2 \\ S_{xy} &= \int_{-h}^0 \overline{\rho uv} dz \end{aligned}$$

where

$$\bar{P} = \rho g (\bar{\eta} - z) + \frac{\partial}{\partial x} \int_z^0 \overline{\rho uw} dz + \frac{\partial}{\partial y} \int_z^0 \overline{\rho vw} dz - \overline{\rho w^2} \quad .$$

The radiation stresses are found to be given by

$$S_{xx} = \frac{\rho g}{4 \sinh 2kh} [a^2 \cos^2 \alpha + b^2 \cos^2 \beta + 2ab \cos \alpha \cos \beta \cos \{2\psi\}] \cdot$$

$$\{2kh + \sinh 2kh\} - \frac{\rho g ab}{8 \sinh 2kh} (\cos \beta - \cos \alpha)^2 \cos \{2\psi\} \cdot$$

$$\{2kh \cosh 2kh - \sinh 2kh\} - \frac{\rho g ab}{8 \sinh 2kh} (\sin \alpha - \sin \beta)^2 \cos \{2\psi\} \cdot$$

$$\{2kh \cosh 2kh - \sinh 2kh\} - \frac{\rho g}{4 \sinh 2kh} [a^2 + b^2 + 2ab \cos \{2\psi\}] \cdot$$

$$\{\sinh 2kh - 2kh\} + \rho g ab \cos^2 \psi + \frac{1}{4} \rho g (b-a)^2$$

$$S_{yy} = \frac{\rho g}{4 \sinh 2kh} [a^2 \sin^2 \alpha + b^2 \sin^2 \beta + 2ab \sin \alpha \sin \beta \cos \{2\psi\}] \cdot \{2kh + \sinh 2kh\}$$

$$- \frac{\rho g ab}{8 \sinh 2kh} (\cos \beta - \cos \alpha)^2 \cos \{2\psi\} \cdot \{2kh \cosh 2kh - \sinh 2kh\}$$

$$- \frac{\rho g ab}{8 \sinh 2kh} (\sin \alpha - \sin \beta)^2 \cos \{2\psi\} \cdot \{2kh \cosh 2kh - \sinh 2kh\}$$

$$- \frac{\rho g}{4 \sinh 2kh} [a^2 + b^2 + 2ab \cos \{2\psi\}] \cdot \{\sinh 2kh - 2kh\}$$

$$+ \rho g ab \cos^2 \psi + \frac{1}{4} \rho g (b-a)^2$$

$$S_{xy} = \frac{\rho g}{4 \sinh 2kh} [a^2 \sin \alpha \cos \alpha + b^2 \cos \beta \sin \beta + ab \cos \{2\psi\} \sin \{\alpha + \beta\}] \cdot$$

$$\{2kh + \sinh 2kh\}$$

where the expression " ψ " is defined as,

$$\psi \equiv \frac{k}{2} (\cos \alpha - \cos \beta) x + \frac{k}{2} (\sin \alpha - \sin \beta) y \quad .$$

The time independent mean free surface displacement, $\bar{\eta}$, is defined by

$$\bar{\eta} \equiv -\frac{1}{2g} \overline{\{u^2 + v^2 + w^2\}}_{z=0}$$

where "—" denotes the time average over one wave period. Substituting the expressions for the velocity components u , v , and w from the velocity potential ϕ_T , $\bar{\eta}$ can be written as,

$$\bar{\eta} = \frac{-k}{2\sinh 2kh} [a^2 + b^2 + 2ab\cos\{2\psi\} \cdot (\cos(\alpha - \beta)\cosh^2 kh - \sinh^2 kh)] \quad (5.3)$$

where " ψ " is the same quantity defined previously. Notice that the mean free surface displacement is modulated in the x and y directions by,

$$\cos\{k(\cos\alpha - \cos\beta)x + k(\sin\alpha - \sin\beta)y\}.$$

Using Snell's Law which states

$$k_o \sin\alpha_o = k \sin\alpha \quad \text{and} \quad k_o \sin\beta_o = k \sin\beta,$$

and using the fact that $k_o \equiv \frac{2\pi}{L_o}$, where "o" denotes deep water values for the wave length, L , and the wave angles, α and β , we see that there is a periodicity of the mean displacement in the longshore direction with a periodic spacing, ℓ , given by,

$$\ell = \frac{L_o}{\sin\alpha_o - \sin\beta_o}$$

This periodicity in water level and wave height causes water to be driven from regions of high mean water level displacement to regions of lower displacement, resulting in the formation of circulation cells.

In order to attempt to model this phenomena, certain simplifications to the model had to be made. Since the refraction and shoaling routines borrowed from the work of Noda,et al., could not treat more than one wave train, they were replaced with routines governed by Snell's Law neglecting wave-current interaction. Again a quadratic, "exact," bottom friction was used including velocities due to mean currents and, this time, the two wave trains. In the momentum equations the advective acceleration terms were retained, horizontal mixing was neglected, and the radiation stresses were calculated using the results presented earlier in this section. The wave height used in calculating the radiation stresses and the bottom frictional stresses is given by

$$H_T = 2.0 \sqrt{a^2 + b^2 + 2ab \cos[k(\cos\alpha - \cos\beta)x + k(\sin\alpha - \sin\beta)y]} .$$

Two runs are presented here using different combinations of wave heights and wave angles. The remainder of the input data for both runs, however, was the same. The waves were run on a plane beach with a slope of 0.025. The planform area of interest was comprised of 25 grids in the x direction with an Δx grid size of 5.0 meters, and 21 grids in the longshore direction with a Δy grid size of 4.0 meters. The time step was chosen to be 0.2 seconds and the model was run for 1500 iterations for both cases. A wave period of 7.159366 seconds was used, which resulted in theoretical rip spacings of 80.0 meters. The bottom friction factor was set equal to 0.12 to allow the system to reach steady state after the 1500 iterations and to decrease the magnitude of the resultant currents.

The first case used waves of equal heights and equal angles to either side of the beach normal. The deep water wave heights were 0.25 meters and

the deep water angles were ± 30.0 degrees. For this case, referring to Eq. (5.3), $a=b$ and $\alpha=-\beta$ resulting in a free surface displacement given by

$$\eta_T = 2a \cos(k_0 \sin \alpha_0 y) \cos(k \cos \alpha x + \sigma t) \quad .$$

This free surface describes a wave train moving in the $-x$ direction with a modulated wave height that is periodic in the longshore direction only. The periodicity in wave height is the driving mechanism producing the rip current perpendicular to the beach, as shown in Figure 5-19. Note the constricted width of the rip current in relation to the width of the inflow region. This is a result of the convective acceleration terms. Also note the weak rip head where the currents diverge from the rip axis and return towards shore.

In the second case, the waves, A and B, had different heights, 0.1 and 0.4 meters, and wave angles of 30.0 and -30.0 degrees, respectively. The resulting circulation pattern is shown in Figure 5-20, and consists of a meandering current with alternating regions of strong and weak longshore velocity along the beach. This circulation would lend itself well to the formation of rhythmic beach features. Looking at Eq. (5.2), we see that there is a non-zero term,

$$(b-a)\cos\{k \cos \beta x + k \sin \beta y + \sigma t\}$$

which is a wave train at an angle to the beach normal with height $2(b-a)$. This wave is present in addition to the normal wave train with the modulated height from the first case, causing a longshore current which is superimposed on the cellular circulation.

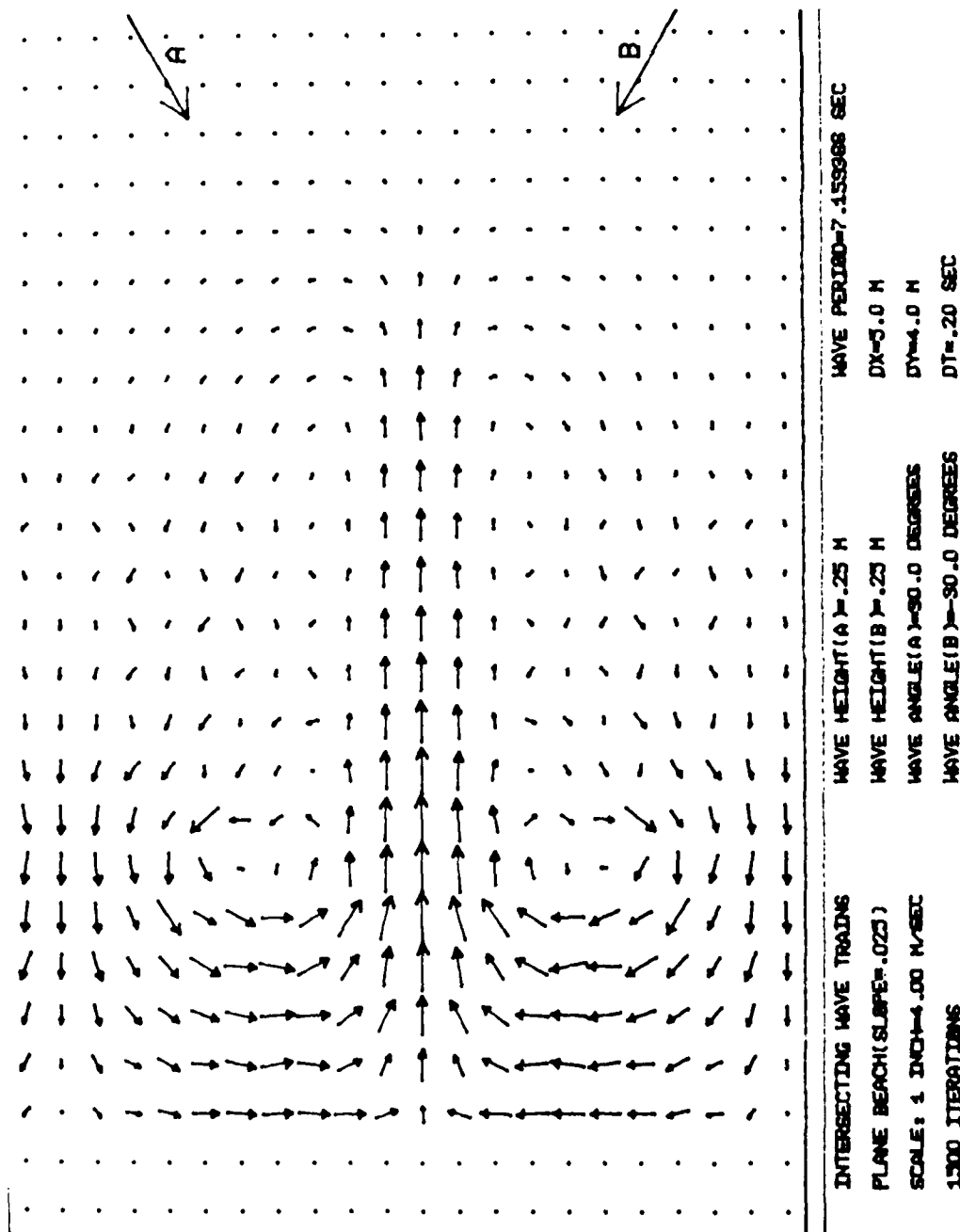


Figure 5-19. Current Vector Plot for Intersecting Waves, Case 1.
Nonlinear Model

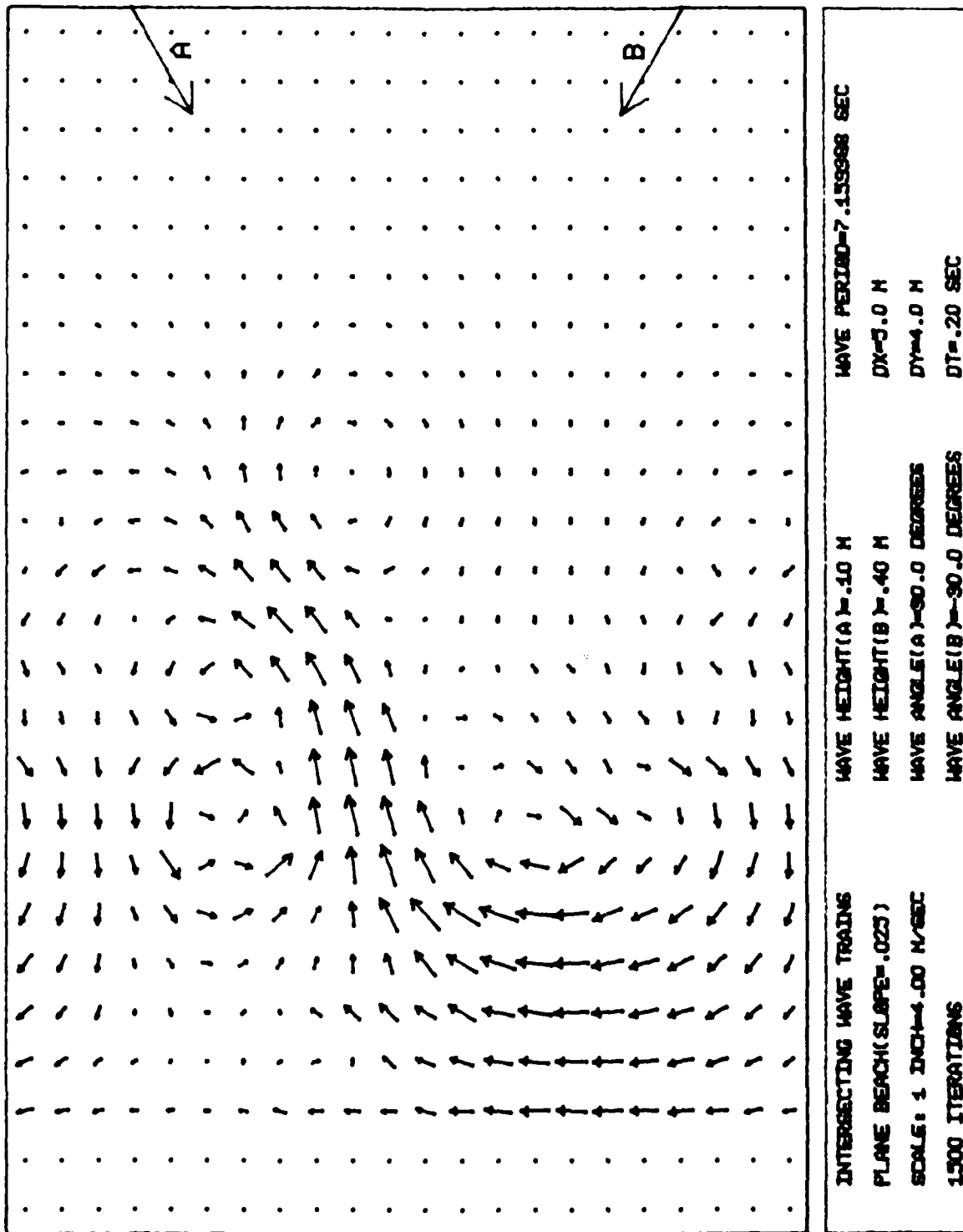


Figure 5-20. Current Vector Plot for the Meandering Circulation Pattern. Nonlinear Model.

Chapter VI

CONCLUSIONS

In this report, the theoretical background and numerical formulation of two models for nearshore circulation have been reviewed. A review of the application of the models to plane beach problems has shown that the models successfully reproduce the characteristics of known analytic solutions. The comments of Basco (1981), who expressed the opinion that the models are invalid due to the effect of numerical viscosity on the calculated velocity profiles, can be seen to be incorrect upon inspection of Figure 5-5, which demonstrates the steep drop in longshore current at the breaker line in the absence of a prescribed lateral mixing. In addition, Figure 5-1 shows that the model reproduces the sharp drop in wave set down at the breaker line, further indicating that the model is capable of reproducing the distinct features of analytic solutions, if the grid scheme chosen is fine enough to resolve the features. It is apparent that any numerical diffusion of solutions for $\bar{\eta}$ or V is confined to one or two grid rows, and can be made insignificant by choosing the grid size small enough. It should also be remarked that the slight decrease in the longshore velocity below the purely linear profile predicted by Longuet-Higgins (1970a) has been explained to be a result of wave-current interaction (Dalrymple, 1980) included in both models, and of finite angle of wave incidence (Liu and Dalrymple, 1978; Krauss and Sasaki, 1979), included in the nonlinear model. In conclusion, there appears to be no discrepancy between numerical solutions using a fine grid and the corresponding analytic solutions.

In practical applications, grid spacings are often chosen which lead to some false numerical averaging of the solutions. In the linear model, this averaging manifests itself most obviously as a smoothing of the longshore profile across the breaker line in the same manner as would be induced by lateral mixing effects (see Figure 4-14). This indicates that the mixing coefficients included in the nonlinear model should be smaller than expected on physical grounds in order to compensate for the numerical effects. With the choice of a friction factor based on the formulae of Jonsson (1966) or Kajiura (1968), the model is then seen to produce realistic current profiles, both in form and magnitude, for the field site chosen. However, it should be noted that no detailed data set currently exists which satisfies the requirement of a monochromatic input wave condition, and which represents a field case for which model results are fairly reliable, such as the absence of a large longshore bar.

The numerical models are shown to be successful predictors of nearshore dynamics in situations dominated by refraction and weak wave-current interaction effects. In this regard, it is noted that the model as currently formulated cannot handle certain effects, such as the influence of finite barriers in the wave field, or strong interaction of waves and opposing currents. The modelling of both of these effects requires the inclusion of a capability for handling wave diffraction.

Finally, the present models require an input wave condition based on a monochromatic wave, whereas wave trains in nature tend to include a spectrum of waves. In the case where the incident wave spectrum is sufficiently narrow-banded in frequency, the incident wave can be represented as a wave of single frequency with a modulated amplitude; such an effect can

be modelled after modification of the programs to handle a time varying deepwater wave height. However, modelling of broad-banded spectra at the level of the treatment here remains a complex problem.

REFERENCES

- Allender, J. H., J. D. Ditmars, A. A. Frigo, and R. A. Paddock (1981), "Evaluation of a Numerical Model for Wave- and Wind-Induced Nearshore Circulation Using Field Data," Report NUREG/CR-1210, ANL/EES-TM-154, Argonne National Laboratory, Argonne, Illinois.
- Basco, D. R. (1981), "Surf Zone Currents," U. S. Army Corps of Engineers, Coastal Engin. Res. Center (in preparation).
- Birkemeier, W. A., and R. A. Dalrymple (1976), "Numerical Models for the Prediction of Wave Set-up and Nearshore Circulation," ONR Tech. Rept. 1, Ocean Engineering Rept. 3, Dept. of Civil Engineering, University of Delaware, Newark, DE.
- Blumberg, A. F. (1977), "Numerical Tidal Model of Chesapeake Bay," ASCE J. Hydraulics Division 103, HY1, 1-9.
- Bowen, A. J., and D. L. Inman (1974), "Nearshore Mixing Due to Waves and Wave-Induced Currents," Rapp. P.-v. Réun. Cons. int. Explor. Mer. 167, 6-12.
- Bowen, A. J., D. L. Inman, and V. P. Simmons (1968), "Wave Set-Down and Set-up," J. Geophys. Res. 73(8), 2569-2577.
- Dalrymple, R. A. (1975), "A Mechanism for Rip Current Generation on an Open Coast," J. Geophys. Res. 80(24), 3485-3487.
- Dalrymple, R. A. (1978), "Rip Currents and their Causes," Proc. 16th Int. Conf. on Coastal Engineering, Hamburg.
- Dalrymple, R. A. (1980), "Longshore Currents with Wave Current Interaction," ASCE J. Waterway, Port, Coast. and Ocean Div. 106 WW3, 414-420.
- Dalrymple, R. A., R. A. Eubanks, and W. A. Birkemeier, (1977), "Wave-Induced Circulation in Shallow Basins," ASCE J. Waterway, Port, Coast. and Ocean Div. 103 WW1, 117-135.
- Dalrymple, R. A., and P. L.-F. Liu (1978), "Waves over Soft Muds: A Two Layer Fluid Model," J. Phys. Oceanogr. 8(6), 1121-1131.
- Dalrymple, R. A., and C. J. Lozano (1978), "Wave-Current Interaction Models for Rip Currents," J. Geophys. Res. 83(C12), 6063-6071.
- Divokey, D., B. LeMehaute, and A. Liu (1970), "Breaking Waves on Gentle Slopes," J. Geophys. Res. 75(9), 1681-1692.
- Ebersole, B. A., and R. A. Dalrymple (1979), "A Numerical Model for Nearshore Circulation including Convective Accelerations and Lateral Mixing," ONR Tech. Rept. 4, Ocean Engineering Rept. 21, Dept. of Civil Engineering, University of Delaware, Newark, DE.

- Cable, C. G. (ed.) (1979), "Report on Data from the Nearshore Sediment Transport Study Experiment at Torrey Pines Beach, California, November-December 1978," IMR Ref. No. 79-8, Institute of Marine Resources, University of California, La Jolla, CA.
- Hildebrand, F. B. (1976), Advanced Calculus for Applications, Prentice-Hall.
- James, I. D. (1974), "Non-linear Waves in the Nearshore Region: Shoaling and Set-up," Est. Coast. Mar. Sci. 2, 207-234.
- Jonsson, I. G. (1966), "Wave Boundary Layers and Friction Factors," Proc. 10th Int. Conf. on Coastal Engineering, Tokyo, 127-148.
- Kajiura, K. (1968), "A Model of the Bottom Boundary Layer in Water Waves," Bull. Earthquake Res. Inst. 46, 75-123.
- Kraus, N. C., and T. O. Sasaki (1979), "Influence of Wave Angle and Lateral Mixing on the Longshore Current," Marine Sci. Comm. 5, 99-126.
- Kurihara, Y. (1965), "On the Use of Implicit and Iterative Methods for Time Integration of the Wave Equation," Monthly Weather Rev. 93(1), 33-46.
- LeBlond, P. H., and C. L. Tang (1974), "On Energy Coupling between Waves and Rip Currents," J. Geophys. Res. 79(6), 811-816.
- Lilly, D. K. (1965), "On the Computational Stability of Numerical Solutions of Time-Dependent Non-Linear Geophysical Fluid Problems," Monthly Weather Rev. 93(1), 11-26.
- Liu, P. L.-F. (1973), "Damping of Waves over a Porous Bed," ASCE J. Hydraulics Div. 99, HY , 2263-2271.
- Liu, P. L.-F. (1982), "Finite Element Modelling of Breaking Wave-Induced Near-shore Currents," Proc. Nearshore Current Model Workshop, CERC, (in preparation) Newark, Del.
- Liu, P. L.-F., and R. A. Dalrymple (1978), "Bottom Frictional Stresses and Longshore Currents Due to Waves with Large Angles of Incidence," J. Mar. Res. 36(2), 357-375.
- Longuet-Higgins, M.S. (1970a), "Longshore Currents Generated by Obliquely Incident Sea Waves, 1," J. Geophys. Res. 75(33), 6778-6789.
- Longuet-Higgins, M.S. (1970b), "Longshore Currents Generated by Obliquely Incident Sea Waves, 2," J. Geophys. Res. 75(33), 6790-6801.
- Longuet-Higgins, M. S., and Stewart, R. W. (1969), "Radiation Stress in Water Waves: A Physical Discussion with Applications," Deep Sea. Res. 4, 529-563.

- Longuet-Higgins, M. S., and J. S. Turner (1974), "An 'Entraining Plume' Model of a Spilling Breaker," J. Fluid Mech. 63(1), 1-20.
- McDougall, W. G. (1979), "A Numerical Model to Predict Surf Zone Dynamics," M.C.E. Thesis, Dept. of Civil Engineering, University of Delaware, Newark, DE.
- Miller, C., and A. Barcelon (1978), "Hydrodynamic Instability in the Surf Zone as a Mechanism for the Formation of Horizontal Gyres," J. Geophys. Res. 83, 4107-4116.
- Noda, E. K. (1973), "Rip Currents," Proc. 13th Int. Conf. on Coastal Engineering, Vancouver, 653-668.
- Noda, E. K., C. J. Sonu, V. C. Rupert, and J. I. Collins (1974), "Nearshore Circulation under Sea Breeze Conditions and Wave-Current Interaction in the Surf Zone," Tetra Tech Report TC-149-4.
- Paddock, R. A., and J. D. Ditmars (1981), "Investigation of the Feasibility of Linking a Sediment Transport Model with a Nearshore Circulation Model," Report NUREG/CR-2237, ANL/EES-TM-155, Argonne National Laboratory, Argonne, Illinois.
- Pawka, S. (1980), personal communication.
- Pearce, B. R. (1972), "Numerical Calculation of the Response of Coastal Waters to Storm Systems with Applications to Hurricane Camille of August 17-22, 1969," College of Engineering Tech. Rept. 12, University of Florida.
- Phillips, O. M. (1977), The Dynamics of the Upper Ocean, 2nd Ed., Cambridge University Press.
- Roache, P. J. (1976), Computational Fluid Dynamics, Hermosa Publishers, Albuquerque.
- Shore Protection Manual (1975), U.S. Army Corps of Engineers, Vol. 1, Government Printing Office.
- Sonu, C. J. (1972), "Field Observations of Nearshore Circulation and Meandering Currents," J. Geophys. Res. 77(18), 3232-3247.
- Sommerfeld, A. (1949), Partial Differential Equations in Physics, Academic Press, New York.
- Symonds, G., D. A. Huntley, and A. J. Bowen (1982), "Two Dimensional Surf Beat: Long Wave Generation by a Time-Varying Breakpoint," J. Geophys. Res. 87(C1), 492-498.
- Van Dorn, W. C. (1953), "Wind Stress on an Artificial Pond," J. Marine Res. 12,

Weggel, J. R. (1972), "Maximum Breaker Height," J. Waterways, Harbors and Coastal Engineering, ASCE 98, WW4, 529-548.

Wilson, B. W. (1966), "Seiche," in Encyclopedia of Oceanography, Reinhold Publishers, New York.

Wu, J. (1968), "Laboratory Studies of Wind-Wave Interactions," J. Fluid Mech. 34(1), 91-111.

Appendix I.

USING THE NEARSHORE CIRCULATION PROGRAM

The nearshore circulation model as described above is supplied in two versions, referred to as the linear and the nonlinear versions. Complete listings of the programs for each version follow. The programs as written are designed to run on a Burroughs B7700. The line

\$RESET FREE

which appears on the front of each program allows for the use of standard Fortran on the B7700. This line should be removed before operating the program on a different system.

The two versions of the model are currently designed to be indistinguishable to the operator, with the input file containing wave and wind information and the depth grid being of identical format for each program. The output file generated currently at a line printer is also identical for each program. The exception to the uniformity between the two models occurs in the output file stored at the end of execution for subsequent restart of the model. Since the nonlinear version of the program requires the storage of three time levels of data, two extra time levels are included in the output. Thus, the nonlinear version of the program can not be started based on intermediate results generated by the linear version, as not enough information is present. It is possible in principle to start the linear version of the program using intermediate results from the nonlinear version, although at present the READ statement in the linear version is not structured to handle this option.

The circulation model is currently designed to be run as a batch job, and as such has all device number specifications for data files in the job file external to the program. This feature may have to be changed depending on the machine to be used. Currently, data files may be named arbitrarily. The program currently requires four IO device specifications:

<u>Logical Device Number</u>	<u>Corresponding Data File</u>
5	User defined input data
6	Output stream, currently directed to a line printer
3	Output file, stores results of last iteration for a later restart
8	Input file used to restart the model

It should be noted that the input file 8 used for restarting the program is identical to, and should be just a renamed version of, the output file 3 generated by the model at the point from which it is desired to continue computation.

Structure of Input Data File 5

The input data file is structured into five groups of data. The first four groups each consist of a single line in the file, with data values entered unformatted; i.e., separated by commas with no requirements on spacing. The fifth data group consists of the depth grid, and requires more space than a single line, as explained below. The information included in the input data file is as follows.

DATA IN INPUT DATA FILE 5

1. Wave Parameters

- T - Wave period (seconds)
- HO - Wave height (meters)
- A - Wave angle, measured clockwise from the +X direction (degrees)

2. Wind Parameters

- WIND - Wind speed (meters/second)
- WINANG - Wind angle, measured clockwise from the -X direction (degrees)

3. Grid Parameters

- M - Number of grid rows in X direction (offshore)
- N - Number of grid columns in Y direction (longshore)
- DX - Grid spacing in X direction (meters)
- DY - Grid spacing in Y direction (meters)
- DT - Size of the time step (seconds)
- INDEX - Specifies the input of depth information
 =1, read data from previous run from file 8
 =2, read depth grid from input file 5
 =3, establish plane beach based on input beach slope
- AM - Beach slope (space in input file must be filled, but value is unused only if INDEX=3)

4. Program Control Parameters

- ITA - Total number of iterations (including the accumulated total from previous runs, if previous run data is used)
- NHIGHT - Number of iterations over which the deep water wave builds up

- ID - Determine if dissipation of wave energy is to be included
 =0, no dissipation
 =1, dissipation due to viscosity and bottom permeability is included
 - KSKIP - Determine frequency of printed iterations in output file 6
5. Depth Grid (required if INDEX=2)
- D - Local water depth with respect to still water level at each grid center.

The depth grid D is input in an unformatted string of length M*N, starting with the fifth line of the input file 5 and continuing to as many lines as necessary. The data values are read off of an established grid row-wise in the +Y direction, starting at the inshore end of the grid.

Coordinate System Used in the Program

The input depth grid and wave and wind parameters should be established using the coordinates shown in Figure 2-1. The models require that the bathymetry be periodic in the longshore direction. Accordingly, for an input depth grid of size (M, N), where (I, J) are X and Y indices and (M, N) are the maximum values of (I, J), the laterally bordering depth values should satisfy the requirement:

$$D(I,N) = D(I,1) \quad .$$

If this condition is not met on input, D(I,1) is redefined to be equal to D(I,N). Both models create two additional rows in the Y direction, (N+1) and (N+2). The grid storage requirement for all variables is thus M by (N+2), with a current

maximum of 50 by 50. The maximum may be enlarged or decreased by alteration of all COMMON and DIMENSION statements in either program.

Wave angle and wind angle are defined as shown in Figure 2-1. Wave angle is measured clockwise from the +X direction. Waves approaching the beach from the right of directly offshore have wave angles $> 180^\circ$. Wind angle is given clockwise from the -X direction, so that winds approaching shore from the right of normal have wind directions greater than 0° .

The program requires that incident waves have longshore components propagating in the +Y direction. For the case of wave angles $= 180^\circ - \theta$, the program flips the depth grid over and rotates the wave and wind directions through $360^\circ - 2\theta$ degrees, and runs the program for waves approaching at $180^\circ + \theta$ and a mirror image depth grid.

Error Messages from the Circulation Models

Each version of the nearshore circulation model will generate various error messages when fatal conditions are met during execution. The messages are, for the most part, identical from either program and correspond to equivalent situations within the programs. A list of possible internally occurring errors leading to the printing of a message follows.

1. Failure of iteration scheme to converge on a wave height at a grid point will cause the message

RELAXATION FOR THE WAVE HEIGHT FAILED TO CONVERGE

followed by an indication of the row and number of iterations tried. This

condition arises in the subroutine HEIGHT. Occurrence of the condition does not lead to termination of the program; iteration continues with the last wave height calculated and the entire iteration is tried again at the next time step.

2. Failure of iteration scheme to converge on a wave angle at a grid point will cause the message

RELAXATION FOR THETA FAILED AFTER -- ITERATIONS

with an indication given of the number of iterations tried. This condition could arise if the magnitude of a current directed against the general direction of wave travel was too strong. The condition arises in the subroutine ANGLE and causes termination of the program.

3. If a negative wave number RK is calculated, the message

RK IS NEGATIVE

is printed, and the program is terminated. This condition occurs in the subroutine WVNUM.

LINEAR MODEL

```

10000 $RESET FREE
10010 C*-----
10020 C*
10030 C* NEARSHORE CIRCULATION MODEL --- LINEAR VERSION
10040 C*
10050 C* THIS COMPUTER PROGRAM IS A NUMERICAL MODEL TO PREDICT SURF-ZONE
10060 C* DYNAMICS, GIVEN A FIXED, PERIODIC TOPOGRAPHY AND DEEPWATER
10070 C* MONOCHROMATIC WAVE CONDITIONS AS INPUT.
10080 C* THE REFRACTION PROGRAM INCLUDING WAVE-CURRENT INTERACTION IS BASED
10090 C* ON THE PROGRAM OF NODA ET AL (TETRA TECH 1974). THE CURRENT
10100 C* PROGRAM IS AN UPDATED VERSION OF THE MODEL DEVELOPED BY
10110 C* BIRKEMEIER AND DALRYMPLE (UNIV. OF DEL. 1977).
10120 C*
10130 C*-----
10140 C* COMMON D(50,50),U(50,50),V(50,50),Z(50,50),SI(50,50),CD(50,50),
10150 C* H(50,50),CG(50,50),S(50,50),HBREAK(50,50),IB(50,50),DDX(50,50),
10160 C* DDDY(50,50),W(50,50),Y(50,50)
10170 C* COMMON/VAL/ETA(50,50)
10180 C* COMMON/STRESS/SIGXX(50,50),SIGYY(50,50),SIGXY(50,50),TAUBX(50,50),
10190 C* TAUBY(50,50),TAUSX(50,50),TAUSY(50,50)
10200 C* COMMON/REF/ZZ(50,50),HNEW(50,50),RKA(50,50)
10210 C* COMMON/CONST/ G,PI,P12,RAD,EPS,DX,DY,DT,DX2,DY2,T,SIGMA,
10220 C* M,N1,N2,M1,M2,AM,DD,IT,RHO,IWET,IDRY,ID
10230 C* DIMENSION DST(50,50)
10240 C*-----
10250 C*
10260 C* NOTES ON RUNNING THE CIRCULATION PROGRAM
10270 C*
10280 C* 1. WAVE ANGLE IS MEASURED CLOCKWISE FROM THE +X DIRECTION
10290 C*
10300 C* 2. WIND ANGLE IS MEASURED CLOCKWISE FROM THE -X DIRECTION
10310 C*
10320 C* 3. ALL INPUT AND OUTPUT DATA IS IN MKS UNITS
10330 C*
10340 C* 4. THE DEPTH GRID IS OFFSET BY -DY FROM ALL THE OTHER VARIABLE
10350 C* FIELDS
10360 C*-----
10370 C*
10380 C* DEFINITIONS OF QUANTITIES USED IN PROGRAM
10390 C*
10400 C* 1. CONSTANTS
10410 C*
10420 C* CF - BOTTOM FRICTION FACTOR (DARCY TYPE)
10430 C* VANCON - WIND SHEAR FACTOR (VAN DORN TYPE)
10440 C*
10450 C* 2. VARIABLE ARRAYS (VALUE AT EACH GRID LOCATION)
10460 C*
10470 C* D - TOTAL WATER DEPTH (D(SW)+ETA)
10480 C* ETA - DEVIATION OF MEAN WATER LEVEL FROM STILL WATER LEVEL
10490 C* Z - WAVE ANGLE
10500 C* CO - COS(Z)
10510 C* SI - SIN(Z)
10520 C* H - WAVE HEIGHT
10530 C* HBREAK - LOCAL BREAKING WAVE HEIGHT
10540 C* IB - BREAKING INDEX
10550 C* IB=0, WAVE IS BREAKING LOCALLY
10560 C* IB=1, WAVE IS NOT BREAKING LOCALLY
10570 C* DDX,DDDY - LOCAL DERIVATIVES OF THE TOTAL DEPTH
10580 C*

```

10590	C*	CG - GROUP VELOCITY	00010590
10600	C*	RKA - WAVE NUMBER	00010600
10610	C*	U,V - X,Y VELOCITIES AT SIDES OF GRID BLOCKS	00010610
10620	C*	W,Y - X,Y VELOCITIES AT CENTERS OF GRID BLOCKS	00010620
10630	C*	NOTE THAT THE U,V AND W,Y ARRAYS ARE INTERCHANGED	00010630
10640	C*	IN SEVERAL SUBROUTINES THROUGH THE COMMON STATEMENTS	00010640
10650	C*	SIGXX,SIGXY,SIGYY - RADIATION STRESSES	00010650
10660	C*	TAUBX,TAUBY - BOTTOM STRESSES	00010660
10670	C*	TAUSX,TAUSY - SURFACE STRESSES	00010670
10680	C*		00010680
10690	C*	3. LOCALLY DEFINED VARIABLES	00010690
10700	C*		00010700
10710	C*	DUDX,DVDX - VELOCITY GRADIENT COMPONENTS	00010710
10720	C*	DCDX,DCDY - WAVE CELERITY GRADIENT COMPONENTS	00010720
10730	C*	DCGDY,DCGDY - GROUP VELOCITY GRADIENT COMPONENTS	00010730
10740	C*	DTDX,DTDY - WAVE ANGLE GRADIENT COMPONENTS	00010740
10750	C*	EPS - ACCURACY VALUE USED IN THE RELAXATION SCHEMES	00010750
10760	C*		00010760
10770	C*		00010770
10780	C*		00010780
10790	C*		00010790
10800	C*	VARIABLES TO BE READ INTO PROGRAM	00010800
10810	C*		00010810
10820	C*	1. WAVE PARAMETERS	00010820
10830	C*		00010830
10840	C*		00010840
10850	C*	T - WAVE PERIOD (SECONDS)	00010850
10860	C*	HO - WAVE HEIGHT (METERS)	00010860
10870	C*	A - WAVE ANGLE, CLOCKWISE FROM +X (DEGREES)	00010870
10880	C*		00010880
10890	C*	2. WIND PARAMETERS	00010890
10900	C*		00010900
10910	C*	WIND - WIND SPEED (METERS/SECOND)	00010910
10920	C*	WINANG - WIND ANGLE, CLOCKWISE FROM -X (DEGREES)	00010920
10930	C*		00010930
10940	C*	3. GRID PARAMETERS	00010940
10950	C*		00010950
10960	C*	M - NUMBER OF GRIDS IN X DIRECTION (OFFSHORE)	00010960
10970	C*	N - NUMBER OF GRIDS IN Y DIRECTION (LONGSHORE)	00010970
10980	C*	DX - GRID SPACING IN X DIRECTION (METERS)	00010980
10990	C*	DY - GRID SPACING IN Y DIRECTION (METERS)	00010990
11000	C*	DT - TIME STEP<DX/SQRT(2*G*DMAX) (SECONDS)	00011000
11010	C*	INDEX - SPECIFY INPUT OF DEPTH INFORMATION	00011010
11020	C*	=1, READ DATA FROM PREVIOUS RUN	00011020
11030	C*	=2, READ DEPTH GRID FROM INPUT DATA FILE	00011030
11040	C*	=3, ESTABLISH PLANE BEACH BASED ON INPUT BEACH SLOPE	00011040
11050	C*	AM - BEACH SLOPE (REQUIRED IF INDEX=3)	00011050
11060	C*		00011060
11070	C*	4. PROGRAM CONTROL PARAMETERS	00011070
11080	C*		00011080
11090	C*	ITA - TOTAL NUMBER OF ITERATIONS (INCLUDING ACCUMULATED	00011090
11100	C*	TOTAL OF PREVIOUS RUNS, IF PREVIOUS RUN DATA IS	00011100
11110	C*	USED)	00011110
11120	C*	NHIGHT - NUMBER OF ITERATIONS OVER WHICH THE DEEPWATER WAVE	00011120
11130	C*	HEIGHT IS BUILT UP	00011130
11140	C*	ID - DETERMINE IF DISSIPATION OF WAVE ENERGY IS TO BE	00011140
11150	C*	INCLUDED	00011150
11160	C*	=0, NO DISSIPATION	00011160
11170	C*	=1, DISSIPATION DUE TO VISCOSITY AND BOTTOM PERM-	00011170
11180	C*	EABILITY	00011180
11190	C*	KSKIP - DETERMINE FREQUENCY OF PRINTED ITERATIONS	00011190
11200	C*		00011200


```

11830 READ(8,107)ITO
11840 DO 10 I=1,M
11850 DO 10 J=1,N2
11860 CO(I,J)=COS(Z(I,J))
11870 SI(I,J)=SIN(Z(I,J))
11880 10 CONTINUE
11890 C*
11900 C* IF WAVE ANGLE IS LESS THAN 180 DEGREES, VARIABLE FIELDS WERE
11910 C* FLIPPED DURING PREVIOUS RUN. ROTATE THE WAVE AND WIND ANGLES
11920 C*
11930 IF(A.GE.180.) GO TO 42
11940 A=360.-A
11950 WINANG=PI2-WINANG
11960 GO TO 42
11970 C*
11980 C* INDEX=2, READ IN DEPTH GRID FROM INPUT DATA FILE 5
11990 C*
12000 2 READ(5,/,END=99)((D(I,J),J=1,N),I=1,M)
12010 99 WRITE(6,120) I,J
12020 C*
12030 C* IF WAVE ANGLE IS LESS THAN 180 DEG., FLIP THE INPUT DEPTH
12040 C* GRID AND ROTATE THE WAVE AND WIND ANGLES
12050 C*
12060 IF(A.GT.180.) GO TO 22
12070 A=360.-A
12080 WINANG=PI2-WINANG
12090 DO 21 I=1,M
12100 DO 20 J=1,N
12110 DST(I,J)=D(I,J)
12120 DO 21 J=1,N
12130 K=(N-J)+1
12140 D(I,K)=DST(I,J)
12150 DO 23 I=1,M
12160 D(1,1)=D(1,N)
12170 D(I,N2)=D(I,3)
12180 D(I,N1)=D(I,2)
12190 23 CONTINUE
12200 GO TO 41
12210 C*
12220 C* INDEX=3, ESTABLISH PLANE BEACH BASED ON VALUE OF AM READ ABOVE
12230 C*
12240 3 DO 31 J=1,N2
12250 DO 31 I=1,M
12260 D(I,J)=((FLOAT(I-2)*DX)*AM)
12270 31 CONTINUE
12280 C*
12290 C* IF WAVE ANGLE IS LESS THAN 180 DEGREES, ROTATE THE WAVE AND WIND
12300 C* ANGLES
12310 C*
12320 IF(A.GE.180.) GO TO 41
12330 A=360.-A
12340 WINANG=PI2-WINANG
12350 41 WRITE(6,108)
12360 WRITE(6,103)((D(I,J),J=1,N1),I=1,M)
12370 DO 65 I=1,M
12380 DO 65 J=1,N2
12390 ETA(I,J)=O.O
12400 U(I,J)=O.O
12410 V(I,J)=O.O
12420 65 CONTINUE
12430 42 DO 15 I=1,M
12440 IF(D(I,1).GT.DD) GO TO 95

```

```

00011830
00011840
00011850
00011860
00011870
00011880
00011890
00011900
00011910
00011920
00011930
00011940
00011950
00011960
00011970
00011980
00011990
00012000
00012010
00012020
00012030
00012040
00012050
00012060
00012070
00012080
00012090
00012100
00012110
00012120
00012130
00012140
00012150
00012160
00012170
00012180
00012190
00012200
00012210
00012220
00012230
00012240
00012250
00012260
00012270
00012280
00012290
00012300
00012310
00012320
00012330
00012340
00012350
00012360
00012370
00012380
00012390
00012400
00012410
00012420
00012430
00012440

```

```

12450      15 CONTINUE
12460      95 IWET=I
12470      IDRY=IWET-1
12480      C*-----
12490      C* MAIN PROGRAM LOOP FOR EACH ITERATION
12500      C*-----
12510      DO 4 IT=(1+ITO), ITA
12520      L=AMOD(FLOAT(IT), FLOAT(KSKIP))
12530      HO=HEIGHT*TANH(FLOAT(IT)/(FLOAT(NHIGHT)/2.0))
12540      IF (IT.LE. (NHIGHT*2.0)) GO TO 12
12550      GO TO 13
12560      12 CALL DGRAD
12570      CALL REFRAC(A,HO,IT,INDEX,NHIGHT,CF)
12580      13 CALL TAUSB(WIND,WINANG,CF,ITO)
12590      CALL UALC
12600      CALL ETAS
12610      SUM=O.O
12620      DO 86 I=1,M
12630      DO 86 J=2,N
12640      SUM=SUM+O.5*(W(I,J)**2+V(I,J)**2)*D(I,J-1)
12650      SUM=SUM+G*ETA(I,J)*(D(I,J-1)-O.5*ETA(I,J))
12660
12670      86 CONTINUE
12680      C*-----
12690      C* WRITE SUM AFTER EACH ITERATION
12700      C*-----
12710      WRITE(6,100) SUM
12720      IF (L.NE.O) GO TO 4
12730      C*-----
12740      C* WRITE WAVE HEIGHT, WAVE ANGLE, VELOCITIES, AND SETUP AT
12750      C* KSKIP INTERVALS
12760      C*-----
12770      WRITE(6,109)
12780      WRITE(6,110) IT,HO
12790      WRITE(6,111)
12800      WRITE(6,112)
12810      WRITE(6,103) ((H(I,J),J=1,N1),I=1,M)
12820      DO 401 I=1,M
12830      DO 401 J=1,N1
12840      401 ZZ(I,J)=360.O-Z(I,J)*RAD
12850      WRITE(6,118)
12860      WRITE(6,103) ((ZZ(I,J),J=1,N1),I=1,M)
12870      WRITE(6,104)
12880      WRITE(6,103) ((U(I,J),J=1,N1),I=1,M)
12890      WRITE(6,105)
12900      WRITE(6,103) ((V(I,J),J=1,N1),I=1,M)
12910      WRITE(6,106)
12920      WRITE(6,103) ((ETA(I,J),J=1,N1),I=1,M)
12930      4 CONTINUE
12940      C*-----
12950      C* WRITE THE RESULTS OF THE LAST ITERATION INTO AN OUTPUT FILE
12960      C* TO BE USED FOR A SUBSEQUENT STARTUP
12970      C*-----
12980      WRITE(3,113)
12990      *((ETA(I,J),J=1,N2),I=1,M),((D(I,J),J=1,N2),I=1,M),
13000      *((U(I,J),J=1,N2),I=1,M),((V(I,J),J=1,N2),I=1,M),
13010      *((Z(I,J),J=1,N2),I=1,M),((H(I,J),J=1,N2),I=1,M),
13020      *((W(I,J),J=1,N2),I=1,M),((Y(I,J),J=1,N2),I=1,M),
13030      *((RKA(I,J),J=1,N2),I=1,M)
13040      WRITE(3,107) ITA
13050      LOCK 3
13060      100 FORMAT(1X,'THE TOTAL ENERGY IS',F14.2)
13070      101 FORMAT (/,'IX','DX=',15.3X,'DY=',15.3X,3X,'DT=',F5.2)

```

```

13070 102 FORMAT(1X,'M=',I5.3X,'N=',I5.3X,'ITERATIONS =',I5)
13080 103 FORMAT(1X,I1F10.4)
13090 104 FORMAT ( 10X,12HX - VELOCITY)
13100 105 FORMAT ( 10X,12HY - VELOCITY)
13110 106 FORMAT (10X,10HETA VALUES)
13120 107 FORMAT(15)
13130 108 FORMAT (// ' THE AUGMENTED MATRIX OF WATER DEPTH IN METERS'//)
13140 109 FORMAT('*****')
13150 110 FORMAT(10X,'ITERATION NUMBER',I6,10X,'WAVE HEIGHT=',F10.5,/)
13160 111 FORMAT (1X,'*****')
13170 112 FORMAT (5X,'WAVE HEIGHTS',/)
13180 113 FORMAT(15F8.4)
13190 114 FORMAT (1X,'WIND SPEED =',F7.3,'M/SEC',5X,'WIND ANGLE =',F7.
13200 *3. DEGREES')
13210 115 FORMAT(5X,'INDEX =',I5.3X,'ID =',I5)
13220 116 FORMAT(10X,'HCF =',F10.3,5X,4HDD =,F10.3)
13230 117 FORMAT(10X,'WAVE HEIGHT BUILDS UP FIRST',I3,' ITERATIONS')
13240 118 FORMAT(2X,'WAVE ANGLE (DEGREES)')
13250 119 FORMAT(1X,'WAVE PARAMETERS',/2X,'PERIOD =',F7.2,' HEIGHT =',F7
13260 *2.3X,7HANGLE =,F7.2,1X,7HDEGREES,4X,12HBEACH SLOPE=,F7.4)
13270 120 FORMAT(" INPUT DEPTH GRID TOO SMALL. LAST I,J VALUES ARE"/
13280 12X,I2,2X,I2)
13290 STOP
13300 END
13310 C*-----
13320 C*
13330 C* SUBROUTINE REFRAC(THETAO,HH,ITER,INDEX,NHIGHT,CF)
13340 C*
13350 C* REFRAC CONTROLS THE CALCULATION OF WAVE ANGLE AND WAVE HEIGHT
13360 C* FOR EACH ITERATION
13370 C*
13380 C*-----
13390 COMMON D(50,50),U(50,50),V(50,50),Z(50,50),SI(50,50),CO(50,50),
13400 *H(50,50),CG(50,50),S(50,50),HBREAK(50,50),IB(50,50),DDX(50,50)
13410 *DDDY(50,50)
13420 COMMON/STRESS/SIGX(50,50),SIGY(50,50),SIGXY(50,50),TAUBX(50,50),
13430 *TAUBY(50,50),TAUSX(50,50),TAUSY(50,50)
13440 COMMON/CONST/ G,PI,P12,RAD,EPS,DX,DY,DT,DX2,DY2,I,SIGMA,
13450 *M,N,N1,N2,M1,M2,AM,DD,IT,RHO,IWET,IDRY,ID
13460 IF (ITER.GT.(NHIGHT)) GO TO 600
13470 C*-----
13480 C* CALL SNELL DURING BUILDUP OF DEEP WATER WAVE
13490 C*-----
13500 THETA=PI2-THETAO/RAD
13510 CALL SNELL (THETA,HH,ITER)
13520 600 DO 50 I=1,IDRY
13530 DO 50 J=1,N2
13540 H(I,J)=O.O
13550 Z(I,J)=PI
13560 SI(I,J)=O.O
13570 CO(I,J)=-1.O
13580 50 CONTINUE
13590 CALL ANGLE(25)
13600 CALL HEIGHT(25,CF)
13610 C*-----
13620 C* CALCULATE THE RADIATION STRESSES
13630 C*-----
13640 DO 57 I=IWET,M1
13650 DO 21 J=3,N1
13660 ENERGY=O.125*RHO*G*(H(I,J)**2)
13670 SIGX(I,J)=SIGX(I,J)*ENERGY
13680 SIGY(I,J)=SIGY(I,J)*ENERGY

```

```

13690 SIGXY(I,J)=SIGXY(I,J)*ENERGY
13700
13710 21 CONTINUE
13720 SIGX(I,1)=SIGX(I,N)
13730 SIGY(I,1)=SIGY(I,N)
13740 SIGX(I,2)=SIGX(I,N1)
13750 SIGY(I,2)=SIGY(I,N1)
13760 SIGX(I,2)=SIGX(I,N1)
13770 SIGY(I,2)=SIGY(I,N1)
13780 SIGX(I,N2)=SIGX(I,3)
13790 SIGY(I,N2)=SIGY(I,3)
13800
13810 57 CONTINUE
13820 DO 59 J=3,N1
13830 SIGXY(M,J)=2.0*SIGXY(M1,J)-SIGXY(M2,J)
13840
13850 59 CONTINUE
13860 SIGXY(M,1)=SIGXY(M,N)
13870 SIGXY(M,2)=SIGXY(M,N1)
13880 SIGXY(M,N2)=SIGXY(M,3)
13890 RETURN
13900 END
13910
13920 C*-----
13930 C* SUBROUTINE GROUP(I,J,DCGDX,DCGDY,FF)
13940
13950 C* GROUP CALCULATES THE GROUP VELOCITY, WAVE CELERITY, AND
13960 C* THEIR SPATIAL DERIVATIVES
13970
13980 C*-----
13990 COMMON D(50,50),W(50,50),Y(50,50),Z(50,50),SI(50,50),CI(50,50),
14000 *H(50,50),CG(50,50),S(50,50),HBREAK(50,50),IB(50,50),DDX(50,50),
14010 *DDY(50,50),U(50,50),V(50,50)
14020 COMMON/CONST/ G,PI,PI2,RAD,EPS,DX,DY,DT,DX2,DY2,T,SIGMA,
14030 *W,N,N1,N2,M1,M2,AM,DD,IT,RHO,IWET,IDRY,ID
14040 COMMON/REF/ZZ(50,50),HNEW(50,50),RKA(50,50)
14050
14060 C* STATEMENT FUNCTIONS DUDX,DUDY,DVDX,DVDY,DTDX,DTDY,E,DKDX,DKDY
14070 C*-----
14080 DUDX(I,J)=(W(I+1,J)-W(I,J))/DX
14090 DUDY(I,J)=(U(I,J+1)-U(I,J-1))/DY2
14100 DVDX(I,J)=(V(I+1,J)-V(I-1,J))/DX2
14110 DVDY(I,J)=(Y(I,J+1)-Y(I,J-1))/DY
14120 DTDX(I,J)=(Z(I+1,J)-Z(I-1,J))/DX2
14130 DTDY(I,J)=(Z(I,J+1)-Z(I,J-1))/DY2
14140 E(I,J)=U(I,J)*COSI+V(I,J)*SINI+O.5*A*(1.0+ARG2/SINH2)/RK
14150 DKDX(I,J)=RK*((U(I,J)*SINI-V(I,J)*COSI)*DTDX(I,J)-(COSI*DUDX(I,J)+
14160 *SINI*DVDY(I,J))-A*DDX(I,J-1)/SINH2)/EE
14170 DKDY(I,J)=RK*((U(I,J)*SINI-V(I,J)*COSI)*DTDY(I,J)-(COSI*DUDY(I,J)
14180 *SINI*DVDY(I,J))-A*DDY(I,J-1)/SINH2)/EE
14190 JJ=J-1
14200 DEP=D(I,JJ)
14210 COSI=CO(I,J)
14220 SINI=SI(I,J)
14230 DCGDX=O.O
14240 DCGDY=O.O
14250
14260 C*-----
14270 C* CHECK FOR DRY LAND
14280 C*-----
14290 IF (DEP.LE.DD) RETURN
14300 CALL WNUM(DEP,COSI,SINI,U(I,J),V(I,J),RK,A)
14310 RKA(I,J)=RK
14320 IF (J.EQ.N) RKA(I,1)=RKA(I,J)
14330 IF (J.EQ.2) RKA(I,N1)=RKA(I,J)

```

```

14310 IF (J.EQ.3) RKA(I,N2)=RKA(I,J)
14320 TA=TANH(RK*DEP)
14330 HBREAK(I,J)=0.12*PI2*TA/RK
14340 COSH1=COSH(RK*DEP)
14350 SECHSQ=1.O/(COSH1**2)
14360 ARG2=2.O*RK*DEP
14370 SINH2=SINH(ARG2)
14380 COSH2=COSH(ARG2)
14390 SINHSQ=SINH2**2
14400 EE=E(I,J)
14410 C=SQRT(G*TA/RK)
14420 FF=0.5*(1.O+ARG2/SINH2)
14430 CG(I,J)=FF*C
14440 P=C*(SINH2-ARG2*COSH2)/SINHSQ
14450 DKDDX=RK*DDDX(I,J)+DEP*DKDY(I,J)
14460 DKDDY=RK*DDDY(I,J)+DEP*DKDX(I,J)
14470 Q=0.5*G/(C*RK**2)
14480 DCDX=Q*(RK*SECHSQ*DKDDX-TA*DKDX(I,J))
14490 DCDY=Q*(RK*SECHSQ*DKDDY-TA*DKDY(I,J))
14500 DCGDX=P*DKDDX+FF*DCDX
14510 DCGDY=P*DKDDY+FF*DCDY
14520 RETURN
14530 END
C*-----
C*
C* SUBROUTINE HEIGHT(ITMAX,CF)
C*
C* HEIGHT CALCULATES THE WAVE HEIGHT
C*-----
COMMON D(50,50),W(50,50),Y(50,50),Z(50,50),SI(50,50),CI(50,50),
*H(50,50),CG(50,50),S(50,50),HBREAK(50,50),IB(50,50),DDX(50,50),
*.DDDY(50,50),U(50,50),V(50,50)
COMMON/CONST/ G,PI,PI2,RAD,EPS,DX,DY,DT,DY2,T,SIGMA,
*M,N,N1,N2,M1,M2,AM,DD,IT,RHO,IWET,IDRY,ID
COMMON/STRESS/SIGX(50,50),SIGY(50,50),SIGXY(50,50),TAUBX(50,50),
*TAUBY(50,50),TAUSX(50,50),TAUSY(50,50)
COMMON/REF/ZZ(50,50),HNEW(50,50),RKA(50,50)
VISCOS=1.OE-05
PERM=1.O6E-09
DO 500 I=2,M1
DO 500 J=2,M1
IF(D(I,J-1).LE.DD) GO TO 499
CALL GROUP(I,J,DCGDX,DCGDY,FF)
DUDX=(W(I+1,J)-W(I,J))/DX
DUDY=(U(I,J+1)-U(I,J-1))/DY2
DVDX=(V(I+1,J)-V(I-1,J))/DX2
DV DY=(Y(I,J+1)-Y(I,J))/DY
DTDX=(Z(I+1,J)-Z(I-1,J))/DX2
DTDY=(Z(I,J+1)-Z(I,J-1))/DY2
501 SS2=SI(I,J)**2
CC2=CI(I,J)**2
CH=COSH(RKA(I,J)*D(I,J-1))
IF(ID.EQ.1) GO TO 301
X=0.O
GO TO 302
301 X=RKA(I,J)*CF*SIGMA*H(I,J)/(6.*PI*(CH**3.-CH))
X=X+G*PERM*RKA(I,J)/(VISCOS*CH*CH)
302 NA=N1
NB=N2
SIGXX=(2.O*FF-0.5)*CC2+(FF-0.5)*SS2
SIGYY=(2.O*FF-0.5)*SS2+(FF-0.5)*CC2
14910
14920

```

```

14930 SIGX(I,J) = SIGXX
14940 SIGY(I,J) = SIGY
14950 TAUXY=FF*SI(I,J)*CO(I,J)
14960 SIGXY(I,J)=TAUXY
14970 S(I,J)=CG(I,J)*(SI(I,J)*DTDX-CO(I,J)*DTDY)-(DUDX*DUDY)-(CO(I,J)*DC
14980 *GDX+SI(I,J)*DCGDY)-(SIGXX*DUDX+TAUXY*DUDY+TAUXY*DUDY+SIGY*DUDY)-X
14990 GO TO 500
15000
15010
15020
15030
15040
15050
15060
15070
15080
15090
15100
15110
15120
15130
15140
15150
15160
15170
15180
15190
15200
15210
15220
15230
15240
15250
15260
15270
15280
15290
15300
15310
15320
15330
15340
15350
15360
15370
15380
15390
15400
15410
15420
15430
15440
15450
15460
15470
15480
15490
15500
15510
15520
15530
15540

SIGX(I,J) = SIGXX
SIGY(I,J) = SIGY
TAUXY=FF*SI(I,J)*CO(I,J)
SIGXY(I,J)=TAUXY
S(I,J)=CG(I,J)*(SI(I,J)*DTDX-CO(I,J)*DTDY)-(DUDX*DUDY)-(CO(I,J)*DC
*GDX+SI(I,J)*DCGDY)-(SIGXX*DUDX+TAUXY*DUDY+TAUXY*DUDY+SIGY*DUDY)-X
GO TO 500
499 H(I,J)=O.O
SIGXY(I,J)=O.O
500 CONTINUE
DO 510 I1=1,M2
I=M-I1
DO 580 I1T=1,ITMAX
IFLAG=1
DO 520 J=2,N1
IF(D(I,J-1).LE. DD) GO TO 520
IB(I,J)=1
CC1=(V(I,J)+CG(I,J)*SI(I,J))/DY
CC2=(U(I,J)+CG(I,J)*CO(I,J))/DX
HNEW(I,J)= (CC1*H(I,J-1)-CC2*H(I+1,J))/(CC1-CC2-S(I,J)/2.O)
IF (HNEW(I,J) .LT. O.O) GO TO 810
IF (HNEW(I,J) .LE. HBREAK(I,J)) GO TO 850
810 HNEW(I,J)=HBREAK(I,J)
IB(I,J)=O
850 CONTINUE
IF (ABS(HNEW(I,J)-H(I,J)) .GT. (EPS*ABS(HNEW(I,J)))) IFLAG=O
C*-----
C* BOUNDARY CONDITIONS
C*-----
IF (J.NE.2) GO TO 800
HNEW(1,N1)=HNEW(1,U)
IB(1,N1)=IB(1,U)
GO TO 520
800 IF (J.NE.3) GO TO 801
HNEW(1,N2)=HNEW(1,U)
IB(1,N2)=IB(1,U)
801 IF (J.NE.N) GO TO 802
HNEW(1,1)=HNEW(1,U)
IB(1,1)=IB(1,U)
GO TO 520
802 IF (J.NE.N1) GO TO 520
HNEW(1,2)=HNEW(1,U)
IB(1,2)=IB(1,U)
520 CONTINUE
DO 625 J=1,N2
H(I,J)=HNEW(I,J)
625 CONTINUE
IF (IFLAG.EQ.1) GO TO 570
580 CONTINUE
WRITE(6,540) I, I1T
540 FORMAT(' RELAXATION FOR THE WAVE HEIGHT FAILED TO CONVERGE ',
*ON ROW ',I5,' AFTER ',I6,' ITERATIONS')
WRITE(6,541)(H(I,J),J=1,N2)
541 FORMAT(' LAST VALUES OF H ARE ',/10F13.5)
C RETURN
570 CONTINUE
510 CONTINUE
510 RETURN
END
C*-----
C* SUBROUTINE ANGLE(ITMAX)

```

```

15550 C*
15560 C* ANGLE CALCULATES THE LOCAL WAVE DIRECTION
15570 C*
15580 C*-----
15590 COMMON D(50,50),W(50,50),Y(50,50),Z(50,50),SI(50,50),CO(50,50),
15600 *H(50,50),CG(50,50),S(50,50),HBREAK(50,50),IB(50,50),DDDX(50,50),
15610 *DDDY(50,50),U(50,50),V(50,50)
15620 COMMON/CONST/ G,PI,P12,RAD,EPS,DX,DY,DT,DX2,DY2,T,SIGMA,
15630 *M,N,N1,N2,M1,M2,AM,DD,IT,RHO,IWET,IDRY,ID
15640 C*-----
15650 C* DEFINE STATEMENT FUNCTIONS - C,SS,DUOX,UDY,DVIX,DVDY,DKDX,
15660 C* DKDY,FAC,F
15670 C*-----
15680 C(I,J)=0.25*(CO(I+1,J)+CO(I-1,J)+CO(I,J+1)+CO(I,J-1))+0.125*((Z(I
15690 *+1,J)-Z(I-1,J))*(SI(I+1,J)-SI(I-1,J))+ (Z(I,J+1)-Z(I,J-1))*(SI(I,
15700 *J+1)-SI(I,J-1)))
15710 SS(I,J)=0.25*(SI(I+1,J)+SI(I-1,J)+SI(I,J+1)+SI(I,J-1))+0.125*((Z(I
15720 *+1,J)-Z(I-1,J))*(CO(I+1,J)-CO(I-1,J)) + (Z(I,J+1)-Z(I,J-1))*(CO(I,
15730 *J+1)-CO(I,J-1)))
15740 DUDX(I,J)=(W(I+1,J)-W(I-1,J))/DX
15750 DUDY(I,J)=(U(I,J+1)-U(I,J-1))/DY2
15760 DVIX(I,J)=(V(I+1,J)-V(I-1,J))/DX2
15770 DVDY(I,J)=(V(I,J+1)-V(I,J-1))/DY
15780 F(I,J)=U(I,J)*COSI+V(I,J)*SINI + 0.5*A*(1.0 + ARG2/SINH2)/RK
15790 DKDY(I,J)=(-(COSI*DUDY(I,J) + SINI*DVDY(I,J))-A*DDDY(I,J-1)/SINH2
15800 */FF
15810 DKDX(I,J)=(-(COSI*DUDX(I,J)+SINI*DVDX(I,J))-A*DDDX(I,J-1)/SINH2)/F
15820 *F
15830 FAC(I,J)=U(I,J)*SINI-V(I,J)*COSI
15840 DO 200 IJT=1,ITMAX
15850 MWET=M-IWET
15860 IFLAG=1
15870 DO 210 II=1,MWET
15880 I=M-II
15890 DO 210 J=2,N1
15900 IF(D(I,J-1).LE.DD) GO TO 210
15910 COSI=C(I,J)
15920 SINI=SS(I,J)
15930 JJ=J-1
15940 CALL WNUM(D(I,J),COSI,SINI,U(I,J),V(I,J),RK,A)
15950 ARG2=2.0*RK*D(I,JJ)
15960 SINH2= SINH(ARG2)
15970 FF=F(I,J)
15980 IF(FF.GT.0.0) GO TO 450
15990 WRITE(6,451) I,J,D(I,JJ),COSI,SINI,U(I,J),V(I,J),RK,A
16000 451 FORMAT(10X'FF IS NEGATIVE--OUTPUT I,J,D,COSI,SINI,U,V,RK,A'/.
16010 *215.7E13.4)
16020 GO TO 210
16030 450 FACI=FAC(I,J)
16040 DEN1=(SINI-COSI*FACI/FF)/DY
16050 DEN2=(COSI+SINI*FACI/FF)/DX
16060 DEN=DEN1-DEN2
16070 ZNEW=(COSI*DKDY(I,J)-SINI*DKDX(I,J)+Z(I,J-1)*DEN1-Z(I+1,J)*
16080 *DEN2)/DEN
16090 IF(ABS(ZNEW-Z(I,J)).GT.(EPS*ABS(ZNEW))) IFLAG=0
16100 Z(I,J)=ZNEW
16110 CO(I,J)=COS(Z(I,J))
16120 SI(I,J)=SIN(Z(I,J))
16130 IF(J.NE.2) GO TO 400
16140 Z(I,N1)=Z(I,2)
16150 CO(I,N1)=CO(I,2)
16160 SI(I,N1)=SI(I,2)

```



```

16170 GO TO 210
16180 IF(J.NE.3) GO TO 401
16190 Z(I,N2)=Z(I,3)
16200 CO(I,N2)=CO(I,3)
16210 SI(I,N2)=SI(I,3)
16220 GO TO 210
16230 IF(J.NE.N) GO TO 402
16240 Z(I,1)=Z(I,N)
16250 CO(I,1)=CO(I,N)
16260 SI(I,1)=SI(I,N)
16270 GO TO 210
16280
16290
16300
16310
16320
16330
16340
16350
16360
16370
16380
16390
16400
16410
16420
16430
16440
16450
16460
16470
16480
16490
16500
16510
16520
16530
16540
16550
16560
16570
16580
16590
16600
16610
16620
16630
16640
16650
16660
16670
16680
16690
16700
16710
16720
16730
16740
16750
16760
16770
16780

      GO TO 210
400 IF(J.NE.3) GO TO 401
      Z(I,N2)=Z(I,3)
      CO(I,N2)=CO(I,3)
      SI(I,N2)=SI(I,3)
      GO TO 210
401 IF(J.NE.N) GO TO 402
      Z(I,1)=Z(I,N)
      CO(I,1)=CO(I,N)
      SI(I,1)=SI(I,N)
      GO TO 210
402 CONTINUE
      IF(J.NE.N1) GO TO 210
      Z(I,2)=Z(I,N1)
      CO(I,2)=CO(I,N1)
      SI(I,2)=SI(I,N1)
210 CONTINUE
      IF(FLAG.EQ.1) GO TO 250
200 CONTINUE
      WRITE(6,220) ITMAX
220 FORMAT(" RELAXATION FOR THETA FAILED AFTER",I4,3X,
+ " ITERATIONS")
      STOP
250 CONTINUE
      RETURN
      END
C*-----
C*
      SUBROUTINE WVNUM(D,COSI,SINI,U,V,RK,A)
C*
C* WVNUM CALCULATES THE WAVE NUMBER INCLUDING THE EFFECTS OF
C* WAVE-CURRENT INTERACTION
C*
C*-----
      COMMON/CONST/ G,PI,P12,RAD,EPS,DX,DY,DT,DX2,DY2,T,SIGMA,
+M,N,N1,N2,M1,M2,AM,DD,IT,RHO,IWET,IDRY,ID
      EPSK=0.001
      RK=PI2/(T*SQRT(G*D))
      DO 1 I=1,50
      A=SIGMA-U*RK*COSI-RK*V*SINI
      A2=A**2
      ARG=RK*D
      F1=EXP(ARG)
      F2=1.0/F1
      SECH=2.0/(F1+F2)
      SECH2=SECH**2
      TT=TANH(ARG)
      FK=G*RK*TT-A2
      FFK=G*(ARG*SECH2+TT)+2.0*(U*COSI+V*SINI)*A
      RKNEW=RK-FFK/FFK
      IF(ABS(RKNEW-RK).LE.(ABS(EPSK*RKNEW)))GO TO 3
      RK=RKNEW
1 CONTINUE
      WRITE(6,2)I,RK,T,D,U,V
2 FORMAT(" ITERATION FOR K FAILED TO CONVERGE: I,K,D,U,V",
+ ,I6.5F10.5)
      CALL EXIT
      RETURN
3 RK=RKNEW
  A=SIGMA-RK*U*COSI-RK*V*SINI
C*-----
C* CHECK IF RK NEGATIVE; THIS CONDITION MAY ARRISE IF CURRENT IS

```

```

16790 C* 100 STRONG
16800 C*
16810 IF(RK.GT.O.O)GO TO 5
16820 WRITE(6,4)D,COSI,SINI,U,V,RK,A
16830 4 FORMAT(' RK IS NEGATIVE: D,COSI,SINI,U,V,RK,A',
16840 *7F10.5)
16850 CALL EXIT
16860 5 RETURN
16870 END
16880 C*
16890 C* SUBROUTINE SNELL(THETAO,HH,ITER)
16900 C*
16910 C* SNELL CALCULATES THE FIRST GUESS AT THE REFRACTION ANGLE
16920 C* AT EACH GRID BY SNELL'S LAW, FOR EACH ITERATION IN WHICH THE
16930 C* DEEPWATER WAVE HEIGHT IS BUILDING UP
16940 C*
16950 C* SNELL ALSO CALCULATES THE WAVE HEIGHT AT THE M GRID ROW
16960 C*
16970 C*
16980 C*
16990 COMMON D(50,50),U(50,50),V(50,50),Z(50,50),SI(50,50),CO(50,50),
17000 *H(50,50),CG(50,50),S(50,50),HBREAK(50,50),IB(50,50),DDX(50,50),
17010 *,DDDY(50,50)
17020 COMMON/CONST/ G,P1,P12,RAD,EPS,DX,DY,DT,DX2,DY2,T,SIGMA,
17030 *M,N,N1,N2,M1,M2,AM,DD,IT,RHO,IWET,IDRY,ID
17040 I=IDRY
17050 30 I=I+1
17060 IF(ITER.GT.1) I=M
17070 DO 600 J=2,N1
17080 CALL WVNUM(D(I,J-1),-1.0,O.O,O.O,O.O,RK,A)
17090 AA = RK* D(I,J-1)
17100 ANG = ARSIN(SIN(THETAO)*TANH(AA))
17110 ANG = PI-ANG
17120 ARG = 2.0*AA
17130 SHOAL = SORT(1.0/(TANH(AA))*(1.0+ARG/SINH(ARG)))
17140 REF = SQRT(COS(THETAO)/COS(ANG))
17150 WVHT = HH*SHOAL*REF
17160 HB = 0.12*TANH(AA)*P12/RK
17170 IF(WVHT.GT.HB) WVHT = HB
17180 IN = 1
17190 IF(WVHT.GT.HB) IN = 0
17200 SS = SIN(ANG)
17210 CC = COS(ANG)
17220 43 CONTINUE
17230 H(I,J) = WVHT
17240 IB(I,J) = IN
17250 Z(I,J) = ANG
17260 SI(I,J) = SS
17270 CO(I,J) = CC
17280 600 CONTINUE
17290 IF(I.EQ.M) GO TO 85
17300 GO TO 30
17310 85 CONTINUE
17320 C*
17330 C* BOUNDARY CONDITIONS
17340 C*
17350 L = 1
17360 K = N
17370 J = 1
17380 45 DO 60 I = 1,M
17390 H(I,J) = H(I,K)
17400 IB(I,J) = IB(I,K)

```

```

17410      Z(I,J)=Z(I,K)
17420      SI(I,J) = SI(I,K)
17430      CO(I,J) = CO(I,K)
17440      L = L+1
17450      IF (L .GT. 3) RETURN
17460      IF (L .EQ. 3) GO TO 610
17470      L = 2
17480      J = 2
17490      K=N1
17500      GO TO 45
17510      610 J = N2
17520      K = 3
17530      GO TO 45
17540      RETURN
17550      END
17560
17570
17580      SUBROUTINE DGRAD
17590
17600      C* DGRAD CALCULATES THE SPATIAL GRADIENTS IN DEPTH AFTER EACH
17610      C* UPDATING OF THE TOTAL DEPTH
17620      C*
17630      C*-----
17640      COMMON D(50,50),U(50,50),V(50,50),Z(50,50),SI(50,50),CO(50,50),
17650      *H(50,50),CG(50,50),S(50,50),HBREAK(50,50),IB(50,50),DDX(50,50),
17660      *DDY(50,50)
17670      COMMON/CONST/ G,PI,P12,RAD,EPS,DX,DY,DT,DX2,DY2,T,SIGMA,
17680      *M,N,N1,N2,M1,M2,AM,DD,IT,RHO,IWET,IDRY,ID
17690      DO 1 I = 2,M1
17700      DO 1 J = 2,N1
17710      DDX(I,J) = -(D(I-1,J)-D(I+1,J))/(2.*DX)
17720      DDY(I,J) = -(D(I,J-1)-D(I,J+1))/(2.*DY)
17730      1 CONTINUE
17740      DO 2 I = 1,M
17750      DDX(I,1)=DDX(I,N)
17760      DDY(I,1)=DDY(I,N)
17770      DDX(I,2)=DDX(I,N1)
17780      DDY(I,2)=DDY(I,N1)
17790      DDX(I,N2)=DDX(I,3)
17800      DDY(I,N2)=DDY(I,3)
17810      2 CONTINUE
17820      RETURN
17830      END
17840
17850      SUBROUTINE TAUSB (WIND, WINANG, CF,ITQ)
17860
17870      C* THIS SUBROUTINE CALCULATES SURFACE SHEAR STRESS BY VAN DORN'S
17880      C* METHOD, AND AN AVERAGE BOTTOM SHEAR STRESS USING A SMALL
17890      C* CURRENT ASSUMPTION
17900      C*
17910      C*-----
17920      COMMON D(50,50),U(50,50),V(50,50),Z(50,50),SI(50,50),CO(50,50),
17930      *H(50,50),CG(50,50),S(50,50),HBREAK(50,50),IB(50,50),DDX(50,50),
17940      *DDY(50,50),W(50,50),Y(50,50)
17950      COMMON/VAL/ETA(50,50)
17960      COMMON/STRESS/SIGXX(50,50),SIGYY(50,50),SIGXY(50,50),TAUBX(50,50),
17970      *TAUBY(50,50),TAUSX(50,50),TAUSY(50,50)
17980      COMMON/REF/ZZ(50,50),HNEW(50,50),RKA(50,50)
17990      COMMON/CONST/ G,PI,P12,RAD,EPS,DX,DY,DT,DX2,DY2,T,SIGMA,
18000      *M,N,N1,N2,M1,M2,AM,DD,IT,RHO,IWET,IDRY,ID
18010
18020

```

```

18030 C* CALCULATE WIND SHEAR STRESS
18040 C*-----
18050 IF (IT.GT.ITO+1) GO TO 21
18060 VANCON=1.1E-06
18070 IF (WIND.GE.7.2) VANCON = 1.1E-06+2.5E-06*((1.-7.2/WIND)**2.)
18080 WINDX = WIND*COS(WINANG)
18090 WINDY = WIND*SIN(WINANG)
18100 CON1 = RHO*VANCON*ABS(WIND)
18110 DO 20 J = 1,N2
18120 DO 20 I = 2,M
18130 TAUSX(I,J) = - CON1 *WINDX
18140 TAUSY(I,J) = CON1 *WINDY
18150 20 CONTINUE
18160 C*-----
18170 C* CALCULATE BOTTOM FRICTION AT EACH GRID POINT
18180 C*-----
18190 21 DO 40 J = 2,N1
18200 K = J-1
18210 DO 40 I = IWET,M1
18220 TAUBX(I,J) = (.5*CF*RHO*H(I,J)*W(I,J))/(T*SINH(RKA(I,J)*D(I,K)))
18230 TAUBY(I,J) = (.25*CF*RHO*H(I,J)*V(I,J))/(T*SINH(RKA(I,J)*D(I,K)))
18240 40 CONTINUE
18250 DO 100 I = 1,M
18260 TAUBX(I,1) = TAUBX(I,N)
18270 TAUBX(I,N1) = TAUBX(I,2)
18280 TAUBX(I,N2) = TAUBX(I,3)
18290 TAUBY(I,1) = TAUBY(I,N)
18300 TAUBY(I,N1) = TAUBY(I,2)
18310 TAUBY(I,N2) = TAUBY(I,3)
18320 100 CONTINUE
18330 RETURN
18340 END
18350 C*-----
18360 C* SUBROUTINE UCALC
18370 C*
18380 C* THIS SUBROUTINE CALCULATES THE MEAN HORIZONTAL VELOCITIES
18390 C* USING THE FINITE DIFFERENCE EQUATIONS
18400 C*
18410 C* NOTE THAT ALL DEPTHS USED ARE OFFSET BY -DY
18420 C*-----
18430 COMMON D(50,50),U(50,50),V(50,50),Z(50,50),SI(50,50),CG(50,50),
18440 *H(50,50),CG(50,50),S(50,50),HBREAK(50,50),IB(50,50),DDX(50,50),
18450 *DDY(50,50),W(50,50),Y(50,50)
18460 COMMON/VAL/ETA(50,50)
18470 COMMON/STRESS/SIGXX(50,50),SIGYY(50,50),SIGXY(50,50),TAUBX(50,50),
18480 *TAUBY(50,50),TAUSX(50,50),TAUSY(50,50)
18490 COMMON/REF/ZZ(50,50),HNEW(50,50),RKA(50,50)
18500 COMMON/CONST/G,PI,P12,RAD,EPS,DX,DY,DT,DX2,DY2,T,SIGMA,
18510 *M,N,N1,N2,M1,M2,AM,DO,IT,RHO,IWET,IDRY,ID
18520 DO 21 J=3,N1
18530 K=J-1
18540 DO 21 I=IWET,M-1
18550 DBAR = (D(I,K)+D(I-1,K))/2.
18560 U(I,J) = U(I,J) +DT*((ETA(I-1,J) - ETA(I,J))*G/DX+(SIGXX(I-1,J)-SI
18570 1GX(I,J))/(DX*RHO*DBAR) - (SIGXY(I,J+1)-SIGXY(I,J-1)+SIGXY(I-1,J
18580 2+1)-SIGXY(I-1,J-1))/(4.*DY*RHO*DBAR)+(TAUSX(I,J)+TAUSX(I-1,J))/(2.
18590 3*RHO*DBAR)-(TAUBX(I,J)+TAUBX(I-1,J))/(2.*RHO*DBAR))
18600 U(IWET,J)=0.0
18610 DBAR = (D(I,K) + D(I,K-1))/2.0
18620 V(I,J)=V(I,J) +DT*((ETA(I,J)-ETA(I,J-1))*G/DY-(SIGXY(I+1,J-1)-SIGX
18630 1Y(I-1,J-1))/(4.*DX*RHO*DBAR)-(SIGXY(I+1,J)-SIGXY(I-1,J))/(4.*DX*RH
18640
00018030
00018040
00018050
00018060
00018070
00018080
00018090
00018100
00018110
00018120
00018130
00018140
00018150
00018160
00018170
00018180
00018190
00018200
00018210
00018220
00018230
00018240
00018250
00018260
00018270
00018280
00018290
00018300
00018310
00018320
00018330
00018340
00018350
00018360
00018370
00018380
00018390
00018400
00018410
00018420
00018430
00018440
00018450
00018460
00018470
00018480
00018490
00018500
00018510
00018520
00018530
00018540
00018550
00018560
00018570
00018580
00018590
00018600
00018610
00018620
00018630
00018640

```

```

18650 20*DBAR)+(SIGYY(I,J-1) - SIGYY(I,J))/(DY*RHO*DBAR)+(TAUSY(I,J) + TA
18660 3USY(I,J-1))/(2.*RHO*DBAR) - (TAUBY(I,J) + TAUBY(I,J-1))/(2.*RHO*DB
18670 4AR))
18680
18690 21 CONTINUE
18700
18710 C*-----
18720 C* BOUNDARY CONDITIONS
18730 C*-----
18740 DO 60 I=1,M
18750 V(I,N2) = V(I,3)
18760 U(I,N2) = U(I,3)
18770 V(I,2) = V(I,N1)
18780 U(I,2) = U(I,N1)
18790 V(I,1) = V(I,N)
18800 U(I,1) = U(I,N)
18810 DO 69 I=1,M1
18820 DO 69 J=2,N1
18830 U(M,J)=O.O
18840 W(I,J)=(U(I,J)+U(I+1,J))/2.O
18850 Y(I,J)=(V(I,J)+V(I,J+1))/2.O
18860 69 CONTINUE
18870 DO 79 I=1,M
18880 V(I,N2)=Y(I,3)
18890 W(I,N2)=W(I,3)
18900 Y(I,1)=Y(I,N)
18910 79 W(I,1)=W(I,N)
18920 DO 80 J=1,N+2
18930 DO 80 Y(M,J)=(V(M,J)+V(M,J+1))/2.O
18940 RETURN
18950 END
18960 C*-----
18970 C* SUBROUTINE ETAS
18980 C*
18990 C* ETAS CALCULATES THE CORRECTION TO SETUP AND TOTAL DEPTH BASED
19000 C* ON CONSERVATION OF MASS
19010 C*-----
19020 COMMON D(50,50),U(50,50),V(50,50),Z(50,50),SI(50,50),CO(50,50),
19030 *H(50,50),CG(50,50),S(50,50),HBREAK(50,50),IB(50,50),DDX(50,50),
19040 *DDY(50,50),W(50,50),Y(50,50)
19050 COMMON/VAL/ETA(50,50)
19060 COMMON/STRESS/SIGXX(50,50),SIGYY(50,50),SIGXY(50,50),TAUBX(50,50),
19070 *TAUBY(50,50),TAUSX(50,50),TAUSY(50,50)
19080 COMMON/REF/ZZ(50,50),HNEW(50,50),RKA(50,50)
19090 COMMON/CONST/ G,PI,P12,RAP,EPS,DX,DY,DT,DX2,DY2,T,SIGMA,
19100 *M,N,N1,N2,M1,M2,AM,DD,IT,RHO,IWET,IDRY,ID
19110 DO 1 J = 3,N1
19120 K = J-1
19130 DO 1 I=IWET,M1
19140 ETAOLD = ETA(I,J)
19150 ETA(I,J)=ETAOLD+DT*(U(I,J)*(D(I,K)+D(I-1,K))/(2.*DX) - U(I+1,J)
19160 * (D(I,K)+D(I+1,K))/(2.*DX)+V(I,J)*(D(I,K-1)+D(I,K))/(2.*DY) - V(I,
19170 2J+1)*(D(I,K+1)+D(I,K))/(2.*DY))
19180 D(I,K) = D(I,K) - ETAOLD + ETA(I,J)
19190 1 CONTINUE
19200
19210 C*-----
19220 C* BOUNDARY CONDITIONS
19230 C*-----
19240 DO 2 I = 1,M
19250 D(I,1)=D(I,N)
19260 D(I,N2) = D(I,3)
19270 D(I,N1) = D(I,2)

```

```

00019270
00019280
00019290
00019300
00019310
00019320
00019330
00019340
00019350
00019360

```

```

      ETA(I,N2) = ETA(I,3)
      ETA(I,2) = ETA(I,N1)
      ETA(I,1) = ETA(I,N)
      DO 3 I=1,M
      IF(D(I,1).GT.DD) GO TO 4
      2 CONTINUE
      3 IWET=I
      4 IDRY=IWET-1
      RETURN
      END

```

```

19270
19280
19290
19300
19310
19320
19330
19340
19350
19360

```

NONLINEAR MODEL

```

1000 $RESET FREE
1100 C*-----
1200 C*
1300 C* NEARSHORE CIRCULATION MODEL --- NONLINEAR VERSION
1400 C*
1500 C* THIS PROGRAM IS A NUMERICAL MODEL TO PREDICT SURF ZONE DYNAMICS,
1600 C* GIVEN A PERIODIC DEPTH GRID AND MONOCHROMATIC WAVE FIELD AS INPUT.
1700 C* THE REFRACTION PROGRAM, INCLUDING THE EFFECTS OF WAVE-CURRENT
1800 C* INTERACTION, WAS DEVELOPED BY NODA ET. AL. (1974). THE LINEAR
1900 C* VERSION OF THIS PROGRAM WAS DEVELOPED BY BIRKEMEIER AND DALRYMPLE
2000 C* (1977). THE PRESENT NONLINEAR VERSION UTILISES THE FULL NON-
2100 C* LINEAR MOMENTUM EQUATIONS (EBERSOLE AND DALRYMPLE(1979)). BOTTOM
2200 C* FRICTION IS CALCULATED USING THE METHOD DEVELOPED BY DALRYMPLE AND
2300 C* LIU
2400 C*
2500 C*-----
2600 COMMON D(50,50),U(50,50),V(50,50),Z(50,50),SI(50,50),CO(50,50),
2700 *H(50,50),CG(50,50),S(50,50),HBREAK(50,50),IB(50,50),DDDX(50,50),
2800 *DDDY(50,50),W(50,50),Y(50,50)
2900 COMMON/VAL/DP1(50,50),DM1(50,50),UP1(50,50),UM1(50,50),
3000 *VP1(50,50),VM1(50,50),ETAP1(50,50),ETAM1(50,50),ETA(50,50)
3100 COMMON/STRESS/SIGXX(50,50),SIGYY(50,50),SIGXY(50,50),TAUBX(50,50),
3200 *TAUBY(50,50),TAUSX(50,50),TAUSY(50,50)
3300 COMMON/REF/ZZ(50,50),HNEW(50,50),RKA(50,50)
3400 COMMON/EDDY/EX(50,50),EY,VCON
3500 COMMON/CONST/ G,PI,P12,RAD,EPHS,EPSS,DX,DY,DT,DX2,DY2,T,SIGMA,
3600 *M,N,N1,N2,M1,M2,AM,DD,IT,RHO,IWET,IDRY,ID
3700 DIMENSION DST(50,50)
3800 C*-----
3900 C*
4000 C* NOTES ON RUNNING THE PROGRAM
4100 C*
4200 C* 1. WAVE ANGLE IS MEASURED CLOCKWISE FROM THE +X DIRECTION
4300 C*
4400 C* 2. WIND ANGLE IS MEASURED CLOCKWISE FROM THE -X DIRECTION
4500 C*
4600 C* 3. ALL INPUT AND OUTPUT VARIABLES ARE IN MKS UNITS
4700 C*
4800 C* 4. THE DEPTH GRID IS OFFSET -DY FROM ALL OTHER VARIABLE GRIDS
4900 C*-----
5000 C*
5100 C* DEFINITIONS OF QUANTITIES USED IN PROGRAM
5200 C*
5300 C* 1. CONSTANTS
5400 C*
5500 C* CF - BOTTOM FRICTION COEFFICIENT (DARCY TYPE)
5600 C* VANCON - WIND SHEAR COEFFICIENT (VAN DORN TYPE)
5700 C* EY - LATERAL EDDY COEFFICIENT, LONGSHORE DIRECTION
5800 C* VCON - EDDY VISCOSITY COEFFICIENT, OFFSHORE DIRECTION
5900 C*
6000 C* 2. VARIABLE ARRAYS (VALUE AT EACH GRID LOCATION)
6100 C*
6200 C* D - TOTAL WATER DEPTH, STILL WATER + SETUP(ETA)
6300 C* DDDX,DDDY - LOCAL DERIVATIVES OF THE TOTAL DEPTH
6400 C* ETA - DEVIATION OF MEAN WATER LEVEL FROM STILL WATER LEVEL
6500 C* Z - WAVE ANGLE
6600 C* CO - COS(Z)
6700 C* SI - SIN(Z)
6800 C*
00001000
00001100
00001200
00001300
00001400
00001500
00001600
00001700
00001800
00001900
00002000
00002100
00002200
00002300
00002400
00002500
00002600
00002700
00002800
00002900
00003000
00003100
00003200
00003300
00003400
00003500
00003600
00003700
00003800
00003900
00004000
00004100
00004200
00004300
00004400
00004500
00004600
00004700
00004800
00004900
00005000
00005100
00005200
00005300
00005400
00005500
00005600
00005700
00005800
00005900
00006000
00006100
00006200
00006300
00006400
00006500
00006600
00006700
00006800

```


6900	C*	H - WAVE HEIGHT	00006900
7000	C*	HBREAK - LOCAL BREAKING WAVE HEIGHT	00007000
7100	C*	IB - BREAKING INDEX	00007100
7200	C*	IB=0. WAVE IS BREAKING LOCALLY	00007200
7300	C*	IB=1. WAVE IS NOT BREAKING LOCALLY	00007300
7400	C*	CG - GROUP VELOCITY	00007400
7500	C*	RKA - WAVE NUMBER	00007500
7600	C*	U,V - X,Y VELOCITIES AT SIDES OF GRID BLOCKS	00007600
7700	C*	W,V - X,Y VELOCITIES AT CENTERS OF GRID BLOCKS	00007700
7800	C*	NOTE THAT THE U,V AND W,V ARRAYS ARE INTERCHANGED	00007800
7900	C*	IN SEVERAL SUBROUTINES THROUGH THE COMMON STATEMENTS	00007900
8000	C*	SIGX,SIGY,SIGZ - RADIATION STRESSES	00008000
8100	C*	TAUBX,TAUBY - BOTTOM STRESSES	00008100
8200	C*	TAUSX,TAUSY - SURFACE STRESSES	00008200
8300	C*	EX - LATERAL EDDY COEFFICIENT, OFFSHORE DIRECTION	00008300
8400	C*		00008400
8500	C*	3. LOCALLY DEFINED VARIABLES	00008500
8600	C*		00008600
8700	C*	DUDX,DVDX - VELOCITY GRADIENT COMPONENTS	00008700
8800	C*	DCDX,DCDY - WAVE CELERITY GRADIENT COMPONENTS	00008800
8900	C*	DCGDY,DCGDY - GROUP VELOCITY GRADIENT COMPONENTS	00008900
9000	C*	DTDX,DTDY - WAVE ANGLE GRADIENT COMPONENTS	00009000
9100	C*	EPS - ACCURACY VALUE USED IN RELAXATION SCHEMES	00009100
9200	C*		00009200
9300	C*		00009300
9400	C*		00009400
9500	C*	VARIABLES TO BE READ INTO PROGRAM	00009500
9600	C*		00009600
9700	C*	1. WAVE PARAMETERS (DEEPWATER)	00009700
9800	C*		00009800
9900	C*	T - WAVE PERIOD (SECONDS)	00009900
10000	C*	HO - WAVE HEIGHT (METERS)	00010000
10100	C*	A - WAVE ANGLE, CLOCKWISE FROM +X (DEGREES)	00010100
10200	C*		00010200
10300	C*	2. WIND PARAMETERS	00010300
10400	C*		00010400
10500	C*	WIND - WIND SPEED (METERS/SECOND)	00010500
10600	C*	WINANG - WIND ANGLE, CLOCKWISE FROM -X (DEGREES)	00010600
10700	C*		00010700
10800	C*	3. GRID PARAMETERS	00010800
10900	C*		00010900
11000	C*	M - NUMBER OF GRIDS IN X DIRECTION	00011000
11100	C*	N - NUMBER OF GRIDS IN Y DIRECTION	00011100
11200	C*	DX - GRID SPACING IN X DIRECTION (METERS)	00011200
11300	C*	DY - GRID SPACING IN Y DIRECTION (METERS)	00011300
11400	C*	DT - TIME STEP, <DX/SQRT(2*G*DMAX) (SECONDS)	00011400
11500	C*	INDEX - SPECIFY INPUT OF DEPTH INFORMATION	00011500
11600	C*	=1. READ DATA FROM PREVIOUS RUN	00011600
11700	C*	=2. READ DEPTH GRID FROM INPUT DATA FILE	00011700
11800	C*	=3. ESTABLISH PLANE BEACH BASED ON INPUT BEACH SLOPE	00011800
11900	C*	AM - BEACH SLOPE	00011900
12000	C*	4. PROGRAM CONTROL PARAMETERS	00012000
12100	C*		00012100
12200	C*		00012200
12300	C*	ITA - TOTAL NUMBER OF ITERATIONS (INCLUDING ACCUMULATED	00012300
12400	C*	TOTAL OF PREVIOUS RUNS IF INDEX=1 IS USED)	00012400
12500	C*	NHIGHT - NUMBER OF ITERATIONS OVER WHICH THE DEEP WATER WAVE	00012500
12600	C*	HEIGHT IS BUILT UP	00012600
12700	C*	ID - DETERMINE IF DISSIPATION OF WAVE ENERGY IS TO BE	00012700
12800	C*	INCLUDED	00012800
12900	C*	=0. NO DISSIPATION	00012900
13000	C*	=1. DISSIPATION DUE TO VISCOSITY AND BOTTOM PERM-	00013000

```

13100      C*      -EABILITY
13200      C*      KSKIP - DETERMINE FREQUENCY OF PRINTED ITERATIONS
13300      C*
13400      C*      5. DEPTH GRID (IF INDEX=2)
13500      C*
13600      C*      D - LOCAL WATER DEPTH W/R MEAN WATER LEVEL.
13700      C*      SEE USERS MANUAL FOR INPUT FORMAT
13800      C*
13900      C*-----
14000      C*      RHO=1000.
14100      C*      G=9.81
14200      C*      PI=3.1415927
14300      C*      P12=PI *2.0
14400      C*      RAD=180.0/PI
14410      C*      CF=0.010
14420      C*      DD=0.0
14430      C*      EY=0.25
14440      C*      VCON=0.0025
14500      C*-----
14600      C*      READ INPUT DATA
14700      C*
14800      C*      1. WAVE PARAMETERS
14900      C*      READ(5,/)T,HO,A
15000      C*      2. WIND PARAMETERS
15100      C*      READ(5,/)WIND,WINANG
15200      C*      3. GRID PARAMETERS
15300      C*      READ(5,/)M,N,DX,DY,DT,INDEX,AM
15400      C*      4. PROGRAM CONTROL PARAMETERS
15500      C*      READ(5,/)ITA,NHIGHT,ID,KSKIP
15600      C*-----
15700      C*      WRITE INPUT DATA ONTO OUTPUT FILE 6 AS HEADER
15800      C*-----
15900      C*      WRITE(6,104)M,N,ITA
16000      C*      WRITE(6,102)DX,DY,DT
16100      C*      WRITE(6,105) T,HO,A,AM
16200      C*      WRITE(6,106) WIND,WINANG
16300      C*      WRITE(6,119) IDDEX,IN,MM
16400      C*      WRITE(6,121) NHIGHT
16500      C*      WRITE(6,120) CF,DD
16600      C*      WRITE(6,123) EY,VCON
16700      C*      ITO=0
16800      C*      HGT=HO
16900      C*      DELTAT=DT
17000      C*      WINANG=WINANG/RAD
17100      C*      N2=N+2
17200      C*      N1=N+1
17300      C*      M2=M-2
17400      C*      M1=M-1
17500      C*      DX2=DX*2.
17600      C*      DY2=DY*2.
17700      C*      SIGMA=PI2/T
17800      C*      EPSH=0.001
17900      C*      EPSA=0.01
18000      C*-----
18100      C*      ESTABLISH BOTTOM TOPOGRAPHY, BASED ON VALUE OF "INDEX"
18200      C*-----
18300      C*      GO TO (1,2,3) INDEX
18400      C*-----
18500      C*      INDEX=1, READ DATA FROM FIE 8 FOR PREVIOUS RUN OF MODEL
18600      C*-----
18700      C*      1 READ(8,116)
18800      C*      *((ETA(I,J),J=1,M),I=1,N2),((D(I,J),J=1,N2),I=1,M),

```

```

18900      *((U(I,J),J=1,N2),I=1,M),((V(I,J),J=1,N2),I=1,M),
19000      *((UM(I,I,J),J=1,N2),I=1,M),((VM(I,I,J),J=1,N2),I=1,M),
19100      *((DM(I,I,J),J=1,N2),I=1,M),((ETAM(I,I,J),J=1,N2),I=1,M),
19200      *((Z(I,J),J=1,N2),I=1,M),((H(I,J),J=1,N2),I=1,M),
19300      *((W(I,J),J=1,N2),I=1,M),((Y(I,J),J=1,N2),I=1,M),
19400      *((RKA(I,J),J=1,N2),I=1,M),
19500      READ(8,118)((SIGXX(I,J),J=1,N2),I=1,M),
19600      *((SIGXY(I,J),J=1,N2),I=1,M),((SIGVY(I,J),J=1,N2),I=1,M),
19700      READ(8,117)ITO
19800      DO 450 I=1,M
19900      DO 450 J=1,N2
20000      CO(I,J)=COS(Z(I,J))
20100      SI(I,J)=SIN(Z(I,J))
20200      450 CONTINUE
20300      C*-----
20400      C* IF WAVE ANGLE IS LESS THAN 180 DEGREES, VARIABLE GRIDS WERE
20500      C* FLIPPED IN PREVIOUS RUN. ROTATE WAVE AND WIND ANGLES
20600      C*-----
20700      IF(A.GE.180.) GO TO 31
20800      A=360.-A
20900      WINANG=PI2-WINANG
21000      GO TO 31
21100      C*-----
21200      C* INDEX=2, READ DEPTH GRID FROM INPUT FILE 5
21300      C*-----
21400      2 READ (5,/) ((D(I,J),J=1,N),I=1,M)
21500      C*-----
21600      C* IF WAVE ANGLE IS LESS THAN 180 DEGREES, FLIP THE INPUT DEPTH
21700      C* GRID AND ROTATE THE WAVE AND WIND ANGLES
21800      C*-----
21900      IF(A.GT.180.) GO TO 161
22000      A=360.-A
22100      WINANG=PI2-WINANG
22200      DO 158 I=1,M
22300      DO 159 J=1,N
22400      159 DST(I,J)=D(I,J)
22500      DO 158 J=1,N
22600      K=(N-J)+1
22700      158 D(I,K)=DST(I,J)
22800      161 DO 160 I=1,M
22900      D(I,1)=D(I,N)
23000      D(I,N2)=D(I,3)
23100      D(I,N1)=D(I,2)
23200      160 CONTINUE
23300      GO TO 146
23400      C*-----
23500      C* INDEX=3, ESTABLISH PLANE BEACH
23600      C*-----
23700      3 DO 30 J=1,N2
23800      DO 30 I=1,M
23900      D(I,J)=((FLOAT(I-2)*DX)*AM)
24000      30 CONTINUE
24100      C*-----
24200      C* IF WAVE ANGLE IS LESS THAN 180 DEGREES, ROTATE WAVE AND WIND ANGLE
24300      C*-----
24400      IF(A.GE.180.) GO TO 146
24500      A=360.-A
24600      WINANG=PI2-WINANG
24700      C*-----
24800      C* WRITE DEPTH GRID ON OUTPUT IF INDEX=2 OR 3
24900      C*-----
25000      146 WRITE(6,108)

```

```

25100      WRITE(6,103)((D(I,J),(J=1,N1),I=1,M)
25200      C*-----
25300      C*  INITIALIZE ARRAYS
25400      C*-----
25500      DO 65 I=1,M
25600      DO 66 J=1,N2
25700      ETA(I,J)=0.0
25800      U(I,J)=0.0
25900      V(I,J)=0.0
26000      ETAM(I,J)=0.0
26100      DM1(I,J)=0(I,J)
26200      UM1(I,J)=0.0
26300      VM1(I,J)=0.0
26400      65 CONTINUE
26500      31 DO 15 I=1,M
26600      IF(D(I,1).GT.DD) GO TO 95
26700      15 CONTINUE
26800      95 IWET=I
26900      IDRY=IWET-1
27000      C*-----
27100      C*  MAIN PROGRAM LOOP FOR EACH ITERATION
27200      C*-----
27300      IT=ITO
27400      IF(ITO.NE.O) GO TO 4
27500      HO=HGT*TANH(1.0/FLOAT(NHIGHT))
27600      CALL DGRAD
27700      CALL REFRAC(A,HO,1,NHIGHT,CF)
27800      CALL TAUSB(WIND,WINANG,CF,ITO)
27900      TSTEP=DT*0.5
28000      CALL CONTIN
28100      CALL ETAS(ETA,TSTEP)
28200      CALL MOMEN
28300      CALL UCALC(D,U,V,TSTEP)
28400      CALL ROLBAC
28500      4 DO 5 IT=(1+ITO),ITA
28600      L=AMOD(FLOAT(IT),FLOAT(KSKIP))
28700      MCOUNT=AMOD(FLOAT(IT),10.0)
28800      HO=HGT*TANH(FLOAT(IT)/(FLOAT(NHIGHT)/2.0))
28900      IF(IT.LE.((NHIGHT*2.0)+5)) GO TO 12
29000      GO TO 13
29100      12 CALL DGRAD
29200      ITP1=IT+1
29300      CALL REFRAC(A,HO,ITP1,NHIGHT,CF)
29400      13 CALL TAUSB(WIND,WINANG,CF,ITP1)
29500      IF(IT.EQ.1) GO TO 51
29600      GO TO 52
29700      51 TSTEP=DT
29800      CALL CONTIN
29900      CALL ETAS(ETAM1,TSTEP)
30000      CALL MOMEN
30100      CALL UCALC(DM1,UM1,VM1,TSTEP)
30200      DO 66 I=1,M
30300      DO 66 J=1,N2
30400      ETA(I,J)=ETAP1(I,J)
30500      D(I,J)=DP1(I,J)
30600      U(I,J)=UP1(I,J)
30700      V(I,J)=VP1(I,J)
30800      66 CONTINUE
30900      GO TO 18
31000      52 TSTEP=DT*2.0
31100      CALL CONTIN
31200      CALL ETAS(ETAM1,TSTEP)
00025100
00025200
00025300
00025400
00025500
00025600
00025700
00025800
00025900
00026000
00026100
00026200
00026300
00026400
00026500
00026600
00026700
00026800
00026900
00027000
00027100
00027200
00027300
00027400
00027500
00027600
00027700
00027800
00027900
00028000
00028100
00028200
00028300
00028400
00028500
00028600
00028700
00028800
00028900
00029000
00029100
00029200
00029300
00029400
00029500
00029600
00029700
00029800
00029900
00030000
00030100
00030200
00030300
00030400
00030500
00030600
00030700
00030800
00030900
00031000
00031100
00031200

```

```

31300 CALL MOMEN
31400 CALL UCALC(DM1,UM1,VM1,TSTEP)
31500 IF(MCOUNT.EQ.O) GO TO 53
31600 CALL ROLBAC
31700 GO TO 18
31800
31900 53 CALL ROLBAC
32000 TSTEP=DT
32100 CALL CONTIN
32200 CALL ETAS(ETAM1,TSTEP)
32300 CALL MOMEN
32400 CALL UCALC(DM1,UM1,VM1,TSTEP)
32500 DO 57 I=1,M
32600 DO 57 J=1,N2
32700 ETA(I,J)=ETAP1(I,J)
32800 D(I,J)=DP1(I,J)
32900 U(I,J)=UP1(I,J)
33000 V(I,J)=VP1(I,J)
33100 57 CONTINUE
33200 18 CONTINUE
33300 SUM=O.O
33400 DO 86 I=1,M
33500 DO 86 J=2,N
33600 SUM=SUM+O.5*(W(I,J)**2+V(I,J)**2)*D(I,J-1)
33700 SUM=SUM+G*ETA(I,J)*(D(I,J-1)-O.5*ETA(I,J))
33800 86 CONTINUE
33900 WRITE(6,101) SUM
34000 IF(L.NE.O)GO TO 5
34100 WRITE(6,112)
34200 WRITE(6,113)IT,H0
34300 WRITE(6,114)
34400 WRITE(6,115)
34500 WRITE(6,103)((H(I,J),J=1,N1),I=1,M)
34600 DO 401 I=1,M
34700 DO 401 J=1,N2
34800 401 ZZ(I,J)=360.O-Z(I,J)*RAD
34900 WRITE(6,122)
35000 WRITE(6,109)((ZZ(I,J),J=1,N1),I=1,M)
35100 WRITE(6,107)
35200 WRITE(6,103)((U(I,J),J=1,N1),I=1,M)
35300 WRITE(6,110)
35400 WRITE(6,103)((V(I,J),J=1,N1),I=1,M)
35500 WRITE(6,111)
35600 WRITE(6,103)((ETA(I,J),J=1,N1),I=1,M)
35700 5 CONTINUE
35800
35900 C*-----
36000 C THE FOLLOWING WRITE STATEMENTS WRITE OUT THE RESULTS OF
36100 C THE LAST ITERATION ONTO AN OUTPUT FILE TO BE USED FOR A
36200 C SUBSEQUENT START-UP
36300 C*-----
36400 WRITE(3,116)
36500 *((ETA(I,J),J=1,N2),I=1,M),((D(I,J),J=1,N2),I=1,M),
36600 *((U(I,J),J=1,N2),I=1,M),((V(I,J),J=1,N2),I=1,M),
36700 *((UM1(I,J),J=1,N2),I=1,M),((VM1(I,J),J=1,N2),I=1,M),
36800 *((DM1(I,J),J=1,N2),I=1,M),((ETAM1(I,J),J=1,N2),I=1,M),
36900 *((Z(I,J),J=1,N2),I=1,M),((H(I,J),J=1,N2),I=1,M),
37000 *((W(I,J),J=1,N2),I=1,M),((Y(I,J),J=1,N2),I=1,M)
37100 *,((RKA(I,J),J=1,N2),I=1,M)
37200 WRITE(3,118)((SIGXX(I,J),J=1,N2),I=1,M),
37300 *((SIGXY(I,J),J=1,N2),I=1,M),((SIGYY(I,J),J=1,N2),I=1,M)
37400 WRITE(3,117)ITA
37500 LOCK 3
37600 101 FORMAT(1X,"THE TOTAL ENERGY IS",F14.2)

```



```

43900      DO 4 I=IWET,M1
44000      DO 3 J=3,N1
44100      ENERGY=O.125*RHO*G*(H(I,J)**2)
44200      SIGX(I,J)=SIGX(I,J)*ENERGY
44300      SIGY(I,J)=SIGY(I,J)*ENERGY
44400      SIGXY(I,J)=SIGXY(I,J)*ENERGY
44500      CONTINUE
44600      SIGX(I,1)=SIGX(I,N)
44700      SIGY(I,1)=SIGY(I,N)
44800      SIGXY(I,1)=SIGXY(I,N)
44900      SIGX(I,2)=SIGX(I,N1)
45000      SIGY(I,2)=SIGY(I,N1)
45100      SIGXY(I,2)=SIGXY(I,N1)
45200      SIGX(I,N2)=SIGX(I,3)
45300      SIGY(I,N2)=SIGY(I,3)
45400      SIGXY(I,N2)=SIGXY(I,3)
45500      CONTINUE
45600      DO 5 J=3,N1
45700      SIGXY(M,J)=2.O*SIGXY(M1,J)-SIGXY(M2,J)
45800      CONTINUE
45900      SIGXY(M,1)=SIGXY(M,N)
46000      SIGXY(M,2)=SIGXY(M,N1)
46100      SIGXY(M,N2)=SIGXY(M,3)
46200      RETURN
46300      END
46400
46500      C*-----
46600      C*
46700      C*
46800      C*
46900      C*
47000      C*
47100      C*-----
47200      SUBROUTINE GROUP(I,J,DCGDX,DCGDY,FF)
47300      C*
47400      C* THIS SUBROUTINE CALCULATES THE GROUP VELOCITY ,WAVE CELERITY
47500      C* AND THEIR SPATIAL DERIVATIVES.
47600      C*
47700      C*-----
47800      COMMON D(50,50),W(50,50),Y(50,50),Z(50,50),SI(50,50),CO(50,50),
47900      *H(50,50),CG(50,50),S(50,50),HBREAK(50,50),IB(50,50),DDDX(50,50),
48000      *,DDDY(50,50),U(50,50),V(50,50)
48100      COMMON/CONST/ G,PI,PI2,RAD,EPHS,EPSS,DX,DY,DT,DX2,DY2,T,SIGMA,
48200      *M,N,N1,N2,M1,M2,AM,DD,IT,RHO,IWET,IDRY,ID
48300      COMMON/REF/ZZ(50,50),HNEW(50,50),RKA(50,50)
48400      DUDX(I,J)=(W(I+1,J)-W(I,J))/DX
48500      DUDY(I,J)=(U(I,J+1)-U(I,J))/DY2
48600      DVDX(I,J)=(V(I+1,J)-V(I,J))/DX2
48700      DVDY(I,J)=(Y(I,J+1)-Y(I,J))/DY
48800      DTDX(I,J)=(Z(I+1,J)-Z(I,J))/DX2
48900      DTDY(I,J)=(Z(I,J+1)-Z(I,J))/DY2
49000      E(I,J)=U(I,J)*COSI+V(I,J)*SINI+O.5*A*(1.O+ARG2/SINH2)/RK
49100      DKDX(I,J)=RK*(U(I,J)*SINI-V(I,J)*COSI)*OTDX(I,J)-(COSI*DUDX(I,J)+
49200      *SINI*DVDX(I,J))-A*DDDX(I,J-1)/SINH2/EE
49300      DKDY(I,J)=RK*(U(I,J)*SINI-V(I,J)*COSI)*OTDY(I,J)-(COSI*DUDY(I,J)
49400      *SINI*DVDY(I,J))-A*DDDY(I,J-1)/SINH2/EE
49500      JU=J-1
49600      DEP=D(I,JJ)
49700      COSI=CO(I,J)
49800      SINI=SI(I,J)
49900      DCGDX=O.O
50000      DCGDY=O.O
50100      C* CHECK FOR DRY LAND
50200      IF (DEP.LE.DD) RETURN
50300      CALL WNUM(DEP,COSI,SINI,U(I,J),V(I,J),RK,A)
50400      RKA(I,J)=RK
50500      IF (J.EQ.N) RKA(I,1)=RKA(I,J)
50600      IF (J.EQ.2) RKA(I,N1)=RKA(I,J)

```



```

56500 SIGX(I,J) = SIGXX                                00056500
56600 SIGY(I,J) = SIGYY                                00056600
56700 TAUXY=FF*SI(I,J)*CO(I,J)                      00056700
56800 SIGXY(I,J)=TAUXY                                00056800
56900 SI(I,J)=CG(I,J)*(SI(I,J)*DTDX-CO(I,J)*DTDY)-(CO(I,J)*DC  00056900
57000 *GDY+SI(I,J)*DCGDY)-(SIGXX*DUDX+TAUXY*DUDY+TAUXY*DUDY)-X  00057000
57100 GO TO 500                                        00057100
499 H(I,J)=O.O                                        00057200
57200 SIGXY(I,J)=O.O                                    00057300
57300 CONTINUE                                         00057400
57400 DO 510 II=1,M2                                  00057500
57500 I=M-II                                           00057600
57600 DO 580 ITT=1,ITMAX                              00057700
57700 IFLAG=1                                          00057800
57800 DO 520 J=2,N1                                    00057900
57900 IF(D(I,J-1).LE.DD) GO TO 520                    00058000
58000 IB(I,J)=1                                         00058100
58100 CC1=(V(I,J)+CG(I,J)*SI(I,J))/DX                 00058200
58200 CC2=(U(I,J)+CG(I,J)*CO(I,J))/DY                 00058300
58300 HNEW(I,J)=(CC1*H(I,J-1)-CC2*H(I+1,J))/(CC1-CC2-S(I,J)/2.O) 00058400
58400 IF (HNEW(I,J).LT.O.O) GO TO 810                  00058500
58500 IF (HNEW(I,J).LE.HBREAK(I,J)) GO TO 850          00058600
58600 HNEW(I,J)=HBREAK(I,J)                            00058700
58700 IB(I,J)=O                                         00058800
58800 CONTINUE                                         00058900
58900 IF (ABS(HNEW(I,J)-H(I,J)).GT.(EPSH*ABS(HNEW(I,J)))) IFLAG=O 00059000
59000 C* BOUNDARY CONDITIONS                          00059100
59100 IF(J.NE.2) GO TO 800                             00059200
59200 HNEW(I,N1)=HNEW(I,J)                             00059300
59300 IB(I,N1)=IB(I,J)                                 00059400
59400 GO TO 520                                         00059500
59500 800 IF(J.NE.3) GO TO 801                          00059600
59600 HNEW(I,N2)=HNEW(I,J)                             00059700
59700 IB(I,N2)=IB(I,J)                                 00059800
59800 801 IF(J.NE.N) GO TO 802                          00059900
59900 HNEW(I,1)=HNEW(I,J)                             00060000
60000 IB(I,1)=IB(I,J)                                 00060100
60100 GO TO 520                                         00060200
60200 802 IF(J.NE.N1) GO TO 520                       00060300
60300 HNEW(I,2)=HNEW(I,J)                             00060400
60400 IB(I,2)=IB(I,J)                                 00060500
60500 CONTINUE                                         00060600
60600 DO 625 J=1,N2                                    00060700
60700 H(I,J)=HNEW(I,J)                                00060800
60800 CONTINUE                                         00060900
60900 IF(IFLAG.EQ.1) GO TO 570                         00061000
580 CONTINUE                                           00061100
540 WRITE(6,540) I,ITT                                00061200
540 FORMAT(' RELAXATION FOR THE WAVE HEIGHT FAILED TO CONVERGE',  00061300
541 *ON ROW ',I5,' AFTER ',I6,' ITERATIONS')          00061400
541 WRITE(6,541)(H(I,J),J=1,N2)                      00061500
541 FORMAT(' LAST VALUES OF H ARE '//,10F13.5)        00061600
541 RETURN                                             00061700
570 CONTINUE                                           00061800
510 CONTINUE                                           00061900
510 RETURN                                             00062000
END                                                     00062100
C*-----
C* SUBROUTINE ANGLE(ITMAX)                             00062200
62300 C* ANGLE CALCULATES THE LOCAL WAVE DIRECTION AT EACH GRID LOCATION 00062300
62400 C* 00062400
62500 C* 00062500
62600 C* 00062600

```

```

62700 C*
62800 C*
62900 COMMON D(50,50),W(50,50),Y(50,50),Z(50,50),SI(50,50),CO(50,50),
63000 *H(50,50),CG(50,50),S(50,50),HBREAK(50,50),IB(50,50),DDDX(50,50),
63100 *DDY(50,50),U(50,50),V(50,50)
63200 COMMON/CONST/ G,PI,P12,RAD,EPHS,EPSSA,DX,DY,DT,DX2,DY2,T,SIGMA,
63300 *M,N,N1,N2,M1,M2,AM,DD,IT,RHO,IWET,IDRY,ID
63400 C*
63500 C* DEFINE STATEMENT FUNCTIONS C,SS,DDDX,DUDY,DVDX,DVDY,DKDX
63600 C* DKDY,FAC,F
63700 C*
63800 C(I,J)=0.25*(CO(I+1,J)+CO(I-1,J)+CO(I,J+1)+CO(I,J-1))+0.125*((Z(I
63900 *+1,J)-Z(I-1,J))*SI(I+1,J)-SI(I-1,J))+ (Z(I,J+1)-Z(I,J-1))*SI(I,
64000 *J+1)-SI(I,J-1)))
64100 SS(I,J)=0.25*(SI(I+1,J)+SI(I-1,J)+SI(I,J+1)+SI(I,J-1))+0.125*((Z(I
64200 *+1,J)-Z(I-1,J))*CO(I+1,J)-CO(I-1,J))+ (Z(I,J+1)-Z(I,J-1))*CO(I,
64300 *J+1)-CO(I,J-1)))
64400 DUDX(I,J)=(W(I+1,J)-W(I-1,J))/DX
64500 DUDY(I,J)=(U(I,J+1)-U(I,J-1))/DY2
64600 DVDX(I,J)=(V(I+1,J)-V(I-1,J))/DX2
64700 DVDY(I,J)=(V(I,J+1)-V(I,J-1))/DY
64800 F(I,J)=U(I,J)*COSI+V(I,J)*SINI + 0.5*A*(1.0 + ARG2/SINH2)/RK
64900 DKDY(I,J)=(-COSI*DUDY(I,J) + SINI*DUDY(I,J)) - A*DDDY(I,J-1)/SINH2
65000 */FF
65100 DKDX(I,J)=(-COSI*DUDX(I,J)+SINI*DUDX(I,J)) - A*DDDX(I,J-1)/SINH2)/F
65200 *F
65300 FAC(I,J)=U(I,J)*SINI-V(I,J)*COSI
65400 DO 200 ITT=1,ITMAX
65500 MWET=M-IWET
65600 IFLAG=1
65700 DO 210 II=1,MWET
65800 I=M-II
65900 DO 210 J=2,N1
66000 IF(D(I,J-1).LE.DD) GO TO 210
66100 COSI=C(I,J)
66200 SINI=SS(I,J)
66300 JJ=J-1
66400 CALL WNUM(D(I,J),COSI,SINI,U(I,J),V(I,J),RK,A)
66500 ARG2=2.0*RK*D(I,J)
66600 SINH2= SINH(ARG2)
66700 FF=F(I,J)
66800 IF(FF.GT.0.0) GO TO 450
66900 WRITE(6,451) I,J,D(I,J),COSI,SINI,U(I,J),V(I,J),RK,A
67000 451 FORMAT(10X'FF IS NEGATIVE--OUTPUT I,J,D,COSI,SINI,U,V,RK,A'/.
67100 *215.7E13.4)
67200 GO TO 210
67300 FACI=FAC(I,J)
67400 DENI=(SINI-COSI*FACI/FF)/DY
67500 DEN2=(COSI+SINI*FACI/FF)/DX
67600 DEN=DEN1-DEN2
67700 ZNEW=(COSI*DKDY(I,J)-SINI*DKDX(I,J)+Z(I,J-1)*DEN1-Z(I+1,J)*
67800 *DEN2)/DEN
67900 IF(ABS(ZNEW-Z(I,J)).GT.(EPSSA*ABS(ZNEW))) IFLAG=0
68000 Z(I,J)=ZNEW
68100 CO(I,J)=COS(Z(I,J))
68200 SI(I,J)=SIN(Z(I,J))
68300 IF(J.NE.2) GO TO 400
68400 Z(I,N1)=Z(I,2)
68500 CO(I,N1)=CO(I,2)
68600 SI(I,N1)=SI(I,2)
68700 GO TO 210
68800 400 IF(J.NE.3) GO TO 401

```

```

68900      Z(I,N2)=Z(I,3)
69000      CO(I,N2)=CO(I,3)
69100      SI(I,N2)=SI(I,3)
69200      GO TO 210
69300      401 IF(J.NE.N) GO TO 402
69400      Z(I,1)=Z(I,N)
69500      CO(I,1)=CO(I,N)
69600      SI(I,1)=SI(I,N)
69700      GO TO 210
69800      402 CONTINUE
69900      IF(J.NE.N1) GO TO 210
70000      Z(I,2)=Z(I,N1)
70100      CO(I,2)=CO(I,N1)
70200      SI(I,2)=SI(I,N1)
70300      210 CONTINUE
70400      IF(IFLAG.EQ.1) GO TO 250
70500      200 CONTINUE
70600      WRITE(6,220) ITMAX
70700      220 FORMAT(" RELAXATION FOR THETA FAILED AFTER",I4,3X,
70800      * "ITERATIONS")
70900      STOP
71000      250 CONTINUE
71100      RETURN
71200      END
71300      C*-----
71400      C*
71500      SUBROUTINE WNUM(D,COSI,SINI,U,V,RK,A)
71600      C*
71700      SUBROUTINE WNUM COMPUTES WAVE NUMBER INCLUDING WAVE-
71800      C* CURRENT INTERACTION.
71900      C*
72000      C*-----
72100      COMMON/CONST/ G,PI,P12,RAD,EP5H,EP5A,DX,DY,DT,DX2,DY2,T,SIGMA,
72200      *M,N,N1,N2,M1,M2,AM,DD,IT,RHO,IWET,IDRY,ID
72300      EPSK=0.001
72400      RK=P12/(1+SQRT(G*D))
72500      DO 100 I=1,50
72600      A=SIGMA-U*RK*COSI-RK*V*SINI
72700      A2=A**2
72800      ARG=RK*D
72900      F1=EXP(ARG)
73000      F2=1 O/F1
73100      SECH=2.O/(F1+F2)
73200      SECH2=SECH**2
73300      TT=TANH(ARG)
73400      FK=G*RK*TT-A2
73500      FFK=G*(ARG*SECH2+TT)+2.O*(U*COSI+V*SINI)*A
73600      RKNEW=RK-FK/FFK
73700      IF (ABS(RKNEW-RK).LE.(ABS(EP5K*RKNEW))) GO TO 110
73800      RK=RKNEW
73900      100 CONTINUE
74000      WRITE(6,101)I,RK,T,D,U,V
74100      101 FORMAT(" INTERATION FOR K FAILED TO CONVERGE: I,K,D,U,V"
74200      *,I6,5F10.5)
74300      CALL EXIT
74400      RETURN
74500      110 RK=RKNEW
74600      A=SIGMA-RK*U*COSI-RK*V*SINI
74700      C*-----
74800      C* CHECK IF RK NEGATIVE, THIS CONDITION CAN ARISE IF LOCAL CURRENT
74900      C* IS TOO STRONG
75000      C*-----

```

```

75100 IF(RK.GT.O.O)GO TO 120
75200 WRITE(6,130)D,COSI,SINI,U,V,RK,A
75300 130 FORMAT(' RK IS NEGATIVE: D,COSI,SINI,U,V,RK,A',
75400 *7F10.5)
75500 CALL EXIT
75600 120 RETURN
75700 END
75800 C*-----
75900 C*
76000 SUBROUTINE SNELL (THETA0,HH,ITER)
76100 C*
76200 C* SNELL CALCULATES THE FIRST GUESS OF THE REFRACTION ANGLE
76300 C* AT EACH GRID, AND ALSO THE WAVE HEIGHT AT THE LAST GRID(M)
76400 C* FOR EACH ITERATION THAT THE DEEPWATER WAVE IS BUILDING UP.
76500 C*
76600 C*-----
76700 COMMON D(50,50),U(50,50),V(50,50),Z(50,50),SI(50,50),CO(50,50),
76800 *H(50,50),CG(50,50),S(50,50),HBREAK(50,50),IB(50,50),DDDX(50,50),
76900 *,DDDY(50,50)
77000 COMMON/CONST/ G,PI,PI2,RAD,EPH,EPHSA,DX,DY,DT,DX2,DY2,T,SIGMA,
77100 *M,N,N1,N2,M1,M2,AM,DD,IT,RHO,IWET,IDRY,ID
77200 I=IDRY
77300 30 I=I+1
77400 IF(ITER.GT.1) I=M
77500 DO 600 J=2,N1
77600 CALL WNUM(D(I,J-1),-1,O,O,O,O,O,C,RK,A)
77700 AA = RK* D(I,J-1)
77800 ANG = ARSIN(SIN(THETA0)*TANH(AA))
77900 ANG = PI-ANG
78000 ARG = 2.O*AA
78100 SHOAL = SQRT(1.O/(TANH(AA)*(1.O*ARG/SINH(ARG))))
78200 REF = SQRT(COS(THETA0)/COS(ANG))
78300 WVHT = HH*SHOAL*REF
78400 HB = O.12*TANH(AA)*PI2/RK
78500 IF(WVHT.GT.HB) WVHT = HB
78600 IN = 1
78700 IF(WVHT.GT.HB) IN = O
78800 SS = SIN(ANG)
78900 CC = COS(ANG)
79000 43 CONTINUE
79100 H(I,J) = WVHT
79200 IB(I,J) = IN
79300 Z(I,J) = ANG
79400 SI(I,J) = SS
79500 CO(I,J) = CC
79600 600 CONTINUE
79700 IF(I.EQ.M) GO TO 85
79800 GO TO 30
79900 85 CONTINUE
80000 C*-----
80100 C* BOUNDARY CONDITIONS
80200 C*-----
80300 L = 1
80400 K = N
80500 J = 1
80600 45 DO 60 I = 1,M
80700 H(I,J) = H(I,K)
80800 IB(I,J) = IB(I,K)
80900 Z(I,J) = Z(I,K)
81000 SI(I,J) = SI(I,K)
81100 CO(I,J) = CO(I,K)
81200 L = L+1

```

```

81300      IF (L .GT. 3) RETURN
81400      IF (L .EQ. 3) GO TO 610
81500      L = 2
81600      J = 2
81700      K=N1
81800      GO TO 45
81900      610 J = N2
82000      K = 3
82100      GO TO 45
82200      RETURN
82300      END
82400
82500
82600
82700
82800
82900
83000
83100
83200
83300
83400
83500
83600
83700
83800
83900
84000
84100
84200
84300
84400
84500
84600
84700
84800
84900
85000
85100
85200
85300
85400
85500
85600
85700
85800
85900
86000
86100
86200
86300
86400
86500
86600
86700
86800
86900
87000
87100
87200
87300
87400

00081300
00081400
00081500
00081600
00081700
00081800
00081900
00082000
00082100
00082200
00082300
00082400
00082500
00082600
00082700
00082800
00082900
00083000
00083100
00083200
00083300
00083400
00083500
00083600
00083700
00083800
00083900
00084000
00084100
00084200
00084300
00084400
00084500
00084600
00084700
00084800
00084900
00085000
00085100
00085200
00085300
00085400
00085500
00085600
00085700
00085800
00085900
00086000
00086100
00086200
00086300
00086400
00086500
00086600
00086700
00086800
00086900
00087000
00087100
00087200
00087300
00087400

IF (L .GT. 3) RETURN
IF (L .EQ. 3) GO TO 610
L = 2
J = 2
K=N1
GO TO 45
610 J = N2
K = 3
GO TO 45
RETURN
END

SUBROUTINE TAUSB (WIND, WINANG, CF, ITD)
THIS SUBROUTINE CALCULATES SURFACE SHEAR STRESS BY VAN DORN'S
METHOD, AND AVERAGE BOTTOM SHEAR STRESS BY THE METHOD OF
DALRYMPLE AND LIU
WIND SPEED MUST BE IN METERS/SECOND

COMMON D(50,50),U(50,50),V(50,50),Z(50,50),SI(50,50),CO(50,50),
*H(50,50),CG(50,50),S(50,50),HBREAK(50,50),IB(50,50),DDX(50,50),
*DDY(50,50),W(50,50),Y(50,50)
COMMON/VAL/DP1(50,50),DM1(50,50),UP1(50,50),UM1(50,50),
*VP1(50,50),VM1(50,50),ETAP1(50,50),ETAM1(50,50),ETA(50,50)
COMMON/STRESS/SIGXX(50,50),SIGYY(50,50),SIGXY(50,50),TAUBX(50,50),
*TAUBY(50,50),TAUSX(50,50),TAUSY(50,50)
COMMON/REF/ZZ(50,50),HNEW(50,50),RKA(50,50)
COMMON/CONST/ G,PI,PI2,RAD,EPHS,EPSA,DX,DY,DT,DX2,DY2,T,SIGMA,
*M,N,N1,N2,M1,M2,AM,DD,IT,RHO,IWET,IDRY,TD
DIMENSION B(40),F(40),GG(40)

COMPUTE SURFACE SHEAR STRESS
IF (IT.GT.ITD+1) GO TO 1
VANCON=1.1E-06
IF (WIND .GE. 7.2) VANCON = 1.1E-06+2.5E-06*((1.-7.2/WIND)**2.)
WINDX = WIND*COS(WINANG)
WINDY = WIND*SIN(WINANG)
CON1 = RHO*VANCON*ABS(WIND)
DO 20 J = 1,N2
DO 20 I = 2, M
TAUSX(I,J) = - CON1 *WINDX
TAUSY(I,J) = CON1 *WINDY
20 CONTINUE
COMPUTE BOTTOM SHEAR STRESS
L=16
DELTA=PI2/L
VALUE=(RHO*CF)/(24.0*L)
DO 4 J=2,N1
K=J-1
DO 4 I=IWET,M1
PHI=Z(I,J)-PI
CC=COS(PHI)
SS=SIN(PHI)
UMAX=(PI*H(I,J))/(T*SINH(RKA(I,J)*D(I,K)))
EXPR1=UMAX*SS
EXPR2=UMAX*CC

```

```

87500      EXPR3=2.0*EXPR2
87600      EXPR4=2.0*EXPR1
87700      WM1=(UM1(I,J)+UM1(I+1,J))/2.0
87800      VM1=(VM1(I,J)+VM1(I,J+1))/2.0
87900      EXPR5=WM1**2
88000      EXPR6=VM1**2
88100      DELX=0.0
88200      DO 2 LL=1,L+1,1
88300      B(LL)=SQRT(EXPR5+EXPR6+(UMAX*COS(DELX))**2+COS(DELX))*
88400      *(WM1*EXPR3+VM1*EXPR4)
88500      GG(LL)=(VM1+EXPR1*COS(DELX))*B(LL)
88600      F(LL)=(WM1+EXPR2*COS(DELX))*B(LL)
88700      DELX=DELX+DELTA
88800      2 CONTINUE
88900      SUM=0.0
89000      SUMM=0.0
89100      DO 3 MM=2,L,2
89200      SUM=SUM+F(MM-1)+4.0*F(MM)+F(MM+1)
89300      SUMM=SUMM+GG(MM-1)+4.0*GG(MM)+GG(MM+1)
89400      3 CONTINUE
89500      TAUBX(I,J)=SUM*VALUE
89600      TAUBY(I,J)=SUMM*VALUE
89700      4 CONTINUE
89800      DO 5 I=1,M
89900      TAUBX(I,1)=TAUBX(I,N)
90000      TAUBX(I,N1)=TAUBX(I,2)
90100      TAUBX(I,N2)=TAUBX(I,3)
90200      TAUBY(I,1)=TAUBY(I,N)
90300      TAUBY(I,N1)=TAUBY(I,2)
90400      TAUBY(I,N2)=TAUBY(I,3)
90500      5 CONTINUE
90600      RETURN
90700      END
C*-----
C*
C* SUBROUTINE DGRAD
C*
C* CALCULATE THE SPATIAL GRADIENTS IN TOTAL DEPTH AFTER EACH
C* UPDATING OF THE TOTAL DEPTH
C*-----
COMMON D(50,50),U(50,50),V(50,50),Z(50,50),SI(50,50),CO(50,50),
+H(50,50),CG(50,50),S(50,50),HBREAK(50,50),IB(50,50),DDX(50,50),
+DDY(50,50)
COMMON/CONST/ G,PI,PI2,RAD,EPSH,EPSA,DX,DY,DT,DX2,DY2,T,SIGMA,
+M,N,N1,N2,M1,M2,AM,OD,IT,RHO,IWET,IDRY,ID
DO 60 I = 2,M1
DO 60 J = 3,N1
DDX(I,J) = -(D(I-1,J)-D(I+1,J))/(2.*DX)
IF(J.EQ.N1) GO TO 61
DDY=D(I,J-2)-8.0*D(I,J-1)+8.0*D(I,J+1)-D(I,J+2)
DDY(I,J)=DDY/(12.0*DY)
GO TO 60
61 DDY=D(I,N-1)-8.0*D(I,N)+8.0*D(I,N+2)-D(I,4)
DDY(I,J)=DDY/(12.0*DY)
60 CONTINUE
DO 70 I = 1,M
DDX(I,1)=DDDX(I,N)
DDY(I,1)=DDDY(I,N)
DDX(I,2)=DDDX(I,N1)
DDY(I,2)=DDDY(I,N1)
DDX(I,N2)=DDDX(I,3)
DDY(I,N2)=DDDY(I,3)

```

```

93700 ODDY(I,N2)=DDY(I,3)
93800 70 CONTINUE
93900 RETURN
94000 END
94100
94200 C*-----
94300 C*
94400 SUBROUTINE MOMEN
94500 C*
94600 C* MOMEN CALCULATES VELOCITIES USING THE FULL NONLINEAR MOMENTUM
94700 C* EQUATIONS
94800 C*-----
94900 COMMON D(50,50),U(50,50),V(50,50),Z(50,50),SI(50,50),CO(50,50),
95000 *H(50,50),CG(50,50),S(50,50),HBREAK(50,50),IB(50,50),DDX(50,50),
95100 *DDY(50,50),W(50,50),Y(50,50)
95200 COMMON/VAL/DP1(50,50),DM1(50,50),UP1(50,50),UM1(50,50),
95300 *VP1(50,50),VM1(50,50),ETAP1(50,50),ETAM1(50,50),ETA(50,50)
95400 COMMON/STRESS/SIGX(50,50),SIGY(50,50),SIGXY(50,50),TAUBX(50,50),
95500 *TAUBY(50,50),TAUSX(50,50),TAUSY(50,50)
95600 COMMON/EDDY/EX(50,50),EY,VCON
95700 COMMON/CONST/ G,PI,P12,RAD,EPHS,EPSSA,DX,DY,DT,DX2,DY2,T,SIGMA,
95800 *M,N,N1,N2,M1,M2,AM,DD,IT,RHO,IWET,IDRY,ID
95900 DO 97 I=IWET,M
96000 DO 96 J=3,N1
96100 EX(I,J)=((I-IWET+1)*DX)*VCON*SQRT(G*DM1(I,J-1))
96200 IF(I.GE.12) EX(I,J)=.875
96300
96400 96 CONTINUE
96500 EX(I,N2)=EX(I,3)
96600 EX(I,2)=EX(I,N1)
96700 EX(I,1)=EX(I,N)
96800
96900 97 CONTINUE
97000 DO 21 I=IWET,M1
97100 K = J-1
97200 UP1(I,J)=((D(I+1,K)+D(I,K))*U(I+1,J)+D(I,K)+D(I-1,K))*
97300 *U(I,J)+((U(I+1,J)+U(I,J))-((D(I,K)+D(I-1,K))*U(I,J)+
97400 *(D(I-1,K)+D(I-2,K))*U(I-1,J)+U(I,J)+U(I-1,J)))/(8.*DX)
97500 UP1(I,J)=UP1(I,J)+((D(I,K)+D(I,K))*V(I,J+1)+D(I-1,K+1)+
97600 *D(I-1,K))*V(I-1,J+1)+((U(I,J)+U(I,J+1))-((D(I,K)+D(I-1,K))*
97700 *V(I,J)+D(I-1,K)+D(I-1,K))*V(I-1,J)+U(I,J)+U(I,J-1))
97800 */(8.*DY)
97900 UP1(I,J)=UP1(I,J)+D(I,K)+D(I-1,K))*((ETA(I,J)-ETA(I-1,J))
98000 *(G/(DX*2.*O))
98100 UP1(I,J)=UP1(I,J)-(TAUSX(I,J)+TAUSX(I-1,J))/(2.*RHO)
98200 UP1(I,J)=UP1(I,J)+(TAUBX(I,J)+TAUBX(I-1,J))/(2.*RHO)
98300 UP1(I,J)=UP1(I,J)+(SIGX(I,J)-SIGX(I-1,J))/(DX*RHO)+(SIGXY(I,
98400 *J+1)-SIGXY(I,J)+SIGXY(I,J+1)-SIGXY(I-1,J-1))/(4.*DY*RHO)
98500 UP1(I,J)=UP1(I,J)-(DM1(I,K)+DM1(I-1,K))*((UM1(I,J+1)-
98600 *UM1(I,J))*EY-(UM1(I,J)-UM1(I,J-1))*EY)/(2.*DY*DY)
98700 UP1(I,J)=UP1(I,J)-(DM1(I,K)+DM1(I-1,K))*((VM1(I,J+1)-
98800 *VM1(I,J))*V(I+1,J)+EX(I,J)+EX(I,J)+EX(I-1,J)+EX(I-1,J+1)-
98900 *(VM1(I,J)-VM1(I-1,J))*EX(I,J)+EX(I,J-1)+EX(I-1,J-1)+
99000 *EX(I-1,J)))/(8.*DX*DY)
99100 VP1(I,J)=((D(I+1,K)+D(I,K))*U(I+1,J)+D(I,K)+D(I-1,K-1))*
99200 *U(I+1,J-1)+((V(I+1,J)+V(I,J))-((D(I,K)+D(I-1,K))*U(I,J)+
99300 *(D(I,K-1)+D(I-1,K-1))*U(I,J-1))*V(I,J)+V(I-1,J))/(8.*DX)
99400 IF (K.EQ.2) GO TO 83
99500 GO TO 84
99600 83 VP1(I,J)=VP1(I,J)+((D(I,K+1)+D(I,K))*V(I,J+1)+D(I,K)+
99700 *D(I,K-1))*V(I,J)+((V(I,J+1)+V(I,J))-((D(I,K)+D(I-1,K))*
99800 *V(I,J)+D(I,K-1)+D(I,N-1))*V(I,J-1))*V(I,J)+V(I-1,J))/(8.*DY)
99900 GO TO 85

```

```

100000      84 VP(I,J)=VP1(I,J)*((D(I,K)+1)+D(I,K))*V(I,J+1)*(D(I,K)+
100100      *D(I,K-1))*V(I,J)*V(I,J+1)+V(I,J)-((D(I,K)+D(I,K-1))*
100200      *V(I,J)+D(I,K-1)+D(I,K-2))*V(I,J-1)*(V(I,J)+V(I,J-1))/(B.O*DY)
100300      85 VP(I,J)=VP1(I,J)*(D(I,K)+D(I,K-1))*ETA(I,J)-ETA(I,J-1))*
100400      *(G/(2.O*DY))
100500      VP(I,J)=VP1(I,J)-(TAUSY(I,J)+TAUSY(I,J-1))/(2.O*RH0)
100600      VP(I,J)=VP1(I,J)*(TAUBY(I,J)+TAUBY(I,J-1))/(2.O*RH0)
100700      VP(I,J)=VP1(I,J)*(SIGXY(I+1,J)-SIGXY(I-1,J-1)+SIGXY
100800      *(I+1,J)-SIGXY(I-1,J))/(4.O*RH0*DX)+(SIGY(I,J)-SIGY(I,J-1))
100900      */(RH0*DY)
101000      VP(I,J)=VP1(I,J)-(DM1(I,K)+DM1(I,K-1))*((EX(I+1,J-1)+
101100      *EX(I+1,J)+EX(I,J-1)+EX(I,J))*(VM1(I+1,J)-VM1(I,J))-
101200      *EX(I,J-1)+EX(I,J)+EX(I-1,J-1)+EX(I-1,J))*(VM1(I,J)-
101300      *VM1(I-1,J))/(8.O*DX*DX)
101400      VP(I,J)=VP1(I,J)-(DM1(I,K)+DM1(I,K-1))*((UM1(I+1,J)-
101500      *UM1(I+1,J-1))*EY-(UM1(I,J)-UM1(I,J-1))*EY)/(2.O*DY*DX)
101600      21 CONTINUE
101700      RETURN
101800      END
101900      C*-----
102000      C*
102100      SUBROUTINE ETAS(ETA,DELT)
102200      C*
102300      C* ETAS CALCULATES THE CHANGE IN MEAN WATER LEVEL DUE TO WAVE ACTION
102400      C*
102500      C*-----
102600      COMMON D(50,50),U(50,50),V(50,50),Z(50,50),SI(50,50),CI(50,50),
102700      *H(50,50),CG(50,50),S(50,50),HBREAK(50,50),IB(50,50),DDX(50,50),
102800      *DDY(50,50),W(50,50),Y(50,50)
102900      COMMON/VAL/DP1(50,50),DM1(50,50),UP1(50,50),UM1(50,50),
103000      *VP1(50,50),VM1(50,50),ETAP1(50,50),ETAM1(50,50),ETA(50,50)
103100      COMMON/CONST/ G,PI,PI2,RAD,EPHS,EPSSA,DX,DY,DT,DX2,DY2,T,SIGMA,
103200      *M,N,N1,N2,M1,M2,AM,DO,IT,RHO,IWET,IDRY,IO
103300      DIMENSION RETA(50,50)
103400      DO 20 J=2,N1
103500      DO 20 I=IWET,M1
103600      K=J-1
103700      ETAP1(I,J)=RETA(I,J)-(DELT*0.5)*ETAP1(I,J)
103800      22 DP1(I,K)=D(I,K)-ETA(I,J)+ETAP1(I,J)
103900      20 CONTINUE
104000      DO 23 J=2,N1
104100      K=J-1
104200      DO 24 I=1,IDRY
104300      DP1(I,K)=D(I,K)
104400      24 CONTINUE
104500      DP1(M,K)=D(M,K)
104600      23 CONTINUE
104700      DO 60 I=1,M
104800      ETAP1(I,N2)=ETAP1(I,3)
104900      ETAP1(I,N1)=ETAP1(I,2)
105000      ETAP1(I,1)=ETAP1(I,N)
105100      DP1(I,N2)=DP1(I,3)
105200      DP1(I,N1)=DP1(I,2)
105300      DP1(I,1)=DP1(I,N)
105400      60 CONTINUE
105500      DO 92 I=1,M
105600      IF(DP1(I,1).GT.DO) GO TO 93
105700      92 CONTINUE
105800      93 IWET=I
105900      IDRY=IWET-1
106000      RETURN
106100      END

```



```

106200      C*-----
106300      C*      SUBROUTINE UCALC(TD,TU,TV,DELTA)
106400      C*
106500      C*      UCALC CALCULATES THE DEPTH AVERAGED VELOCITIES BASED ON THE
106600      C*      RESULTS OF SUBROUTINE WOMEN
106700      C*
106800      C*-----
106900      C*      COMMON D(50,50),U(50,50),V(50,50),Z(50,50),SI(50,50),CO(50,50),
107000      C*      H(50,50),CG(50,50),S(50,50),HBREAK(50,50),IB(50,50),DDX(50,50),
107100      C*      DDDY(50,50),W(50,50),Y(50,50)
107200      C*      COMMON/VAL/DP1(50,50),DM1(50,50),UP1(50,50),UM1(50,50),
107300      C*      VP1(50,50),VM1(50,50),ETAP1(50,50),ETAM1(50,50),ETA(50,50)
107400      C*      COMMON/CONST/ G,PI,P12,RAD,EPHS,EPSSA,DX,DY,DT,DX2,DY2,T,SIGMA,
107500      C*      M,N,N1,N2,M1,M2,AM,DD,IT,RHO,IWET,IDRY,TD
107600      C*      DIMENSION TD(50,50),TU(50,50),TV(50,50)
107700      C*      DO 24 I=IWET,M1
107800      C*      DO 24 J=3,N1
107900      C*      K=J-1
108000      C*      UP1(I,J)=((TD(I,K)+TD(I-1,K))*TU(I,J))/(DP1(I,K)+DP1(I-1,
108100      C*      *K))-((DELTA*2.0)/(DP1(I,K)+DP1(I-1,K)))*UP1(I,J)
108200      C*      VP1(I,J)=((TD(I,K)+TD(I-1,K))*TV(I,J))/(DP1(I,K)+
108300      C*      *DP1(I,K-1))-((DELTA*2.0)/(DP1(I,K)+DP1(I,K-1)))*VP1(I,J)
108400      C*      24 CONTINUE
108500      C*      DO 22 J=3,N1
108600      C*      DO 27 I=1,IWET
108700      C*      UP1(I,J)=0.0
108800      C*      27 CONTINUE
108900      C*      UP1(M,J)=VP1(M1,J)
109000      C*      VP1(M,J)=0.0
109100      C*      22 CONTINUE
109200      C*      DO 60 I=1,M
109300      C*      UP1(I,N2)=UP1(I,3)
109400      C*      UP1(I,2)=UP1(I,N1)
109500      C*      UP1(I,1)=UP1(I,N)
109600      C*      VP1(I,N2)=VP1(I,3)
109700      C*      VP1(I,2)=VP1(I,N1)
109800      C*      VP1(I,1)=VP1(I,N)
109900      C*      60 CONTINUE
110000      C*      DO 69 J=2,N1
110100      C*      DO 68 I=1,M1
110200      C*      W(I,J)=(UP1(I,J)+UP1(I+1,J))/2.0
110300      C*      Y(I,J)=(VP1(I,J)+VP1(I,J+1))/2.0
110400      C*      68 CONTINUE
110500      C*      Y(M,J)=0.0
110600      C*      69 CONTINUE
110700      C*      DO 79 I=1,M
110800      C*      W(I,N2)=W(I,3)
110900      C*      W(I,2)=W(I,N1)
111000      C*      W(I,1)=W(I,N)
111100      C*      Y(I,N2)=Y(I,3)
111200      C*      Y(I,2)=Y(I,N1)
111300      C*      Y(I,1)=Y(I,N)
111400      C*      79 CONTINUE
111500      C*      RETURN
111600      C*      END
111700      C*-----
111800      C*      SUBROUTINE ROLBAC
111900      C*
112000      C*      ROLBAC UPDATES THE VALUES OF ETA,U,V,AND D FOR THE NEXT
112100      C*      ITERATION
112200      C*
112300      C*-----
00106200
00106300
00106400
00106500
00106600
00106700
00106800
00106900
00107000
00107100
00107200
00107300
00107400
00107500
00107600
00107700
00107800
00107900
00108000
00108100
00108200
00108300
00108400
00108500
00108600
00108700
00108800
00108900
00109000
00109100
00109200
00109300
00109400
00109500
00109600
00109700
00109800
00109900
00110000
00110100
00110200
00110300
00110400
00110500
00110600
00110700
00110800
00110900
00111000
00111100
00111200
00111300
00111400
00111500
00111600
00111700
00111800
00111900
00112000
00112100
00112200
00112300

```

```

112400      COMMON D(50,50),U(50,50),V(50,50),Z(50,50),SI(50,50),CO(50,50),
112500      *H(50,50),CG(50,50),S(50,50),HBREAK(50,50),IB(50,50),DDDX(50,50),
112600      *DDDY(50,50),W(50,50),Y(50,50)
112700      COMMON/VAL/DP1(50,50),DM1(50,50),UP1(50,50),UM1(50,50),
112800      *VP1(50,50),VM1(50,50),ETAP1(50,50),ETAM1(50,50),ETA(50,50)
112900      COMMON/CONST/ G,PI,P12,RAD,EPHS,EPSA,DX,DY,DT,DX2,DY2,T,SIGMA,
113000      *M,N,N1,N2,M1,M2,AM,DD,IT,RHO,IWET,IDRY,ID
113100      DO 1 I=1,M
113200      DO 1 J=1,N2
113300      ETAM1(I,J)=ETA(I,J)
113400      ETA(I,J)=ETAP1(I,J)
113500      UM1(I,J)=U(I,J)
113600      U(I,J)=UP1(I,J)
113700      VM1(I,J)=V(I,J)
113800      V(I,J)=VP1(I,J)
113900      D(I,J)=DP1(I,J)
114000      DM1(I,J)=D(I,J)
114100      1 CONTINUE
114200      RETURN
114300      END
114400
114500
114600
114700
114800
114900
115000
115100
115200
115300
115400
115500
115600
115700
115800
115900
116000
116100
116200
116300
116400
116500
116600
116700
116800
116900
117000
117100
117200
117300
117400

C*-----
C*      COMMON D(50,50),U(50,50),V(50,50),Z(50,50),SI(50,50),CO(50,50),
*H(50,50),CG(50,50),S(50,50),HBREAK(50,50),IB(50,50),DDDX(50,50),
*DDDY(50,50),W(50,50),Y(50,50)
COMMON/VAL/DP1(50,50),DM1(50,50),UP1(50,50),UM1(50,50),
*VP1(50,50),VM1(50,50),ETAP1(50,50),ETAM1(50,50),ETA(50,50)
COMMON/CONST/ G,PI,P12,RAD,EPHS,EPSA,DX,DY,DT,DX2,DY2,T,SIGMA,
*M,N,N1,N2,M1,M2,AM,DD,IT,RHO,IWET,IDRY,ID
DO 1 I=1,M
DO 1 J=1,N2
ETAM1(I,J)=ETA(I,J)
ETA(I,J)=ETAP1(I,J)
UM1(I,J)=U(I,J)
U(I,J)=UP1(I,J)
VM1(I,J)=V(I,J)
V(I,J)=VP1(I,J)
D(I,J)=DP1(I,J)
DM1(I,J)=D(I,J)
1 CONTINUE
RETURN
END
C*-----
C*
SUBROUTINE CONTIN
C*
CONTIN CALCULATES THE FINAL CORRECTION TO TOTAL DEPTH BASED
C* ON THE EQUATION OF CONTINUITY
C*
C*-----
COMMON D(50,50),U(50,50),V(50,50),Z(50,50),SI(50,50),CO(50,50),
*H(50,50),CG(50,50),S(50,50),HBREAK(50,50),IB(50,50),DDDX(50,50),
*DDDY(50,50),W(50,50),Y(50,50)
COMMON/VAL/DP1(50,50),DM1(50,50),UP1(50,50),UM1(50,50),
*VP1(50,50),VM1(50,50),ETAP1(50,50),ETAM1(50,50),ETA(50,50)
COMMON/CONST/ G,PI,P12,RAD,EPHS,EPSA,DX,DY,DT,DX2,DY2,T,SIGMA,
*M,N,N1,N2,M1,M2,AM,DD,IT,RHO,IWET,IDRY,ID
DO 20 J=2,N1
K=J-1
DO 20 I=IWET,M1
IF (K.EQ.1) GO TO 21
ETAP1(I,J)=((D(I+1,K)+D(I,K))*U(I+1,J)-
*(D(I,K)+D(I-1,K))*U(I,J))/DX+((D(I,K+1)+D(I,K))*V(I,J+1)-
*(D(I,K)+D(I,K-1))*V(I,J))/DY)
GO TO 20
21 ETAP1(I,J)=((D(I+1,K)+D(I,K))*U(I+1,J)-
*(D(I,K)+D(I-1,K))*U(I,J))/DX+((D(I,K+1)+D(I,K))*V(I,J+1)-
*(D(I,K)+D(I,N-1))*V(I,J))/DY)
20 CONTINUE
RETURN
END

```

Distribution

Office of Naval Research
Coastal Science Program
Code 42205
Arlington, VA 22217

Defense Documentation Center
Cameron Station
Alexandria, VA 22314

Director, Naval Research Lab.
ATTN: Technical Information Officer
Washington, D. C. 20375

Director
Office of Naval Research Branch Office
1030 East Green Street
Pasadena, CA 91101

Chief of Naval Research
Code 100M
Office of Naval Research
Arlington, VA 22217

Office of Naval Research
Operational Applications Division
Code 200
Arlington, VA 22217

Office of Naval Research
Scientific Liaison Officer
Scripps Institution of Oceanography
La Jolla, CA 92093

Director Naval Research Laboratory
ATTN: Library, Code 2628
Washington, D. C. 20375

ONR Scientific Liaison Group
American Embassy - Room A-407
APO San Francisco, CA 96503

Commander
Naval Oceanographic Office
ATTN: Library, Code 1600
Washington, D. C. 20374

Naval Oceanographic Office
Code 3001
Washington, D. C. 20374

Chief of Naval Operations
OP 987P1
Department of the Navy
Washington, D. C. 20350

Oceanographer of the Navy
Hoffman II Building
200 Stovall Street
Alexandria, VA 22322

Naval Academy Library
U. S. Naval Academy
Annapolis, MD 21402

Commanding Officer
Naval Coastal Systems Laboratory
Panama City, FL 32401

Director
Coastal Engineering Research Center
U. S. Army Corps of Engineers
Kingman Building
Fort Belvoir, VA 22060

Officer in Charge
Environmental Research Productn Felty.
Naval Postgraduate School
Monterey, CA 93940

Director
Amphibious Warfare Board
U. S. Atlantic Fleet
Naval Amphibious Base
Norfolk, Little Creek, VA 23520

Commander, Amphibious Force
U. S. Pacific Fleet
Force Meteorologist
Comphibpac Code 25 5
San Diego, CA 93155

Librarian, Naval Intelligence
Support Center
4301 Suitland Road
Washington, D. C. 20390

Commanding Officer
Naval Civil Engineering Laboratory
Port Hueneme, CA 93041

Chief, Wave Dynamics Division
USAE-WES
P. O. Box 631
Vicksburg, MS 39180

Commandant
U. S. Coast Guard
ATTN: GECV/61
Washington, D. C. 20591

Office of Research and Development
%DS/62
U. S. Coast Guard
Washington, D. C. 20591

National Oceanographic Data
Center %D764
Environmental Data Services
NOAA
Washington, D. C. 20235

Prof. Dr. Fuehrboeter
Lehrstuhl F. Hydromechanik U. Kuestenw
Technische Hochschule Braunschweig
Beethovenstrasse 51A
D-3300 Braunschweig, West Germany

Prof. Dr. Walter Hansen
Direktor D. Instituts F. Meereskunde
Universitaet Hamburg
Heimhuderstrasse 71
D-2000 Hamburg 13, West Germany

Prof. Dr. Klaus Hasselmann
Institut F. Geophysik
Universitaet Hamburg
Schleuterstrasse 22
D-2000 Hamburg 13, West Germany

Coastal Studies Institute
Louisiana State University
Baton Rouge, LA 70803

Dr. Edward Thornton
Department of Oceanography
Naval Postgraduate School
Monterey, CA 93940

Dr. Douglas I. Inman
University of California A-009
Shore Processes Laboratory
La Jolla, CA 92093

Dr. Bruce Heyden
Dept. of Environmental Sciences
University of Virginia
Charlottesville, VA 22903

ATE
LMED
-8